UNIVERSITÀ DEGLI STUDI DI MILANO

PhD School in Molecular and Cellular Biology
XXXII Ciclo

ROLE OF *ALOG* FAMILY GENES IN INFLORESCENCE PATTERNING IN *ORYZA SATIVA* AND *ARABIDOPSIS THALIANA*

EMANUELA FRANCHINI
PhD Thesis

Scientific tutor: **Professor Martin M. Kater**

Table of contents

RIASSUNTO

L'architettura dell'infiorescenza è uno dei tratti agronomici che influenza la resa pertanto comprendere i meccanismi genetici che sono alla base di essa contribuirebbe a chiarire i meccanismi di evoluzione e domesticazione dei cereali e a migliorarne la resa.

Le piante a fiore hanno sviluppato diversi tipi di infiorescenza. L'architettura dell'infiorescenza è stabilita nelle prime fasi dello sviluppo riproduttivo ed è determinata dall'attività di diversi tipi di meristema e dal tempo di transizione da meristema indeterminato a meristema determinato.

Diversi sono i geni già noti coinvolti in questo processo; molti però devono essere ancora caratterizzati per capire meglio come lo sviluppo dell'infiorescenza sia regolato.

L'analisi transcrittomica eseguita, tramite l'uso della MicroDissezione Laser (LMD), in Arabidopsis e in riso, nei diversi meristemi riproduttivi, ha evidenziato che geni appartenenti alla famiglia degli ALOG, in particolare *G1L1, G1L2* and *G1L5* in riso e *LSH1, LSH3* e *LSH4* in Arabidopsis, risultano differenzialmente espressi nei campioni considerati e che possono essere coinvolti nello sviluppo dell'infiorescenza. È infatti noto che *G1L5* regola l'architettura dell'infiorescenza mentre *LSH3* e *LSH4* sono coinvolti nel mantenimento del meristema e nell'organogenesi. Il ruolo degli altri geni è stato indagato.

Analisi di espressione mediante qRT-PCR e ibridazione *in situ* sui tessuti meristematici in entrambe le specie hanno confermato i dati di RNAseq.

Per investigare meglio il ruolo di questi geni nell' organizzazione dell'infiorescenza sono stati generati singoli e multipli mutanti, in combinazioni diverse attraverso il sistema di genome editing CRISPR-Cas9.

I risultati ottenuti rivelano che *G1L1* e *G1L2* regolano il numero di ramificazioni infiorescenziali e di spighette e suggeriscono un ruolo di *G1L2* anche nello sviluppo radicale; indicano anche un coinvolgimento di *LSH1* nel mantenimento del meristema ascellare e nell'organogenesi, il ruolo di *LSH3* nella lunghezza dello stelo e una funzione ridondante di *LSH1, LSH3* e *LSH4* nello sviluppo dell'infiorescenza.

ABSTRACT

Inflorescence architecture is a key agronomical trait that determines fruit and seed yield.

Understanding the genetic basis of inflorescence architecture will not only contribute to elucidate crop evolution/domestication mechanisms but also improve crop grain yield.

Flowering plants develop different types of inflorescences, such as racemes in Arabidopsis and panicles in rice. The architecture is established during the early stages of reproductive development and it is determined by the activity of different meristem types and by the timing of the transition between indeterminate meristems to determinate ones.

Inflorescence development is finely regulated by a genetic network that includes meristem identity genes and genes that regulate their expression; many genes are already known but others have still to be characterized to provide insight into how this complex process is controlled.

Transcriptomic analysis performed in rice and in Arabidopsis through laser microdissection of different meristematic tissues highlighted differentially expressed genes belonging to the ALOG family suggesting their role in inflorescence patterning.

We focus on *G1L1, G1L2* and *G1L5* of rice and on *LSH1, LSH3* and *LSH4* of Arabidopsis. *G1L5* is already known to be a major regulator of inflorescence architecture, whereas *LSH3* and *LSH4* seem to have a role in meristem maintenance and organogenesis. Their expression profiles were analysed by qRT-PCR and RNA in situ hybridization experiments using meristematic tissues from both species. We are also generating single and double/triple K.O mutants in different combinations by CRISPR-Cas9 genome editing technology to have a better understanding of their role in inflorescence patterning.

The data so far obtained demonstrate the role of *G1L1* and *G1L2* in inflorescence branching and spikelet number determination and we also propose a role for *G1L2* in root development. Furthermore, *LSH1* seems to be involved in axillary meristem maintenance and organogenesis, and *LSH3* in stem elongation. We propose the hypothesis that *LSH1, LSH3* and *LSH4* play a redundant function in inflorescence development.

AIM OF THESIS

The architecture of the inflorescence is an important agronomical trait. Meristem activity and timing of transitions from indeterminate to determinate meristems is a crucial step that determines the whole structure of the inflorescence. Unravelling the roles of genes putatively involved in this process will provide insight into how the molecular mechanisms are controlled and hence it will contribute to improving crop grain yield.

Transcriptomic analysis performed in reproductive meristems by Mantegazza et al. (2014)[1] and by Harrop et al. (2016)[2], in Arabidopsis and rice, respectively, indicated that *ALOG* family genes might have a role in inflorescence development in both species. In Arabidopsis, *AtLSH1*, *AtLSH3* and *AtLSH4* are the only genes of the ALOG family resulting differentially expressed in different reproductive meristems with a similar expression profile; whereas in Rice *OsG1L1, OsG1L2* and *OsG1L5* are the only *ALOG* genes resulting differentially expressed in reproductive meristems with a similar expression profile. It is already known that *AtLSH3* and *AtLSH4* are involved in meristem maintenance and organogenesis [3,4] whereas *OsG1L5* is a major regulator of rice inflorescence architecture, it controls the timing of transition from indeterminate to determinate meristems [5]. Furthermore, phylogenetic analysis performed by Yoshida et al. (2009)[6] showed that *AtLSH3* and *AtLSH4* are paralogues and closely related to *AtLSH1*; in the same way, *OsG1L1* and *OsG1L2* are paralogues and close related to *OsG1l5*. Therefore, *AtLSH1* might have the same function or might be involved in the same pathway such as *AtLSH3, AtLSH4,* and the genes *OsG1L1* and *OsG1L2*, like *OsG1L5,* could play a role in determination of inflorescence architecture.

The aim of my thesis was to functionally characterize these genes in Arabidopsis and rice to unravel their role in inflorescence development and to understand if their functions are conserved between monocot and dicot species.

To address this goal, first, expression analysis by qRT-PCR has been done on reproductive meristems to confirm the RNAseq data and also on all the different plant tissues to investigate their pattern of expression during plant development. Subsequently, the spatial/temporal expression of the transcript in different meristematic tissues by *in situ* hybridization has been characterized.

Second, single and double mutants in different combinations using CRISPR-Cas9 genome editing technology were generated and subsequently analysed by genotyping and phenotyping. Phenotypical analysis in Arabidopsis was performed measuring length of primary shoot, number of secondary shoots and number of siliques produced on primary shoot; whereas in rice the main traits of the panicle such as panicle length, number and length of branches, number of spikelets and also the grains

structure were analysed. The *g1l2* mutant showed a more severe phenotype than *g1l1*, therefore we decided to further investigate in more detail the role of *G1L2* in inflorescence architecture determination. However, for both genes, we also generated rice overexpression lines.

In Arabidopsis, to unravel putative interactors of LSHs factors protein-protein interaction assay was performed using the Yeast 2-Hybrid system and BiFC assays.

All these experiments together will lead to a better understanding of the role that ALOG family genes play in the control of inflorescence development and will be a starting point to elucidate these genetic networks and their conservation between monocot and dicot species.

1. INTRODUCTION

1.1 MODEL PLANTS

The Angiosperm phylum counts more than 250.000 species and it is formed by two major classes: Monocotyledons, which includes major cereals like rice, maize, barley and wheat and Dicotyledons such as Arabidopsis, tomato, Antirrhinum etc. *Oryza sativa* and *Arabidopsis thaliana* are considered important model plant systems for the following features: their genome size is relatively small when compared to other plants; completely sequenced and annotated genome; easily manipulation of the genome; short life cycle and high reproductive success. The study of these two model plants provide insights into how plants develop and the molecular mechanism underlying plant processes [7].

1.1.1 *Arabidopsis thaliana*: a model for plant research

Arabidopsis thaliana is a winter annual plant belonging to the *Brassicaceae* family, which includes cultivated species such as cabbage, cauliflower and radish. Arabidopsis is not agronomical relevant but it offers advantages for basic research in genetics and molecular biology. Arabidopsis was discovered by Jhoannes Thal in the 16th century and its potential as model organism was already revealed by F. Laibach [8]. His student, Erna Reinholz, made the first mutant collection, induced by X-Rays, and published it in his thesis in 1947.

The Arabidopsis genome was the first completely sequenced plant genome and was made available in the year 2000 by the Arabidopsis Genome Initiative [9]. The genome size is 125 Mb and it is organized in 5 chromosomes **[Figure 1]**. According to the TAIR10 annotation *(https://www.arabidopsis.org)*, the genome has 33.602 genes grouped in about 11.000 families. Furthermore, Arabidopsis is easily transformed by *Agrobacterium tumefaciens* using the floral dip method [10].

It is a small self-fertilizing plant easily cultivated in large numbers occupying little space; its life cycle is very short: six to eight weeks from seed to seed and it produces a large number of seeds; a single plant can produce up to 10.000 seeds.
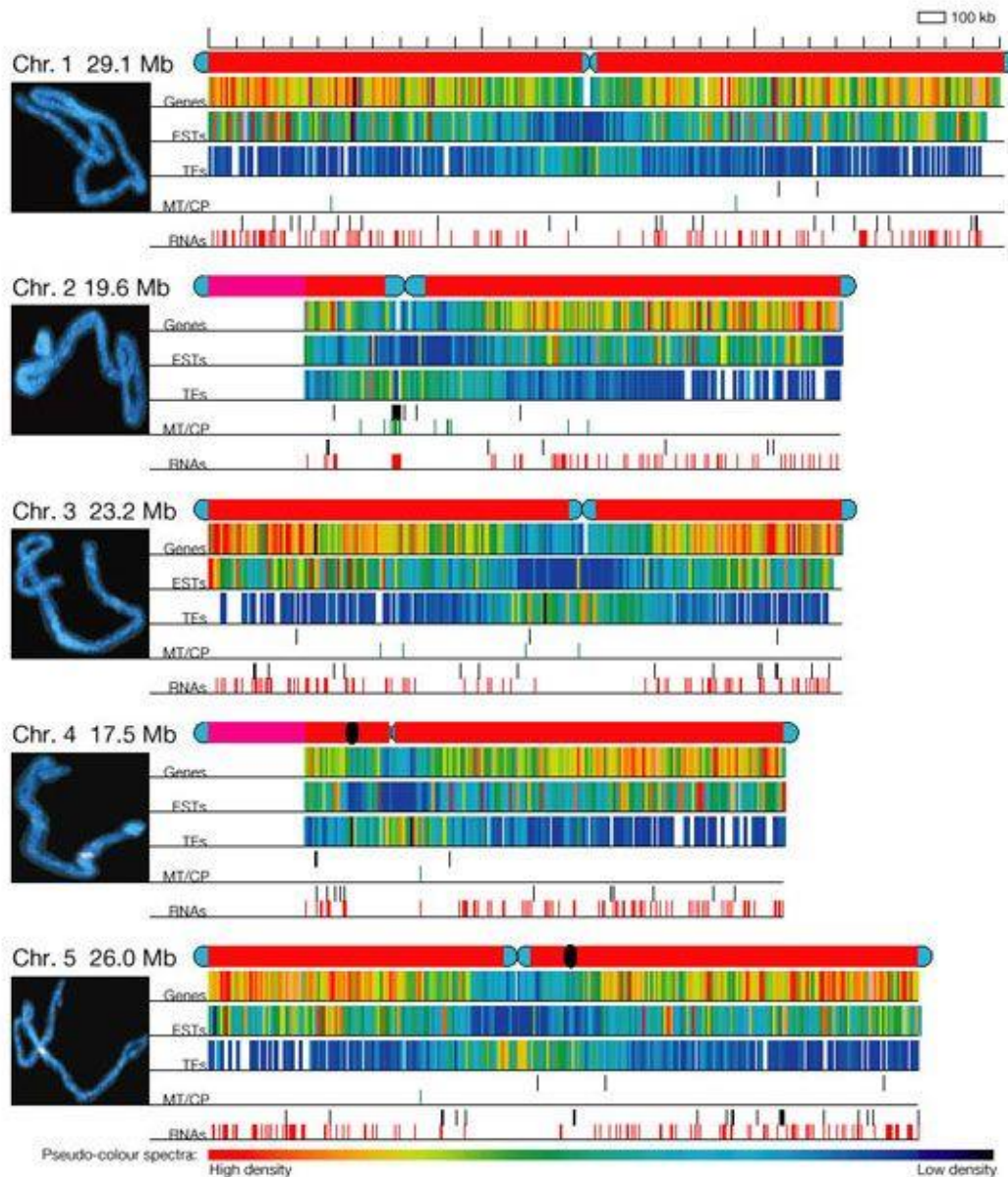
Figure 1. Arabidopsis chromosome organization [9].

1.1.2 Oryza sativa: a model plant for cereals

Rice is an annual plant belonging to the *Oryza* genus that belongs to *Poaceae* (grass) family. The *Oryza genus* has two domesticated species: *sativa* and *glaberrima.* The domestication of *Oryza sativa* started 10.000 years ago in the present China, while domestication of *Oryza glaberrima,* was more recent, starting from 3000 years ago along the Niger river [11]. *Oryza sativa* has three subspecies (*ssp.):*

Indica: non-sticky, long-grain, typical of tropical climate, more resistant to adverse weather conditions, diffused in Asia;

Japonica: sticky, short-grain, more yield, adapted to temperate climates like for instance in parts of Asia, Europe and Northern America;

Javanica: long and thick grain, cultivated in Indonesia and not very diffused.

Rice is a staple plant and with other cereals form the major source of food for half of the world population, especially in Asia, Arica and South America [12], therefore rice research has an important agronomical relevance.

The rice genome is 390 Mb in size [13], rather small when compared to other cereals but three times larger than the genome of Arabidopsis [12,14]. It is a diploid species and its genome is organized in 12 chromosomes [15–17] **[Figure 2]**.

The genome of cultivar Nipponbare (*ssp. Japonica)* was completely sequenced and mapped in 2000 by the International Rice Genome Sequencing Project (IRGSP) [12,15,17] and improved with next generation sequencing techniques by *Kawahara et al.* in 2013. Recently, also the near-completely version of *Indica* reference genome was built by sequencing and de novo assembly [18] since the previous one was incomplete and with fragmented genes [19–21].

The rice life cycle, from seed to seed takes more or less six months, depending on the cultivar. It is an autogamy plant and it is highly suitable for use in the laboratory for experimentation [7].

Many rice accessions can be efficiently transformed using *Agrobacterium tumefaciens* and protocols are already available since 1994 [22] which were later optimised. Furthermore, the monophyletic origin revealed by Clark et al., 1995[23] and high syntenic genomes among rice and other cereals [24], make it possible to transfer the knowledge acquired from rice to other cereals [7].
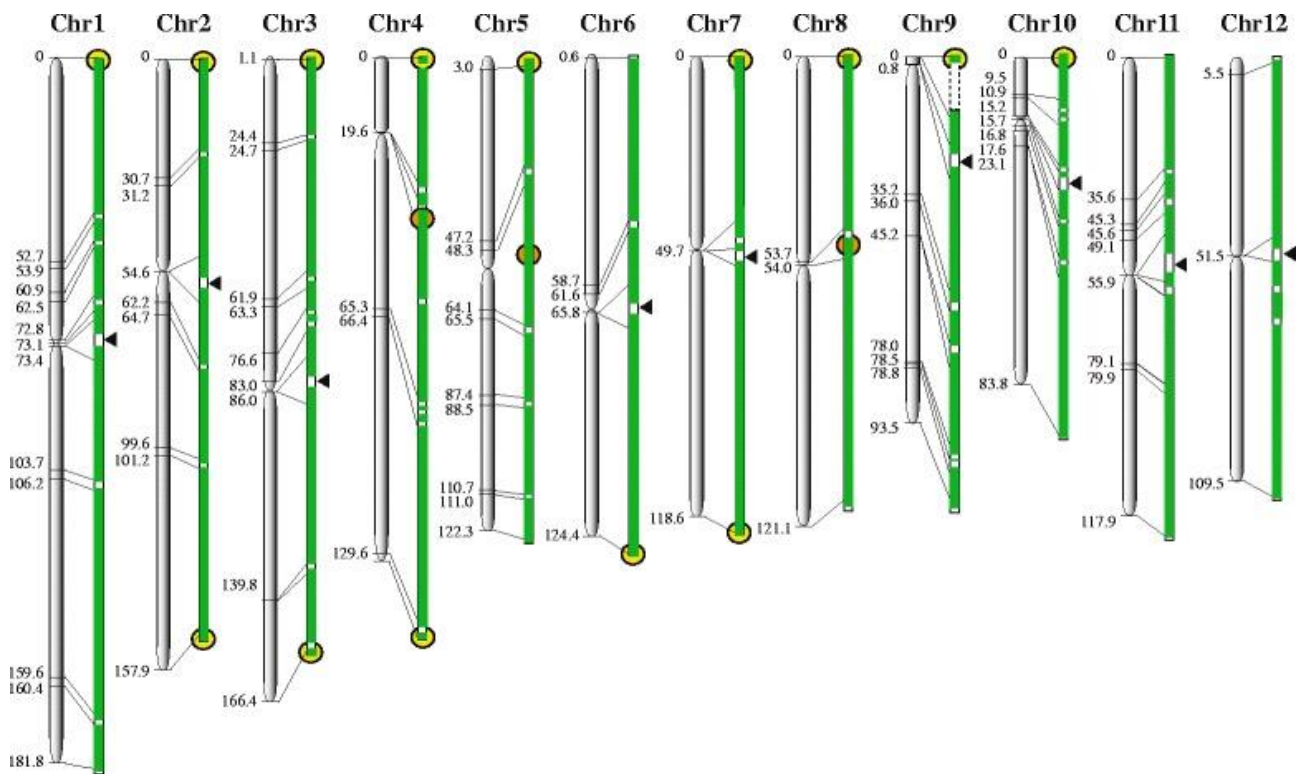
Figure 2. Chromosome organization of rice genome.

1.2. INFLORESCENCE ARCHITECTURE AND DEVELOPMENT

Inflorescence architecture is an important agronomical trait that determines yield in many seed crops and for this reason is a major target for crop domestication and improvement [25]. Crop yield has become a major issue for agriculture because there is a decrease in arable land, the availability of water for plant irrigation is more and more limited and climate change affects negatively yield.

Flowering plants evolved different kinds of inflorescences, which can be grouped into different classes. First, we can group inflorescence architectures into unbranched (simple) and branched (compound). Second, concerning whether the Inflorescence Meristem (IM) ends in a terminal flower or continues to produce structures, including branches and flowers, we can recognise determinate or indeterminate inflorescences, respectively. Therefore, based on these key parameters, we can distinguish at least three groups of inflorescence architectures: the raceme (simple, indeterminate, like in Arabidopsis), the cyme (complex, determinate, for instance, tomato), and the panicle (complex, determinate, like in rice or complex, indeterminate, for instance, maize (*Zea mays)* [26–28] **[Figure 3]**.
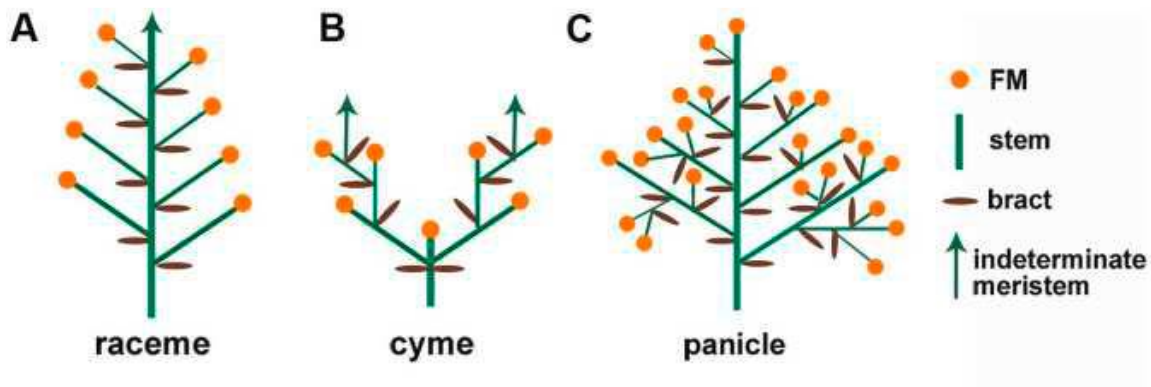
Figure 3. Three main groups of inflorescence architectures.

The three distinct inflorescences result from different developmental programs.

In Arabidopsis, the raceme inflorescence, after the transition from vegetative meristem (Shoot Apical Meristem (SAM)) to reproductive meristem (IM), produces directly on its flanks and in a spiral way the Floral Meristem (FM), the FM is a determinate meristem, that through several developmental stages differentiates the floral organs [**Figure 4**].

In rice, inflorescence development is more complex. After the transition from SAM to IM, the IM gives rise to primary Branch Meristems (pBMs) that elongate and produce secondary Branch Meristems (sBMs), which is another indeterminate meristem. However, the pBM can also directly develop Spikelet Meristems (SM). All sBMs elongate and produce SMs that initiate FMs and differentiate in their turn floral organs, exhausting the pool of meristematic cells **[Figure 4]**.
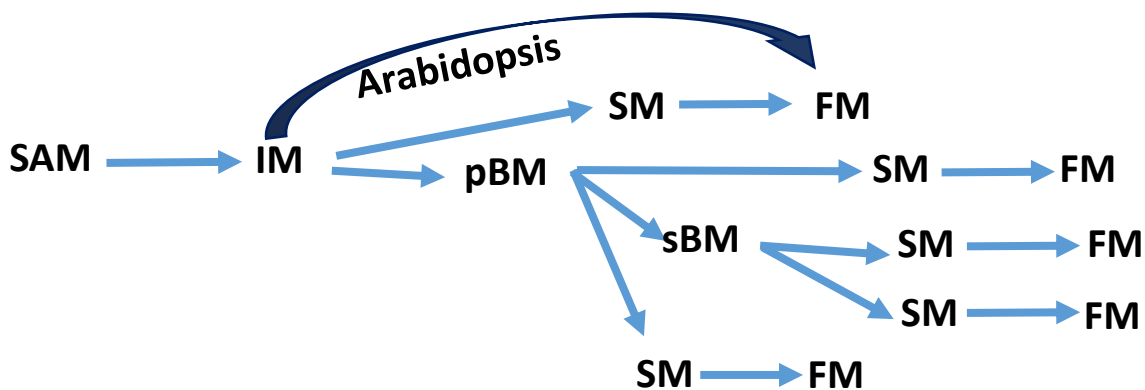
Figure 4. Simplified scheme of inflorescence development in rice and in Arabidopsis (adapted from Han, Yang, & Jiao, 2014[27]**).**

The inflorescence architecture is established during the early stages of reproductive development and it is determined by the activity of different meristem types and by the timing of the transition between indeterminate meristems to determinate ones. The longer the inflorescence meristem retains its undifferentiated state, the more branch meristems or more flower meristems are formed increasing the number of seeds produced by a plant. Furthermore, a prolonged undifferentiated state of meristems influences also meristem size that tends to become larger [27,29–31].

1.2.1 Morphology of Arabidopsis inflorescence

The activity of the SAM determines the architecture of the aerial part of the plant. During the vegetative phase, the SAM produces leaves on its flanks forming the rosette. After the floral transition, the shoot bolts and the SAM becomes the reproductive IM that produces flowers or inflorescence shoots [32]. Arabidopsis develops a main inflorescence shoot, called the primary shoot and also other shoots which arise from secondary meristems located in the axils of cauline or rosette leaves called secondary shoots or lateral shoots respectively.

On the primary shoot, the first nodes generate secondary shoots that bear lateral flowers, subsequent nodes instead bear directly flowers.

The same pattern of development is followed also by secondary shoots which give rise to secondary lateral shoots, called tertiary shoots [33] **[Figure 5A].** In Arabidopsis, each FM produces a single fertile flower [34].

The Arabidopsis flower is organised in four concentric whorls in which arise four different floral organs: sepals, petals, stamens (male reproductive organ) and carpels (female reproductive organ). The four sepals in the first most outer whorl, are leaf-like organs. The 4 petals arise in the second whorl, six stamens with anthers that produce pollen arise from the third whorl and the pistil, composed of two fused carpels, develops from whorl 4 in the center of the flower. The pistil contains ovules and after fertilization, the carpel develops into fruits called silique and the ovules in the ovary develop into seeds [35] **[Figure 5B]**.

A

B

carpels   anthers

petals

sepals

Flower

Tertiary
shoot

Secondary
shoot

Cauline
leaf   Primary
              shoot

Rosette
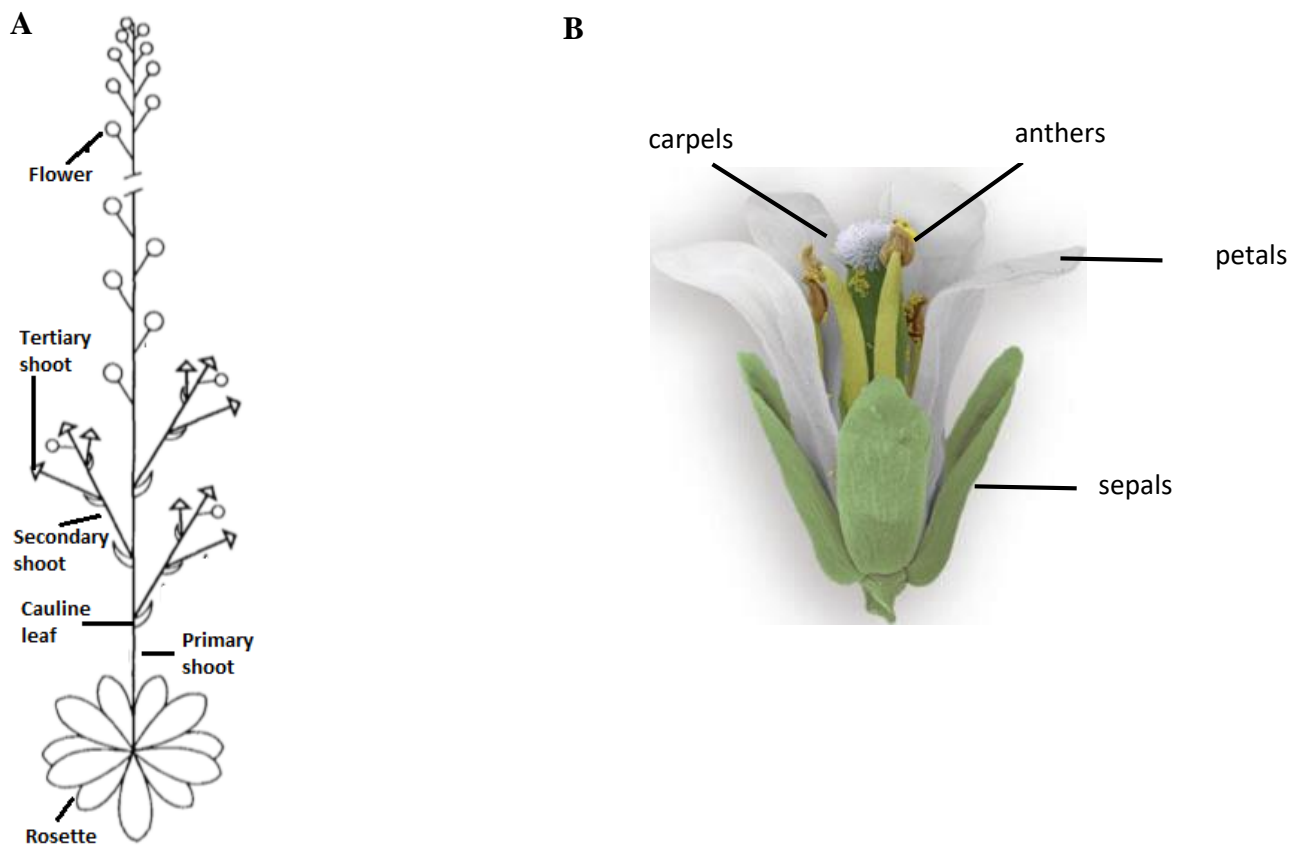
Figure 5A. Aerial part architecture of Arabidopsis thaliana. 5B. Arabidopsis Flower (Adapted by Huijser & Schmid, 2011[32]).

1.2.2 Morphology of the rice inflorescence

The morphology of the rice inflorescence has been described exhaustively by Hoshikawa (1989)[36] and Ikeda et al., (2004) [37]. The main axis is known as rachis, which starts from the upper node of the highest internode. A mature rachis is more or less 18 cm in length and has from 6 to 15 nodes from which the lateral ramification (primary branches) arise. The whole panicle is around 22 cm long. However, depending on rice cultivar, rachis length and consequently panicle length can vary. The length of the internodes is also variable and sometimes from one node more than one primary branch may develop. In the panicle the primary branches vary in length, in particular, they become shorter acropetally. Primary branches follow a spiral phyllotaxy and similar to the rachis they have nodes that give rise to secondary branches. Rarely secondary branches develop tertiary branches from their nodes, but they may develop pedicels or peduncles which terminate in a single spikelet. Secondary branches and spikelets, unlike primary branches, follow a distichous phyllotaxy, with a divergent angle of 110° [37] **[Figure 6A]**.

The rice inflorescence has two different meristem types that follow 2 different fates: the rachis meristem and the branch meristems. Each branch meristem terminates in a flower, whereas the rachis meristem not. Indeed, the rachis produces a certain number of primary branches and then loses its meristem activity and aborts. In the mature inflorescence, at the base of the last developing primary branch, is a small knot like node present, which is the sign of rachis abortion **[Figure 6B]**.

A Spikelet is a basic unit of the rice inflorescence and it is formed by bract-like organs, known as glumes, and by reproductive organs that constitute the androecia and gynaecium of the flower [38]. In rice, each spikelet has a single fertile floret and a couple of sterile rudimentary glumes at the spikelet base. The floret is formed by a couple of fertile glumes, bigger than the previous ones, known as lemma and palea that envelop the internal flower organs and protect them that are considered equivalent to sepals [39]. The lodicules, instead, are small membranous and white floral structures that are equivalent to petals in the second whorl. They are responsible for flower opening at anthesis. More inside, six stamens with respective anthers are developing in the third whorl and in a central 4th whorl there is a pistil with one carpel and a bifid stigma **[Figure 6C]** [37,38].
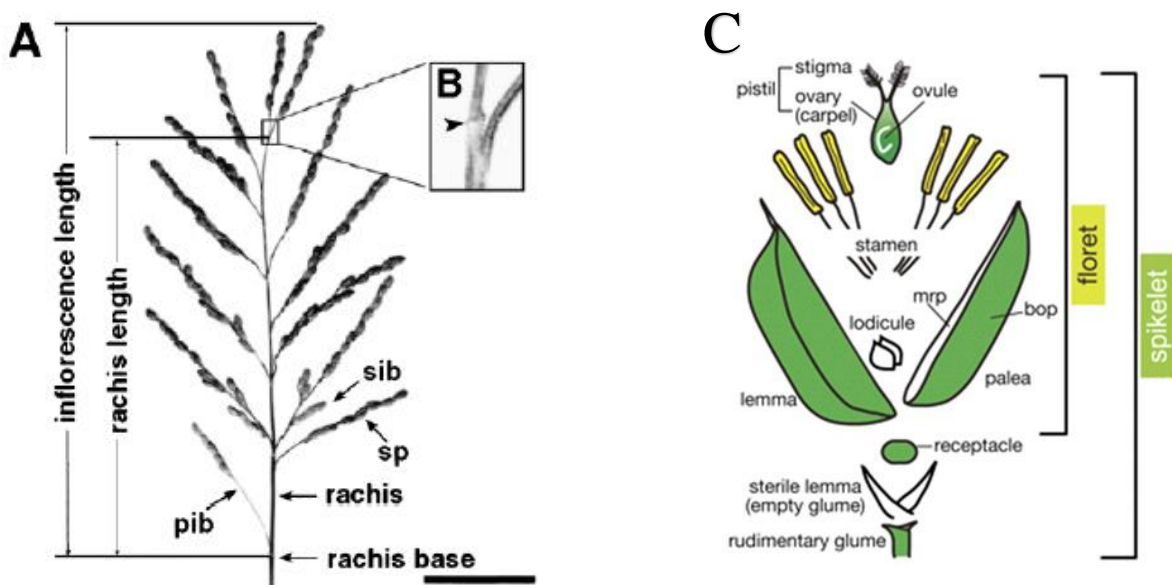
Figure 6A. Rice inflorescence morphology (pib, primary inflorescence branch; sib, secondary inflorescence branch; sp, spikelet). 6B. Vestigial rachis meristem. 6C. Schematic representation of spikelet structure, mrp, marginal region of palea; bop, body of palea.

1.2.3 Floral transition and inflorescence development in Arabidopsis

Inflorescence development is finely regulated by a genetic network that includes meristem identity genes and genes that regulate their expression. Endogenous and exogenous inputs trigger the switch from vegetative to inflorescence meristem, the flowering time [40]. This comprises the formation of FLAVIN BINDING KELCH REPEAT F-BOX PROTEIN 1 (FKF1) and GIGANTEA (GI) containing protein complex [41] that targets CYCLING DOF FACTORs (CDFs), for proteasome-mediated degradation. *CDFs* encode transcriptional repressors that regulate the activities of *CONSTANTS* (*CO*), a gene that encodes a zinc finger transcription factor; accumulation of CO leads to *FLOWERING LOCUS T* (*FT*) expression, a gene that encodes a "florigen" protein [42–45] **[Figure 7].** FT moves from the leaves to the SAM, through the phloem, and together with its partner FD, triggers the activation of the transcription factor *SUPPRESSOR OF OVEREXPRESSION OF CONSTANS1 (SOC1)* and induce flowering [46,47].
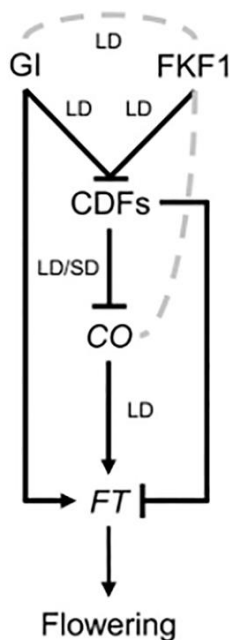
Figure 7. Flowering time scheme in Arabidopsis; LD, Long Day; SD, Short Day; GI, Gigantea; FKF1, Flavin Binding Kelch Repeat F-Box Protein 1; CDFs, Cycling Dof Factors; CO, Constants*;* FT, Flowering Locus T.

SOC1 and the *FT/FD* complex determine inflorescence meristem identity, inducing the expression of the floral meristem identity genes *LEAFY* (*LFY*) and *APETALA1* (*AP1*) in the cells that will give rise to the floral meristem (FM) [48–50]. SOC1 bind directly the *LFY* promoter, rich in cis-regulatory elements.

LEAFY (LFY), APETALA1 (AP1) together with *TERMINATING FLOWER1 (TFL1)* are three major regulators of IM- FM transition. *LFY* and *AP1* establish the FM meristem identity whereas *TFL1*, which is expressed in the IM, prevents FM identity.

LFY encodes plant-specific transcription factor and it is strongly expressed at very early stages of FM development [51]. *LFY* expression is activated by flowering time genes such as *SVP, AGL24* and *SOC1* but it also promoted by MONOPTEROS (MP), an auxin response factor that in absence of auxin, is inactivated by its interaction with BODENLOS (BDL), but in presence of auxin, which cause BDL degradation, cause *LFY* upregulation [52].

The *lfy* mutant shows structures with shoot characteristics instead of flowers [33,53]. Moreover, when *LFY* is constitutively expressed, the plant shows an early conversion of all shoots into flowers, indicating that *LFY* is both necessary and sufficient for the FM differentiation and strictly related to the timing of floral transition [54].

LFY regulates flower development by regulating *AP1* expression, which activates the transcription of several genes implied in flower determination and by acting with the auxin carriers, in particular with *PIN-FORMED1 (PIN1),* to promote primordium development. *lfy pin1* double mutant shows more defects in floral primordium formation compare to *pin1* single mutants [55,56]. Furthermore, LFY at floral stage 1 first activates *LATE MERISTEM IDENTITY1* (*LMI1*) and, in combination with LMI1, up-regulates the expression of the MADS-box gene *CAULIFLOWER (CAL)* [57]. CAL and LFY, partially in combination with LMI2, activate *AP1* expression [58–60] that in turn binds LFY regulatory region to form a positive feedback loop [50,61]. *AP1* is a MADS-box gene, expressed in the young FMs and later in sepals and petals. The *AP1* expression pattern follows *LFY*, but is slightly delayed [62]. However, *AP1* expression is not regulated entirely by LFY since in *lfy* mutant it is expressed [63], there are indeed other factors involved in *AP1* upregulation such as *LATE MERISTEM IDENTITY2 (LMI2), AGAMOUS-LIKE24 (AGL24)* and *SHORT VEGETATIVE PHASE (SVP)* [59,64]. In an *ap1* loss of function mutant meristems that would normally develop into flowers are partly converted in a shoot-like structure [65,66] whereas constitutive expression of *AP1* under the *CaMV 35S* promoter, as *LFY* overexpression line, causes early flowering shoots, a phenotype similar to the *tfl* mutant. The shoot apex meristem indeed terminates prematurely as floral meristem producing terminal flower and also all lateral meristems were converted into a single flower instead of producing inflorescence shoots [67]. The *ap1 lfy* double mutant shows a more severe phenotype compare to the two single mutants, suggesting that *AP1* and *LFY* act redundantly in FM identity specification [51]. At the same time, *LFY* and *AP1* regulate also the expression of negative flowering regulators. AP1 suppresses the expression of *TERMINAL FLOWER1 (TFL1), TARGET OF EAT1 (TOE1), TOE3, TEMPRANILLO1 (TEM1)* and *TEM2* (two important inhibitors of the FM identity gene *FLOWERING LOCUS T)* [50,68], while LFY suppresses only expression of *TFL1, TOE3* and *TEM1* [60,69].

CAL activates with LFY, *AP1* expression but is also partially redundant with AP1. The *cal* mutant has a WT phenotype but in the *cal ap1* double mutant the "FMs" that develop on the flanks of the IM

does not acquire FM identity and maintain IM identity. On these secondary IMs, the process repeats and new IMs develop, this process is the end result in the formation of enormous amounts of proliferating IM meristems forming a cauliflower-like curd [66,67]. The shape of a fully develop *ap1 cal* mutant, similar to a cauliflower, gives the name to the gene.

AP1 shares also high homology with another MADS-box gene, *FRUITFULL (FUL)* [70]. *FUL* is a transcription factor previously demonstrated to be involved in fruit development [71]. It also plays a role during the floral transition [67,72]. *FUL* is closely related to the meristem identity genes *AP1* and *CAL*. [73]. *FUL* and *AP1* proteins are expressed in mutually exclusive domains, *FUL* expression starts in the early phases of IM development and decreases while *AP1* expression increases during flower development [74]. Interestingly, promoter-swap experiments proved that they can substitute each other, confirming a similar molecular function [75]. In addition, the triple mutant *ful ap1 cal* shows a dramatic non-flowering phenotype where leaves are continuously produced in place of flowers [73], indicating a molecular function with CAL as well. Furthermore, they also observed that overexpression of *LFY* in triple mutant partially restore flowering phenotype suggesting that these genes act redundantly in boosting LFY expression and that other factors are able to induce LFY expression initially. Several MADS-box genes, like *AP1*, *SOC1, FUL, AGAMOUS-LIKE24 (AGL24)* and *SHORT VEGETATIVE PHASE (SVP)*, are involved in the timing of the floral transition. The *svp* mutant shows an early flower phenotype whereas the *agl24* mutant shows a late flowering phenotype indicating their action as respectively repressor and promoter of flowering time [76–78]. SVP indeed is able to directly repress the expression of *FT* and *SOC1* [79], whereas AGL24 together with SOC1 directly activates *LFY* expression [80]. *LFY* and *AP1* are repressors of *AGL24* and *SVP* in a negative-feedback loop. The *agl24 svp lfy* triple mutant enhances the *lfy* phenotype and is a phenocopy of *lfy ap1* [64]. The *ap1 agl24 svp* triple mutant continuously produces inflorescence meristems instead of flowers in a "cauliflower" shape, similar to *ap1 cal1* double mutants. *AP1*, *AGL24* and *SVP* act redundantly to maintain FM in undifferentiated state at first stages preventing the precocious activation of floral homeotic genes, in particular they directly repress Arabidopsis class B-C floral homeotic genes [81]. Furthermore, AGL24 and SVP repress SOC1 during stages 1 and 2. SOC1 normally doesn't play a role during the early stages of development, it starts to be expressed in flowers at stage 3 when floral organs start to develop; interestingly, its expression is found at stage 1 and 2 in the *agl24 svp* mutant background [81]. Liu et al., (2008) demonstrated by Chip analysis that AGL24 and SOC1 act in a positive-feedback loop when they activate each other, binding each other regulatory region.

Recently, it is also demonstrated that also *miR156* is involved in regulation of floral transition, by regulation of *SQUAMOSA PROMOTER BINDING PROTEIN-LIKE SPL3, SPL4* and *SPL5* expression. These genes indeed function with FT-FD to activate directly *AP1, LFY* and *FUL* [83–85].

Furthermore, Lal et al., 2011[86] demonstrated that also two genes belong to *BELL1* family, *PENNYWISE* and *POUND-FOOLISH* contribute to meristem maintenance and flowering [87]. PNY-PNF works together with FT-FD and with AGL24-SOC1 to promote flower development. In addition, they also promote the expression of *SPL3, SPL4,* and *SPL5* that directly activate FMI genes in parallel with FT-FD [86]. Compatible with this, miR156 is up-regulated in *pny pnf* apices and ectopic expression of *SPL4* in *pny pnf* restores accumulation of *LFY* and *AP1* transcripts and partially restores flower formation [86].

TERMINAL FLOWER1 (TFL1), belongs to the phosphatidylethanolamine binding protein *(PEBP)* family present in all eukaryote kingdoms. This family gene acts in the signalling pathway that controls growth and differentiation but acts also in transition from the vegetative to the reproductive phase and in the determination of plant architecture [88]. *TFL* is responsible for IM identity maintenance. The *tfl* mutant shows a similar phenotype *AP1* overexpression line: early conversion of all shoot meristems in FMs with cauline that subtend flowers and IMs converted into terminal flowers [89,90]. On the other hand, *35S::TFL1* transgenic lines show a strong delay in development, slowing down the rate of progression of the shoot apex [91]. *TFL1* plays a role in flowering time, repressing gene activated by *FT,* like *LFY* and *AP1* [92]that in the *tfl* mutant, indeed, result expressed in IM [51,93]. *TFL1* and *FLOWERING LOCUS T (FT)* belong to the same family; they are very similar in sequence, in structure but they have an opposite function; they differ for only 39 non-conservative residues [94,95].

Meristem identity is also related to hormonal levels; cytokinins and auxins have opposite functions: cytokinins promote an undifferentiated state of the meristem whereas auxin leads to phase change and specification of meristematic tissues. Gibberellins promote floral transition as well [96]. A lower level of gibberellins led to a premature FM differentiation [97]. Genes involved in the cytokinin pathway are key regulators of the inflorescence architecture. There is a relationship between meristem size and cytokinin levels, a higher concentration of the hormone leads to a bigger meristem, while a lower level of CK led to a smaller meristem [98–100]. *LONELY GUY (LOG)* genes encode cytokinin riboside 5'-monophosphate phosphoribohydrolases, enzymes involved in cytokinin biosynthesis. In Arabidopsis, the *LOG* family counts 9 members with high sequence similarity. Septuple T-DNA insertion mutants have defects in the maintenance of shoot apical meristems and *LOG7* has a central role in the regulation of meristem size [31,101]. *AP1* regulate cytokinin level by directly silencing *LOG1* and activating *CYTOKININ OXIDASE/DEHYDROGENASE3 (CKX3)*, to lower cytokinin levels and trigger FM differentiation [102,103]. *CKX* genes control cytokinin concentration: overexpression of *CKX1* or *CKX2* leads to the production of fewer flowers [104], while the *ckx3 ckx5* double mutant is characterized by a strong delay in development, bigger meristems and consequently larger inflorescences.

Also AHK histidine-kinases cytokinin receptors have an important role in inflorescence development. The single mutant doesn't show an obvious phenotype, the multiple mutants instead show strong growth defects due to a slower meristematic activity [105]. In particular, *ahk2 ahk3 ahk4* triple mutants have smaller meristems that terminate very early and produce fewer flowers than the WT. A schematic representation of a regulatory network controlling IM and FM development is shown in **[Figure 8].**
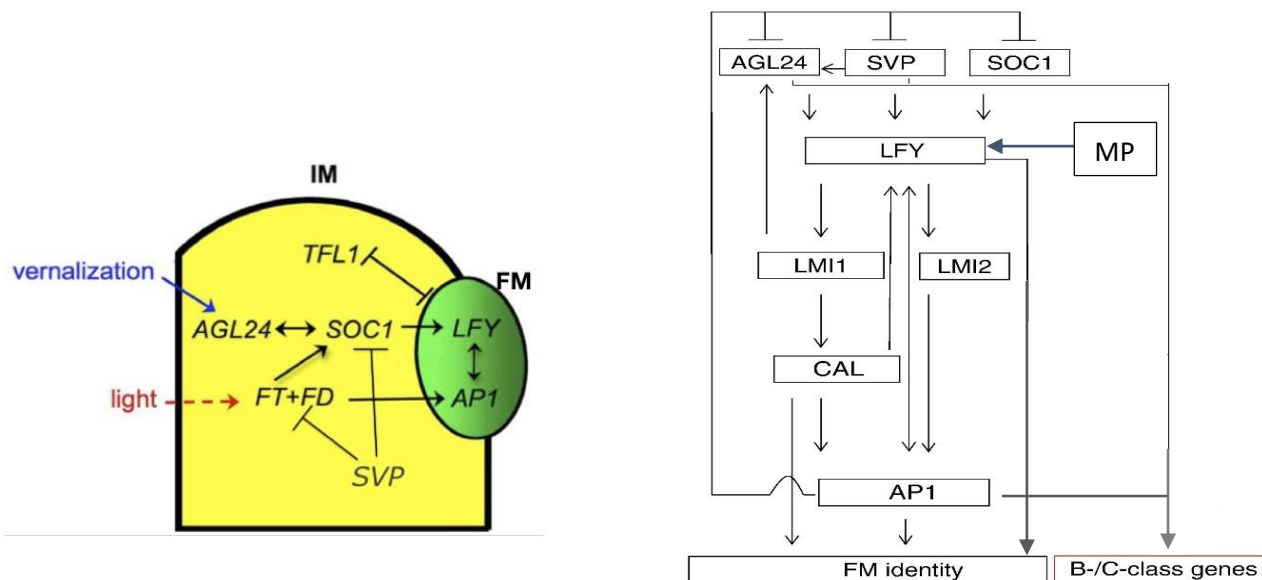
Figure 8. Images adapted from Alvarez-Buylla, 2010 [34] and Wils et al., (2017)[48] showing , schematically, exogenous input, like vernalization and light, and regulatory network that control IM and FM development in Arabidopsis.

1.2.4 Floral transition and inflorescence development in rice

In rice, the regulatory pathways that regulate flowering, under short day and long day conditions are more complex than in Arabidopsis due to the presence of several genes involved in heading date unique in rice, not present in Arabidopsis [42,106]. The homolog of Arabidopsis *CO* in rice is *Heading date 1* (*Hd1*). *Hd1* is regulated by *OsGI* and activates the expression of *Hd3a*, an orthologue of *Arabidopsis FT*, which triggers flowering in SD. *Hd3a* is suppressed in LD condition [107,108] **[Figure 9]**. There is an alternative and independent pathway of the Hd1 pathway, whose main player is *EARLY HEADING DATE 1* (*Ehd1*), unique to rice and having no counterpart in *Arabidopsis*. It encodes a B-type response regulator and activates the expression of *RICE FLOWERING LOCUS T1* (*RFT1*), and *Hd3a* [109] respectively in LD and SD. In response to an increase in day length above 13.5h *Hd3a* expression result low in "Norin8", a *japonica* rice (*Oryza sativa*), while expression of *RFT1* is less affected [110]. Geographic distribution and sequence variation indicates that *RFT1* functional alleles were selected in the process for adaptation to regions with high latitude and SD length [111]. Several factors are involved in a regulation of *Ehd1* expression, some of them act as repressors of *Ehd1*, such

as *Heme Activator Protein like 1* (*OsHAPL1*) [112], *Grain number, plant height and heading date 7* (*Ghd7*) [113], *Pseudo-response regulator 7-like or Heading date 2 (PRR37 or Hd2), Days To Heading on chromosome 8 (DTH8/Ghd8/OsHAP3H)* [113,114], *OsCOL4* [115] and *OsCOL10* [116]; other genes such as *Rice Indeterminate1* (*RID1*)/*Early heading date 2* (*Ehd2*) [117,118], *Early heading date 3 (Ehd3), Early heading date 4 (Ehd4)* [119,120] and *OsMADS51* [121] instead positively regulate its expression. Perhaps, several flowering pathways and multiple gene interactions lead to targeting *Hd3a* and *RFT1*, which encode florigen proteins that move from leaves to the shoot apical meristem (SAM) through the phloem and play a key role in reprogramming of meristem identity and floral transition [122]. Hd3a forms a complex with an intracellular receptor 14-3-3 that links OsFD1, a bZIP transcription factor, to Hd3a and form the florigen activation complex (FAC) in the SAM, which activates the transcription of the downstream target genes *OsMADS14* and *OsMADS15*. These two genes belong to *AP1/FUL* family, a subgroup of the *MADS-box* gene family [123] and together with *OsMADS18*, another member of this family, and *PAP2*, a SEPALLATA subfamily MADS-box gene acts co-ordinately in the specification of IM identity downstream of the florigen signal [124].

Transcriptomic analysis of meristem phase transition from SAM to IM revealed these four genes show overlapping expression patterns. The *PAP2* loss of function mutant (*pap2-1*) doesn't show any phenotype at early inflorescence developmental stages, however, suppression of *OsMADS14*, *OsMADS15*, and *OsMADS18*, by RNAi, in a *pap2-1* background, resulted in a delay of phase transition from SAM to IM with a production of multiple shoots instead of inflorescences. This indicates that these genes promote IM identity [124].
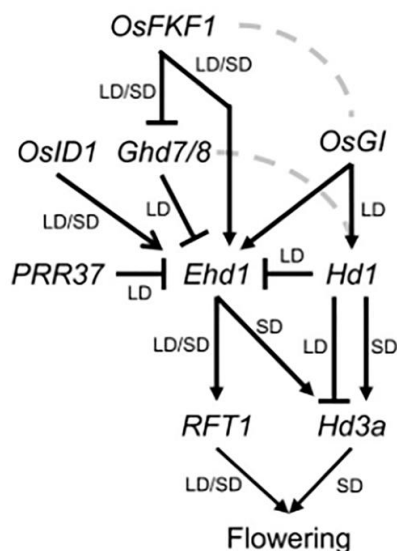
Figure 9. A schematic representation of genetic network controlling photoperiodic flowering in Rice [42]. **LD, Long Day; SD, Short Day.**

Several genes are involved in determination of inflorescence architecture; some of them are regulator of axillary meristem, others are involved in spikelet o flower meristem identity and development.

MONOCULM1 (MOC1) and *LAX PANICLE1 (LAX1)* genes that encode a transcription factor are involved in axillary meristems (AMs) formation [125].

MONOCULM1 (MOC1), an orthologue of *LATERAL SUPPRESSOR (LAS)* in *A. thaliana,* belongs to GRAS (GAI, RGA and SCR) family genes and its expression is confined in axillary buds [126]. *MOC1* controls the initiation of (AMs) during the vegetative and reproductive phases promoting respectively culm and branches formation [125,127]. The *moc1* mutant loses its capability to form culms and shows a monoculm panicle [127]. Furthermore, *MOC1* regulates expression of *Oryza sativa homeobox 1* (*OSH1*) e *TEOSINTE BRANCHED1 (OsTB1),* genes that play a role respectively in initiation/maintenance of IM/BMs and in regulation of AMs growth [126]. The *osh1* mutant has a smaller inflorescence and a decreased number of spikelets [128] The *OsTB1* overexpression line is affected in the propagation of axillary buds and exhibits a reduction in lateral branching [129,130].

LAX1 encodes a basic helix-loop-helix (bHLH) protein and it is expressed where the AM develops [125,127]. *LAX1* is necessary for branch formation and for spikelet meristem specification. The *lax1* K.O mutant is impaired in branches and spikelets formation due to the indeterminate growth of rachis and branch meristem [127,131]. There is another gene, *SMALL PANICLE (SPA),* involved in AM initiation; even mild *lax* alleles in combination with *spa* show dramatic defects in AM formation [132].

Deshpande et al., (2015)[133] demonstrated that the *RFL (RICE FLORICAULA/LEAFY)/ABERRANT PANICLE 2 (APO2)* gene, an orthologue of Arabidopsis *LFY,* regulates *LAX1* e *CUC* during AMs specification, promoting AM development via auxin transport. The *rfl/apo2* knockdown mutant shows defects in AM specification and also reduced expression of auxin transporter genes in the culm. *RFL/APO2* encodes for a transcription factor and together with *ABERRANT PANICLE 1 (APO1),* an orthologue of Arabidopsis *UFO (Unusual Floral Organization)* [30], are mainly expressed in IM and in BMs, where they promote cellular proliferation. They play also a role in the transition from BMs to SMs, suppressing an early conversion [30,134]. The two *apo1* and *apo2* mutants show an early conversion of IM/BM in SM and hence smaller panicles with fewer branches compared to WT [30,38,134–136]. The gain of function mutant instead shows an opposite phenotype [30,38,137].

Another key regulator of the transition from indeterminate to determinate meristem is *TAWAWA1 (TAW1)*. *It* belongs to the ALOG (*Arabidopsis* LSH1 and *Oryza* G1) family genes and encodes a nuclear protein containing an uncharacterized DUF640 domain or ALOG domain, which is conserved in all land plants.

TAW1 shows high expression in the SAM and in reproductive meristems; it promotes BM maintenance and at the same time suppresses SM specification by activating genes involved in

repression of floral transition. In the dominant gain of function mutant *tawawa1-D* three genes, *OsMADS22*, *OsMADS47*, and *OsMADS55* belongs to *SVP* subfamily of MADS-box genes are highly up-regulated while spikelet identity genes, such as *OsMADS7* (*SEP3*), *OsMADS8* (*SEP3*), *OsMADS16* (*AP3*), *OsMADS4* (*PI*), *OsMADS3* (*AG*), and *OsMADS58* (*AG*) show a reduced expression [5].

Tawawa1-D is characterized by an extended indeterminate meristem activity and by delay in SM specification, resulting in panicles with more secondary and tertiary inflorescence branches and more spikelets; opposite phenotype is observed in mutant that shows a reduction in *TAW1* expression: small panicles with fewer branches. When the SVP gene *OsMADS22*, *OsMADS47* or *OsMADS55* are constitutive expressed by the cauliflower mosaic virus (CaMV) 35S promoter an increase in inflorescence branching is observed. These results suggest that *TAW1* suppresses the acquisition of SM identity through the induction of *SVP* genes, which consequently, promote or prolong BM identity.

FRIZZY PANICLE (FZP) encodes an APETALA2/ETHYLENE RESPONSE FACTOR (AP2/ERF) protein which is expressed at the boundaries of rudimentary glumes during differentiation.

In *fzp1* mutant, floret formation is arrested and several branches are produced instead of spikelets [131,132]. *fzp2* shows a similar phenotype; the *lax1 fzp2* double mutant is unable to form spikelets and doesn't develop SBs, but forms new meristems in the axis of lateral bracts, growing PBs in a zigzag shape [131]. The orthologues of *Arabidopsis TFL1, Oryza sativa RICE CENTRORADIALIS (RCN)*, conserves the same function in rice [138]. There are four *RCN* genes in rice, mainly expressed in the vasculature and then transported to the inflorescence where they act as regulators [139]. Overexpression of *RCN1* or *RCN2* leads to a delay in flowering time resulting in a more branched panicle [38,138,140]. As already observed for *TFL1 Arabidopsis*, *RCNs* conserve the function as *FT* repressors [139]. We can observe the *RCNs* phenotypes also when specific *OsMADS* genes like *OsMADS50* and *OsMADS56* (the orthologues of Arabidopsis *SOC1*) or *OsMADS22*, *OsMADS47* and *OsMADS55* (orthologues of Arabidopsis SVP and AGL24) are downregulated [141]. This observation indicates that these genes in rice, as well as their orthologues in Arabidopsis, regulate panicle branching by suppressing *RCNs* genes [142].

Last but not least, *PAP2* already mentioned to be involved in IM promotion is also a strong candidate for SM identity as well as floral organ identity. The *pap2* mutant shows floral organ homeotic transformations but more intriguing show branching and spikelet phenotypes. It produces more highly branched bearing spikelets with more leaf-like glumes (occasionally with axillary branches) in addition to leaf-like palea. A highly branching phenotype is caused by an inability to establish SM identity. Therefore, meristems continue as indeterminate BMs, and when SMs are eventually formed,

they are incapable of producing organs of the correct identity. Furthermore, unlike *FZP, PAP2* is expressed in the meristem proper, with expression increasing as the meristems acquire SM identity. Thus both the expression and phenotype of *pap2* suggest its role in SM identity specification [143].

SQUAMOSA PROMOTER BINDING PROTEIN-LIKE14 (OsSPL14) encodes a transcription factor that belongs to the *WEALTHY FARMER'S PANICLE (WFP)* locus, involved in panicle branching and tiller number [144]. Overexpression line of *OsSPL14* shows a reduction in tiller number, more resistant to lodging and with more branches. *OsSPL14* promotes the indeterminate branch phase, delaying the transition to SM identity. It is expressed in SAM, IM and BMs and its expression is post-transcriptionally regulated by *OsmiR156*. A single point mutation in the *OsmiR156* target site leads to increased branching [144,145].

Dense e Erect Panicle1 (DEP1) is a QTL that encodes an unknown protein characterized by the presence of the Phosphatidylethanolamine-Binding Protein (PEBP) domain. It is a positive regulator of panicle branching as it promotes cellular proliferation and meristematic activity [146,147].

SUPERNUMERARY BRACT (*SNB*) and *INDETERMINATE SPIKELET-1* (*OsIDS1*) are two genes belong to AP2 family genes, functionally associated that control FM specification.

Compared to the *snb* mutant, the *snb osids1* double mutant shows a further delay in FM transition and the mutants exhibit fewer inflorescence branches and spikelet numbers [148]. A similar phenotype is observed when the microRNA *OsmiR172* was overexpressed [148,149]. This indicates that *miR172* is involved in the regulation of *IDS1-like* genes in rice. Furthermore, either *IDS* or *SNB* genes are positively regulated by *MULTI-FLORET SPIKELET 1* (*MFS1*), another member of the AP2/ERF family, expressed, in turn, in the spikelet and floral meristems. It regulates SM fate and determines FM identity. In *mfs1* mutants, the transition to FM is suppressed and identity of floral organs is altered. *MFS1* positively regulates also *G1/ELONGATED EMPTY GLUME* (*ELE*), a member of the ALOG family, which specifies sterile lemma identity [150].

In rice, as well as Arabidopsis, the phytohormones Auxin and Cytokinin play a very important role in inflorescence development. Auxin is involved in axillary meristem initiation [151]. Many genes involved in the auxin biosynthesis, transport and signalling pathways have been identified. Mutations in these genes affect axillary meristem initiation and outgrowth and resulted in reduced inflorescence branching.

In rice, seven YUCCA (*OsYUCCA1-7*) genes have been identified, in particular, *OsYUCCA-1* has a key role in IAA biosynthesis. Constitutive expression of *OsYUCCA-1* resulted in increased levels of IAA and plants displayed characteristic phenotypes similar to auxin overproduction [152].

Auxin transport during inflorescence development is mediated through phosphorylation of *OsPIN1* and its homologous (auxin efflux carrier) by *OsPID/OsBIF2,* an Arabidopsis orthologue of *PINOID (PID)* that encode Ser/Thr protein kinase [153–156].

ABERRANT SPIKELET AND PANICLE 1 (*ASP1*) a homolog of *TOPLESS* (*TPL*), a transcriptional corepressor in Arabidopsis, plays a role in auxin-related inflorescence development. The *asp1* mutant produces fewer inflorescence branches and flowers, similar to auxin-related pleiotropic defects [157]. Yoshida et al., (2012) [157] proposed a putative link between *ASP1* function and the auxin response although the exact function of *ASP1* in auxin signalling has not been clearly demonstrated yet.

Cytokinin plays a role in the regulation of inflorescence architecture and meristem function. Cks promote cellular divisions and meristem size [27,158].

The *LONELY GUY* (*LOG1*) gene, specifically expressed in the apical and axillary meristems, is involved in cytokinin biosynthesis, it encodes a cytokinin-activating enzyme that catalyses the final step in the bioactivation pathway. This gene is required for the continuous function of meristems during inflorescence development [31]. A *LOG* homolog, *LONELY GUY LIKE PROTEIN6* (*OsLOGL6*) or *An-2* gene, is shown to promote awn length by increasing the level of endogenous cytokinin [159].

Gn1a, known also as *CYTOKININOXIDASE/DEHYDROGENASE (OsCKX2)*, encodes an enzyme involved in cytokinin degradation [160]. A mutant with low expression of *OsCKX2* leads to increased levels of cytokinin in reproductive meristems and hence a higher yield of plants with more branches and more grains. In contrast, mutants with a high level of CKX2 showed an opposite phenotype: panicles with fewer branches and hence with less yield [13]. Type-A response regulators (ARRs) instead are genes involved in cytokinin signalling such as *OsRR1, OsRR4, OsRR6, OsRR9* and *OsRR10*. Overexpression of these genes alters plant morphology [161].

Recently, a new gene that encodes a cytochrome P450 protein involved in BRs biosynthesis has been identified: *PANICLE MORPHOLOGY MUTANT* (*PMM1*). *pmm1* mutant shows strong morphological defects in panicle architecture: clustered primary branching, opposite grains, and small grains [162]. This means that also BRs are involved in inflorescence architecture.

A list of genes involved in inflorescence development is reassumed in **Figure 10**.
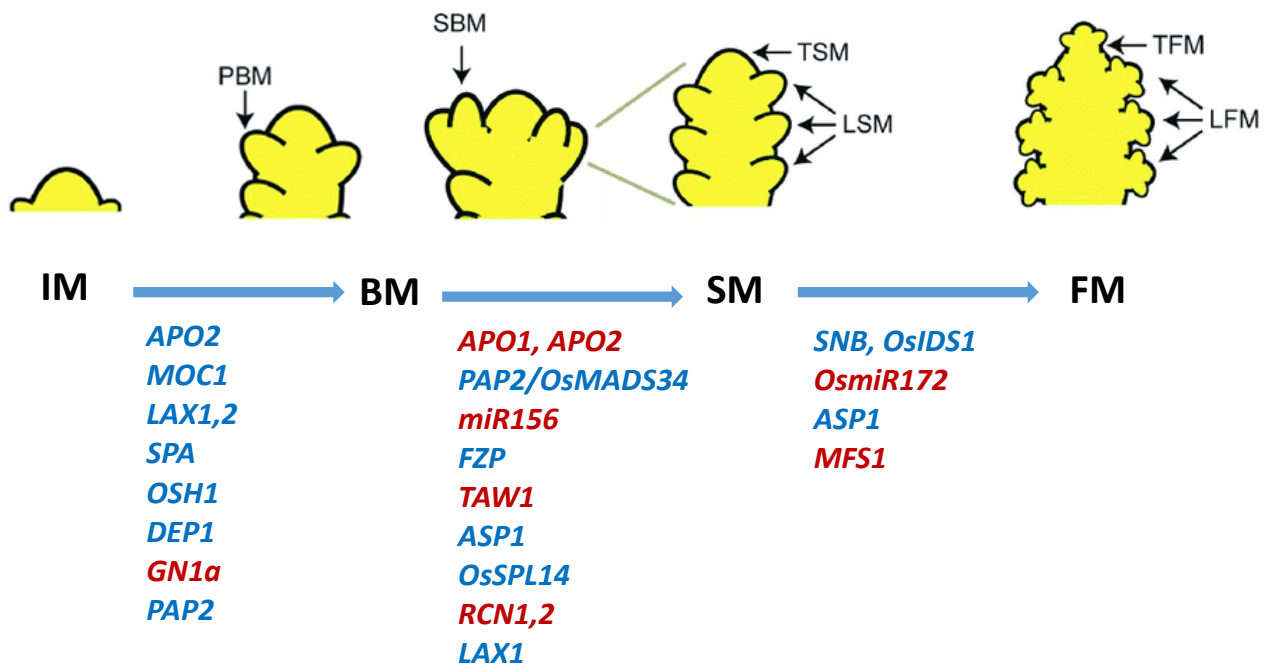
Figure 10. A Schematic representation of genes involved in different meristems transition during inflorescence development. IM, inflorescence Meristem; BM, branches meristem; PBM, primary branch meristem; SBM, secondary branch meristem; SM, spikelet meristem; TSM and LSM, terminal and lateral spikelet meristem; FM, floral meristem; TFM and LFM, terminal and later meristem (adapted from Yamburenko et al., 2017 [163] **) Genes that promote Meristem transition are written in Blue whereas genes that Inhibit the meristem transition are written in red.**

1.3. ALOG FAMILY GENES

ALOG genes [6,164] form a family of eukaryotic putative transcription factors that encode nuclear proteins. They have a predicted Nuclear Localization Signal (NLS), KKRKR, and a conserved DUF640 domain, considered a putative DNA Binding Domains (DBDs) since it is thought to be derived from the XerC/D like recombinases of a novel class of DIRS-1-like retroposons [165]. However, the DNA-binding specificity and mechanism of action are still unclear.

ALOG stands for **A**rabidopsis **L**SH1 **O**ryza **G**1, the first members that have been identified in Arabidopsis and in rice and that gave the name to the other members of this family in the respective species. The ALOG genes count 10 members in Arabidopsis, also known as *LIGHT-DEPENDENT SHORT HYPOCOTYLS (LSH)/ ORGAN BOUNDARY (OBO)* genes, and 14 members in rice [166] also known as *G1 like* genes.

LSH1 plays a role in the regulation of hypocotyl length. *35S::LSH1* transgenic plants are hypersensitive to continuous red, far red and blue light and show a very short hypocotyl compared to WT [164]. The 35S::*GUS-LSH1* line shows expression in the hypocotyl, shoot apices and lateral root primordia while the fluorescent protein LSH1-GFP resulted to be nuclear localised [164].

LSH3 and *LSH4* are the other two *ALOG* genes characterized in Arabidopsis [3,4]. These genes are phylogenetically close to each other and they are a direct target of CUP SHAPED COTYLEDON1

27

(CUC1). They are specifically expressed in the boundary region between the SAM and lateral organs. Gain-of-function mutants of both genes develop flowers with increased numbers of sepals, flowers with extra floral organs or chimeric floral organs with identities of sepal and petal, or of petal and stamen and ectopic meristem formation [3,4]. *lsh3 RNAi* lines and the *lsh1-4 T-DNA* insertion mutant didn't show any phenotypical defects, maybe due to redundancy with other ALOG genes. The experimental data so far obtained suggests that they play a role in meristem maintenance and organogenesis.

The phenotype emerging from *LSH3* and *LSH4* overexpression is similar to *ufo* KO mutants, indicating that these genes might share the same pathway.

It is already known that *LSH4* is repressed by *REPLUMLESS (RPL)*, a gene that controls the morphogenesis of the Rib Zone (RZ) [167]. The *rpl* mutant has defects in stem elongation and fruit development because it fails to orient the growth of the cells in the RZ tissue correctly. By ChIP-seq analysis with a specific antibody that binds the GFP on *pRPL::RPL-GFP* lines, *LSH4* came out as one of RPL targets [168]. They also demonstrated that *lsh4* mutation can revert the *rpl* phenotype, restoring directional growth in the RZ and a normal stem elongation, concluding that *RPL* controls the stem elongation in the RZ by repressing *LSH4* [168].

LONG STERILE LEMMA G1 (G1), is a homeotic rice gene involved in the specification of sterile lemma in spikelets by repressing lemma identity [6]. In WT rice spikelets the sterile lemma is much smaller than the lemma and is attached to its base. In recessive mutant *g1-1*, instead, the sterile lemma enlarges and acquires lemma identity [6].

TRIANGULAR HULL1 (TH1) is a rice ALOG gene that regulates spikelet formation [169,170]. The *th1* mutant shows a narrower lemma and palea than WT even if in the *th1 g1* double mutant there is any detectable effect [170]. The TH1 protein forms a homodimer that localizes in the nucleus where it acts as a transcriptional repressor. When the dimerization is hampered the lemma and palea become narrower, especially in the apical region, resulting in a "beak-shape" [169].

As already mentioned *TAW1*, is fundamental for a correct panicle development and architecture: by keeping the branch meristem identity from progressing to Spikelet Meristem it allows a proper panicle development and hence a proper number of branches before meristem determination [5].

TERMINATING FLOWER (TMF) is the tomato orthologue of *TAW1* and has been shown to have a similar function. It is expressed in the shoot apex and in the vegetative stages of the Primary Shoot Meristem (PSM); The *tmf loss-of-function* mutant is early flowering and shows flowers with leaf-like sepals and a primary SAMs that generate a single flower instead of producing a sympodial inflorescence. Moreover, when *TMF* is expressed under *CaMV 35S* promoter, inflorescences display

a gain-of-function phenotype with ectopic leave formation, reversion to vegetative meristem and more branches [171].

TMF downregulates *ANANTHA (AN)*, *FALSIFLORA (FA)* and *MACROCALYX (MC)* [171], the tomato orthologues of *Arabidopsis UFO*, *LFY* and *AP1,* the major players in the FM identity acquisition and maintenance [53,66,172]. The qRT-PCR expression analysis performed in *tmf* mutant by MacAlister et al., (2012) on these genes and on different meristematic stages, Early Vegetative Meristem (EVM), Transition Meristem (TM) and Floral Meristem (FM), shows that genes typically expressed in the Transition Meristem (TM), like *FRUITFULL (FUL)* and *COMPOUND INFLORESCENCE (S)* result undetected while genes related with FM identity, like *SEPALLATA3 (SEP3)* and *ANANTHA (AN)* showed a precocious activation. Consistent with that, when *AN* is overexpressed, it is precocious activated and mutant show a similar phenotype as *tmf*. These data suggest that TMF, like TAW1, regulates inflorescence development by repressing FM identity genes, like *AN* and *FA*, up to the TM stage.

Yeast two-hybrid screen showed that TMF interacts with two homologs of the *Arabidopsis* BLADE-ON-PETIOLE (BOP), BOP1 and BOP2 transcriptional coactivators (SlBOP1 and SlBOP2), which have a role in growth and development, and in particular in leaf complexity and organ abscission [173,174]. In tomato, there is also a third *BOP SlBOP3*. *Xu et al. (2016)* suggest the formation of a transcriptional complex including *TMF* and three tomato *SlBOPs* since they interact with themselves and each other, and *TMF* recruits *SlBOPs* to the nucleus. The *SlBOP* expression pattern is similar to *TMF*; they are highly expressed in vegetative and transitional stages of meristem maturation and are very low expressed in the FM. Furthermore, mutations in *SlBOP* genes cause pleiotropic defects, that are more severe in double and triple mutants, with single flower inflorescences, such as *tmf* mutants [175].

TFAM1 and *TFAM2,* other ALOG genes in tomato have a similar expression profile of *TFM* [175].These three ALOGs form homodimers and heterodimers in double hybrid assay an in BiFC assay performed in tomato protoplast, where they show also a nuclear localization. The *tfm-1 tfam1tfam2* triple mutant generated by the CRISPR-Cas system has a more drastic phenotype when compare to *tmf*-1: it flowers after only two to three leaves and the sepals of these flowers are more leaf-like, suggesting that flower identity is acquired early during meristem maturation [176]. These genetic studies underline a synergic interaction between these three ALOG genes, that can form a high order complex and function together during reproductive development.

In maize, an ALOG gene named *ALOG*1* was identified by transcriptome analysis of SAMs during embryogenesis and is expressed in the boundaries between SAM and the lateral meristems [177].

Also in *Lotus japonicus*, a model plant for legumes, recently a member of the *ALOG* family, LjALOG1 was functionally characterized. It has high levels of expression in nodules and at the base of nodules primordia. This gene, in fact, promotes nodulation in roots after inoculation with rhizobia [178]. The *ljalog1* mutant produces fewer nodules and upregulates *LjCLE-RS1*, a known repressor of nodulation.

Transcriptomic analysis performed in Arabidopsis [1] and in rice [2] on reproductive meristems highlighted a possible role in inflorescence development of other *ALOG* genes, like the partially characterized *LSH1* and the uncharacterized *G1L1* and *G1L2*. They sampled IM, Stage 2 (ST2) and ST3 of Flower development in Arabidopsis and IM, PBM, ePBM/AM and SM in rice. By bioinformatics analysis, genes were grouped in clusters, that show their pattern of expression during each meristematic stage. *LSH1* is in the same cluster with *LSH3* and *LSH4,* and *G1L1* and *G1L2* are in the same cluster of *G1L5*. They are the only ALOG genes differentially expressed in meristems and they show a downtrend expression. *LSH* genes show a high level of expression in IM (20/100 Transcripts Per Million (TPM)), then decreasing in ST2 (10 TPM) and in ST3 where expression is close to 0 TPM **[Figure 11].** *G1-like* genes are highly expressed in the IM (35/50 TPM) and decreased by 3 or 4 folds in the PBM (15/20 TPM), to reach the lowest expression level in the ePBM/AM (5/15 TPM) and then go up in SM (10/15 TPM) **[Figure 12].** The reads counts were expressed in Transcripts Per Million (TPM) which is a good way to compare the expression of specific genes and between samples. This normalization takes into account first, the length of each gene (more reads can map on a longer gene), and then normalizes for sequencing depth (more reads can map on a gene if the total reads number of the sample is higher).

More investigation has to be done to elucidate the role of *LSH1, G1L1* and *G1L2* in inflorescence patterning in both species.
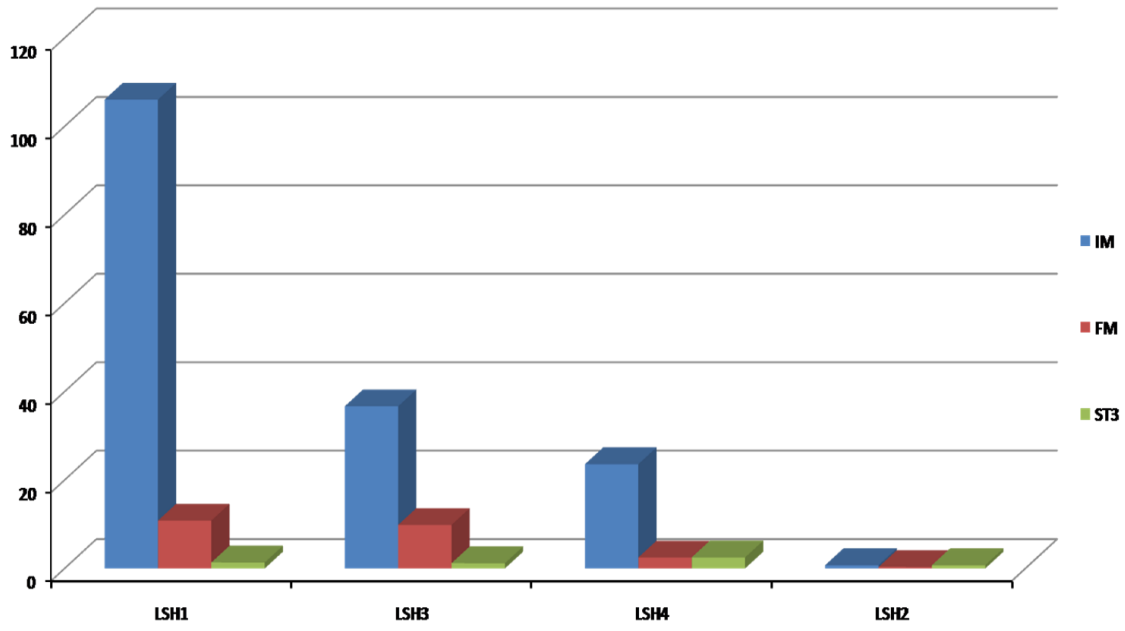
Figure 11. Expression of *LSHs* genes in TPM.
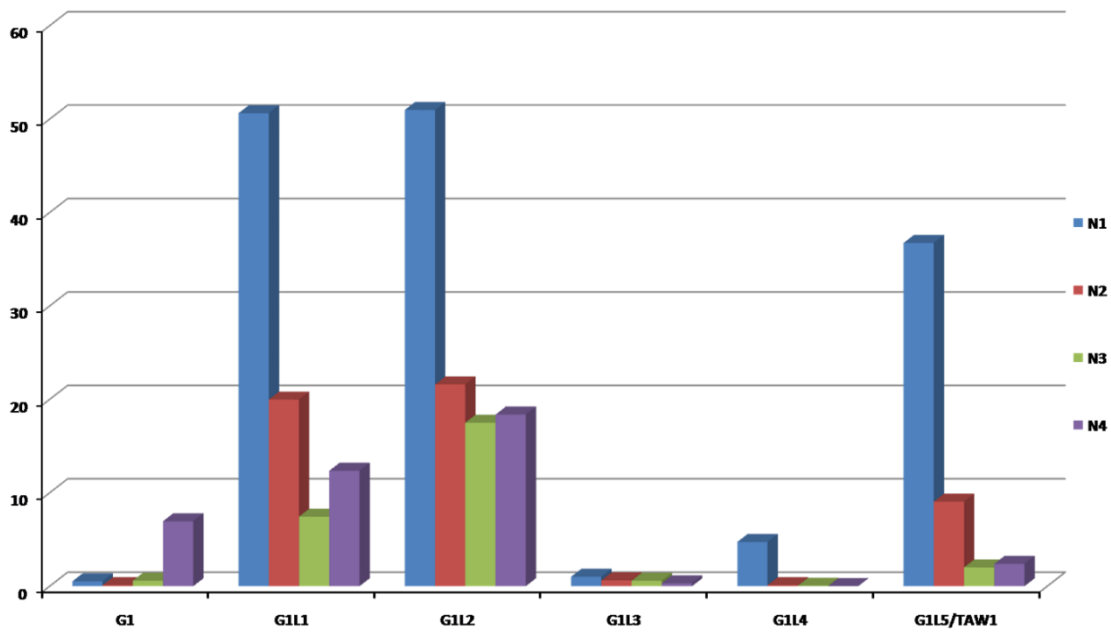
Figure 12. Expression of *G1-like* genes in TPM; N1 =IM; N2= PBM; N3=SBM; N4=SM.

2. RESULTS

2.1 GENOMIC LOCATION AND DOMAIN CONSERVATION OF ALOG GENES IN ARABIDOPSIS

The ALOG gene family in Arabidopsis is composed of 10 members. The locus distribution on the 5 chromosomes is shown in Figure 13. *LSH6, LSH7* and *LSH8* are located on Chr1; *LSH2* and *LSH10* on Chr2; *LSH2* and *LSH4* on Chr3; *LSH9* is the only genes located on Chr4 and finally, *LSH1* and *LSH5* are located on Chr5. These genes encode nuclear proteins and their size ranges from 182 to 219 amino acids with a mass range from 19.689 to 24.123 Da. All members are different in sequence at their N- and C-terminal regions but they have highly conserved region in the middle of the protein, corresponding to 4 α-helixes and Zinc Ribbon insert of the ALOG domain (shown in **Figure 13**) [165].

Figure 13. A schematic representation of genomic location of *ALOG* genes in Arabidopsis.

```
LSH1    1   MDLISH----------------QPN-KN------PN-----------SSTQLTPPSSSRY   26
LSH2    1   MDLISQ---------------NHNNRN------PN----TSLSTQTPSSFSSPPSSSRY   34
LSH3    1   MDMIPQLMEGSSAYGGVTNLNIISNNSSSVTGA-TG----GEATQPLSSSSSPSANSSRY   55
LSH4    1   MDHIIG-------FMGTTNMSHNTNLMIAAAATTTT----TSSSSSSSSGGGSGTNQLSRY   49
LSH5    1   ------------------------------M---------EGE-TAAKAAASSSSSPSRY   20
LSH6    1   -----------------MESADSGRSDPV---------KGDDPGPSFVSSPPATPSRY   32
LSH7    1   -------------MA--S--HSNKGKGIAEGSSQP-QSQPQPQPHQPQSPPNPPALSRY   41
LSH8    1   -------------MTSTN--TRNKGKCI--------------------VEGPPPTLSRY   24
LSH9    1   -------------MSSD--------RHTPTKDPPDHPSSSSNHHKQPLPPQPQQPLSRY   38
LSH10   1   ----------------------------MSSPRE----RGKSLMESSGSEPPVTPSRY   26
                                                                    ***

            Helix-1                        Helix-2          Zinc ribbon insert

LSH1    27  ENQKRRDWNTFCQYLRNHRPPLSLPSCSGAHVLEFLRYLDQFGKTKVHHQNCAFFGLPNP   86
LSH2    35  ENQKRRDWNTFCQYLRNHHPPLSLASCSGAHVLDFLRYLDQFGKTKVHHQNCAFFGLPNP   94
LSH3    56  ENQKRRDWNTFGQYLRNHRPPLSLSRCSGAHVLEFLRYLDQFGKTKVHTNICHFYGHPNP   115
LSH4    50  ENQKRRDWNTFGQYLRNHRPPLSLSRCSGAHVLEFLRYLDQFGKTKVHTHLCPFFGHPNP   109
LSH5    21  ESQKRRDWNTFLQYLRNHKPPLNLSRCSGAHVLEFLKYLDQFGKTKVHATACPFFGQPNP   80
LSH6    33  ESQKRRDWNTFLQYLKNHKPPLALSRCSGAHVIEFLKYLDQFGKTKVHVAACPYFGHQQP   92
LSH7    42  ESQKRRDWNTFCQYLRNQQPPVHISQCGSNHILDFLQYLDQFGKTKVHIHGCVFFGQVEP   101
LSH8    25  ESQKSRDWNTFCQYLMTKMPPVHVWECESNHILDFLQSRDQFGKTKVHIQGCVFFGQKEP   84
LSH9    39  ESQKRRDWNTFVQYLKSQNPPLMMSQFDYTHVLSFLRYLDQFGKTKVHHQACVFFGQPDP   98
LSH10   27  ESQKRRDWNTFGQYLKNQRPPVPMSHCSCNHVLDFLRYLDQFGKTKVHVPGCMFYGQPEP   86
            * .**  *****  ***  .:  **: :    *::.**:  ********  *  ::*   :*

                    Helix-3                        Helix-4

LSH1    87  PAPCPCPLRQAWGSLDALIGRLRAAYEENG-GPPEANPFGSRAVRLFLREVRDFQAKARG   145
LSH2    95  PAPCPCPLRQAWGSLDALIGRLRAAYEENG-GAPETSPFGSRSVRIFLREVRDFQAKSRG   153
LSH3    116 PAPCPCPLRQAWGSLDALIGRLRAAFEENG-GKPETNPFGARAVRLYLREVRDMQSKARG   174
LSH4    110 PAPCACPLRQAWGSLDALIGRLRAAFEENG-GSPETNPFGARAVRLYLREVRDSQAKARG   168
LSH5    81  PSQCTCPLKQAWGSLDALIGRLRAAFEEIGGGLPESNPFAAKAVRIYLKEVRQTQAKARG   140
LSH6    93  PSPCSCPLKQAWGSLDALIGRLRAAYEEN-GGRPDSNPFAARAVRIYLREVRESQAKARG   151
LSH7    102 AGQCNCPLKQAWGSLDALIGRLRAAFEENG-GLPERNPFAGGGIRVFLREVRDSQAKARG   160
LSH8    85  PGECNCPLKQAWGSLDALIGRLRAAYEENG-GLTEKNPFARGGIRIFLREVRGSQAKARG   143
LSH9    99  PGPCTCPLKQAWGSLDALIGRLRAAYEEHGGSPDTNPFANGSIRVHLREVRESQAKARG   158
LSH10   87  PAPCTCPLRQAWGSLDALIGRLRAAYEENG-GPPETNPFASGAIRVYLREVRECQAKARG   145
            . *  ***:****************:** *  : .**.  .:*:.*:*** *:*:**

LSH1    146 VSYEKKRKRVNRQK-----PQTQPPLQLQQQQQQPQQGQSMM--ANYSGATV------   190
LSH2    154 VSYEKKRKRVNNKQITQSQPQSQPPPLPQQ---PQQEQGQSMM--ANYHHGATQ-----   201
LSH3    175 VSYEKKRKRPLPSSSTSSSSAVASHQQ----FQMLPGTSSTTQLKFEK---------   219
LSH4    169 ISYEKKRKRPPPPLPPAQPAISSSPN-----------------------------   195
LSH5    141 IPYDKKKKRPHTDTATPIAGDGDDAEG-------SGGAA----LVVTAAT---TV--   182
LSH6    152 IPYEKKKKRPPTVTTVRVDVASSR--Q-------SDGDP----CNVGAPSVAEAVPP   196
LSH7    161 VPYKKRKKRKKRNPMKSHDGEDGTTG-----------TSSSS--NLAS---------   195
LSH8    144 VLYKKKKKRLVVVGTGTSTT------------------------WT----------   164
LSH9    159 IPYRKKKKRRKTKNEVVVVKKDVANSSTPN-QSFT----------------------   191
LSH10   146 IPYKKKKKKKPTPEMGGGREDSSSSSSS----FSFS--------------------   177
            : * *:::
```

Figure 14. Sequence alignment of Arabidopsis ALOG proteins. In dark grey are indicated the identical or similar a.a residues among all members; in light grey instead are indicated the a.a residues conserved by at least half of the family members.

2.1.1 Gene structure of *LSH1, LSH3* and *LSH4*

This research project is focussing on the functional characterization of *LSH1, LSH3* and *LSH4* to investigate their role in inflorescence development. Phylogenetic analysis showed that they are closely related and therefore they might act redundantly **[Figure 15].**
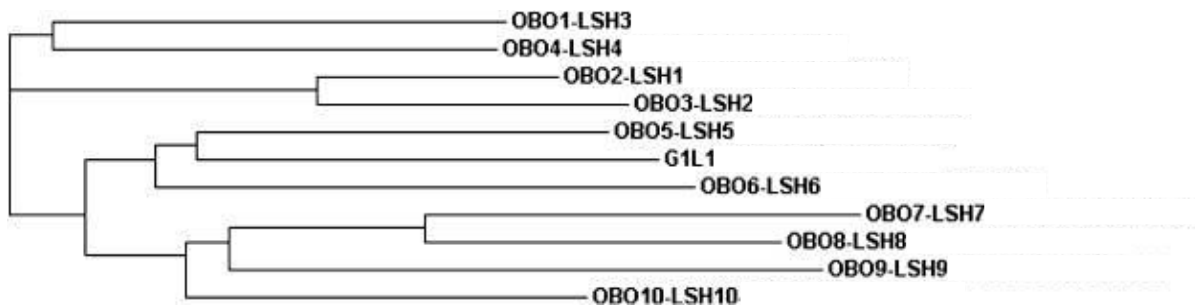
Figure 15. Phylogenetic tree of ALOG proteins.

LSH1 (At5g28490) has no introns and the CDS (blue box) is 574 nucleotides long. The protein consists is 190 a.a with a mass of 21.653 Da **[Figure16 A].** *LSH3 (AT2G31160)* has also no introns and its CDS is 660 nucleotides long that encodes a protein of 24.123 Da **[Figure 16B].** *LSH4 (AT3G23290)* has 1 intron and the CDS encodes a protein with a mass of 21.434 Da **[Figure 16C].**
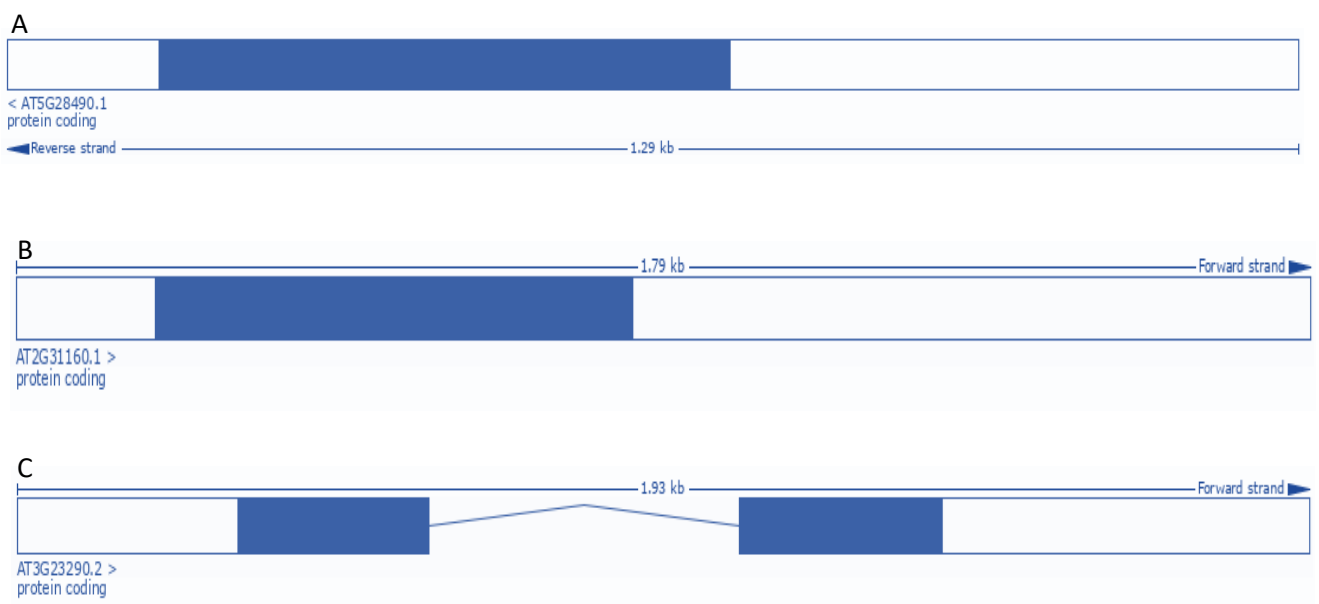
Figure 16. Structures and orientation of *AtLSH1* (A)*, AtLSH3* (B) and *LSH4I* (C) in the Arabidopsis genome. The white boxes represent the 5' and 3' UnTranslated Regions (UTRs), the blue box indicates the translated region.

2. 2 EXPRESSION ANALYSIS OF *LSH1, LSH3* AND *LSH4* GENES IN ARABIDOPSIS

2.2.1 Expression analysis by qRT-PCR across plant tissues

Analysis of the RNAseq data, performed on reproductive meristems in Arabidopsis [1], showed that *LSH1, LSH3* and *LSH4* have a similar downtrend expression profile: high expression in the IM and progressively lower expression levels in Stage 2 (ST2) and Stage 3 (ST3) of the Flower Meristem (FM). The similarity in sequence and the overlapping expression following a similar trend suggests that *LSH1, LSH3* and *LSH4* might have a redundant function during inflorescence development.

To confirm the RNAseq data and to better understand the pattern of expression of these genes during plant development we performed an expression analysis by qRT-PCR using different plant tissues. This analysis provides also information about the transcript levels of these genes in the different tissues.

We analysed vegetative tissues, in particular, roots, hypocotyls, cotyledons, leaves (rosette and cauline); reproductive tissues (inflorescence and siliques) **[Figure 17].**
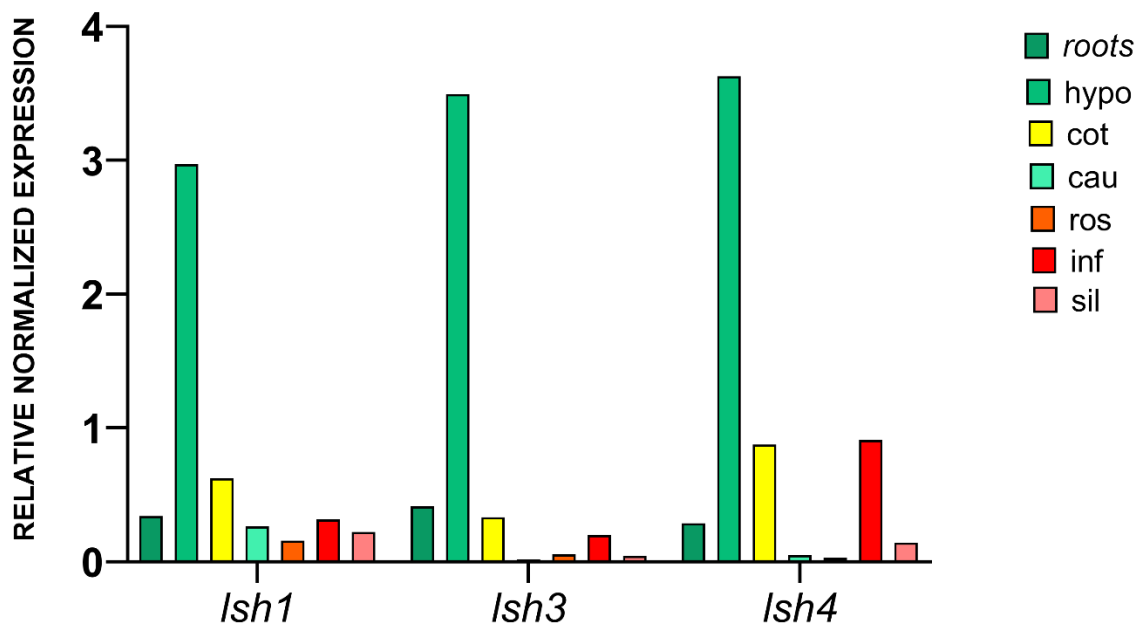

Figure 17. Relative expression of *LSH1, LSH3, LSH4* in three biological replicates normalized with *ACTIN*; roots (roots); hypocotyl (hypo); cotyledons (cot), cauline (cau), rosette (ros), inflorescences (inf); siliques (sil)

LSH1, LSH3 and *LSH4* showed a similar expression profile across all plant tissues. They were mainly expressed in the hypocotyl but were also expressed in cotyledons, roots and inflorescences. Furthermore, *LSH1* showed low levels of expression in leaves and in siliques. *LSH3* didn't show expression in these tissues while *LSH4* showed a mild expression in siliques. Notably, in contrast to

the RNAseq data, *LSH4* resulted higher expressed in inflorescences. However, the obtained data confirm their similar expression profile not only in reproductive tissues but in all plant tissues suggesting a possible functional redundancy throughout the plant.

2.2.2 Expression analysis of *lsh1, lsh3* and *lsh4* by *in situ* hybridization across reproductive meristems

Previously it has been reported that *LSH3* and *LSH4* are expressed in IM and in the boundary cells of floral organs [4]. To further investigate the spatial and temporal expression of *LSH1* in reproductive tissue and to see whether these genes show a similar expression profile we performed *in situ* hybridization with all three genes on IM and first stages of flower development **[Figure 18]**. A specific antisense digoxigenin- labelled RNA probes for *LSH3, LSH4* and *LSH1* was used. *LSH1* showed a similar expression profile as *LSH3* and *LSH4*: they were all expressed in IM but also in a boundary region between IM and FM. This confirmed the data already published for *LSH3* and *LSH4* and showed that also *LSH1* was expressed in the same tissues.
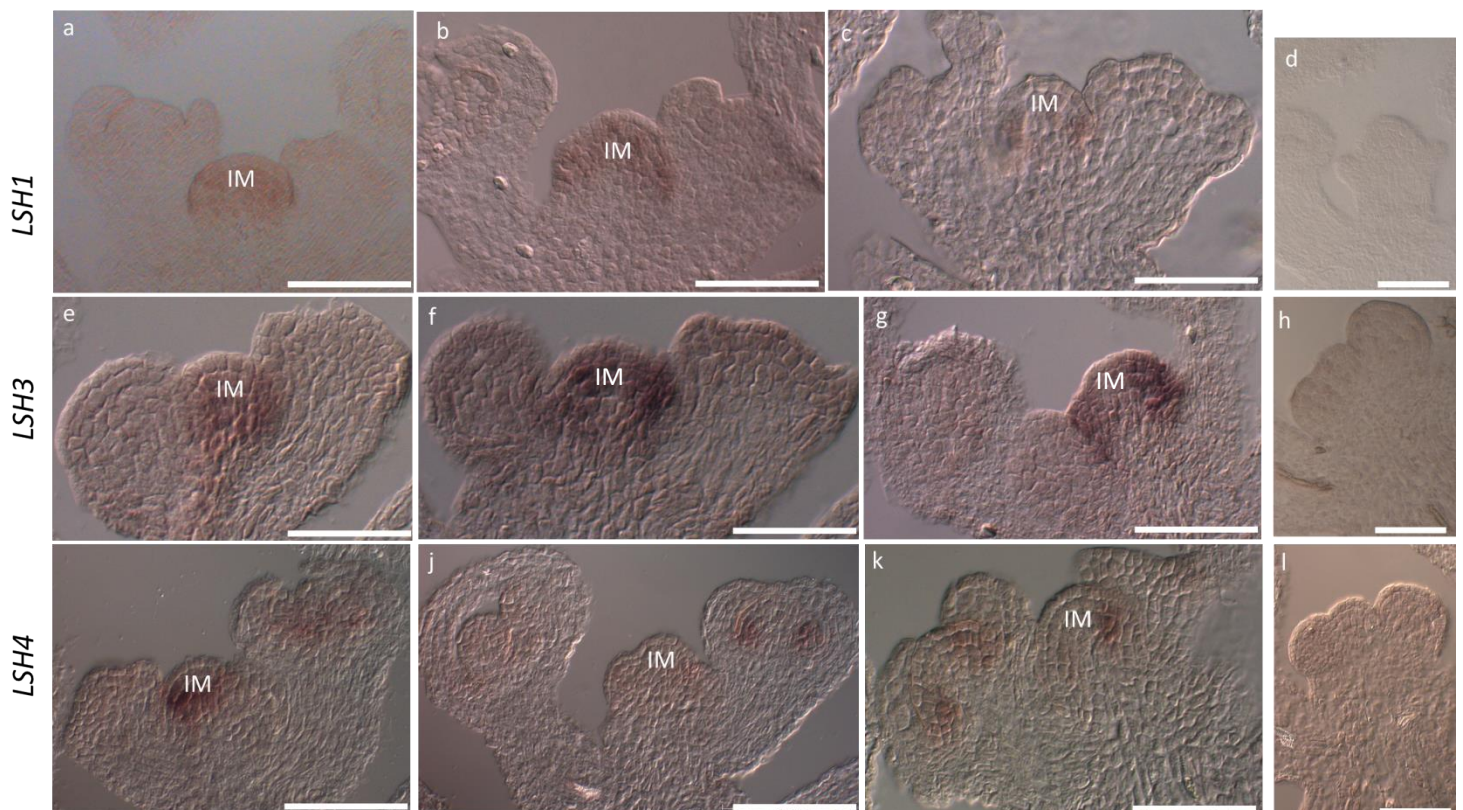
Figure 18. Expression pattern of *LSH1, LSH3* and *LSH4* by in situ hybridization in reproductive meristems. *LSH1* antisense probe (a-c), *LSH1* sense negative control probe (d), *LSH3* antisense probe (e-g), *LSH3* sense negative control probe (h), *LSH4* antisense probe (i-k), *LSH4* sense negative control probe (l). Scale bars represent 100 µm.

2.3 GENERATION OF SINGLE AND MULTIPLE K.O MUTANT COMBINATIONS FOR *LSH1, LSH3* AND *LSH4*.

From literature is already known that the downregulation of *LSH3*, *LSH4* or both *LSH3* and *LSH4* by RNAi didn't result in any obvious phenotype [4]. This could be due to the fact that the genes were partially downregulated and not complete KO mutants, or more probably, to redundancy with other genes, such as *LSH1*. To test this hypothesis our goal was to obtain double mutants in different combinations and to generate the *lsh1 lsh3 lsh4* triple mutant.

2.3.1 *lsh3* and *lsh4* T-DNA insertion lines analysis

Screening the SALK database for T-DNA insertions in the *LSH1*, *LSH3* and *LSH4* genes we identified for *LSH4* a line (SALK_067722C) with the T-DNA inserted in intron. This *lsh4-1* T-DNA insertion line was already published as a strong knockdown mutant, showing a remaining 3% expression of *LSH4* respect to the WT [4] and hence could be considered a K.O. mutant. Although, the *lsh4-1* mutant didn't show an aberrant phenotype, it proved when combined with the *rpl* mutant to partially restore the *rpl* phenotype [168]. We also identified an unpublished T-DNA insertion line for *LSH3*, SALK_123953C, with an insertion in the 5'-UTR **[Figure 19]** while there wasn't any SALK line available with a T-DNA insertion in *LSH1*.

lsh3 -> SALK_123953C: T-DNA insertion in the 5'-UTR of the gene at 300 bp from the ATG
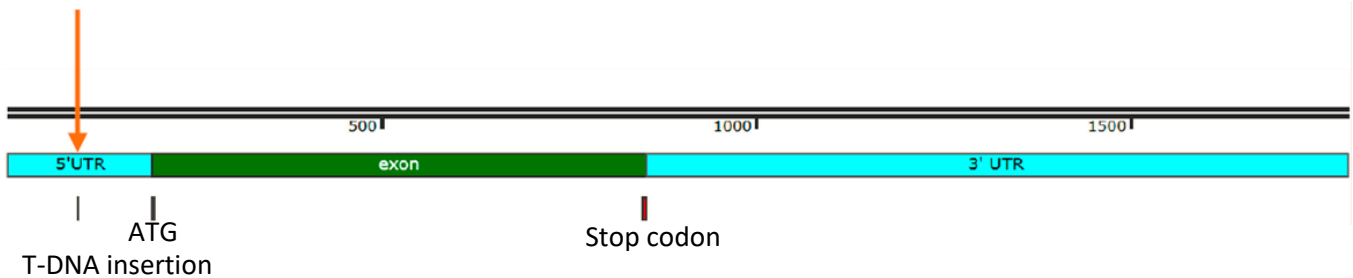
Lsh4-> SALK_067722C: T-DNA insertion in the intron
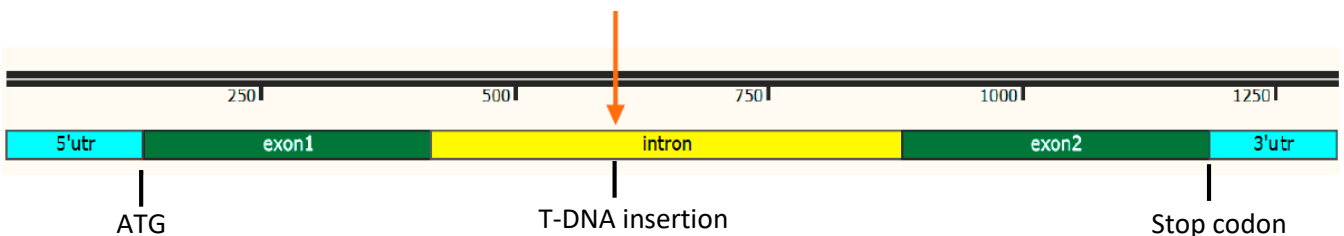
Figure 19. SALK T-DNA line available for *LSH3* and *LSH4*.

The *lsh3* and *lsh4* plants were genotyped by PCR to identify lines homozygous for the T-DNA insertion, using specific primer sets that amplify the WT or mutant alleles.

We obtained several homozygous mutants that were subsequently confirmed by sequencing:

- *lsh3* 5/22 homozygous (22,7%)

- *lsh4* 10/30 homozygous (33,3%)

We checked the expression of *LSH3* in the *lsh3* T-DNA line by qRT-PCR. Since the T-DNA insertion is in the 5'-UTR, it could have disrupted a regulatory region upstream of *LSH3*, changing its expression. The *LSH3* expression in this line is reduced to 40-50 %, therefore we consider this line a knockdown mutant instead of a K.O **[Figure 20]**.
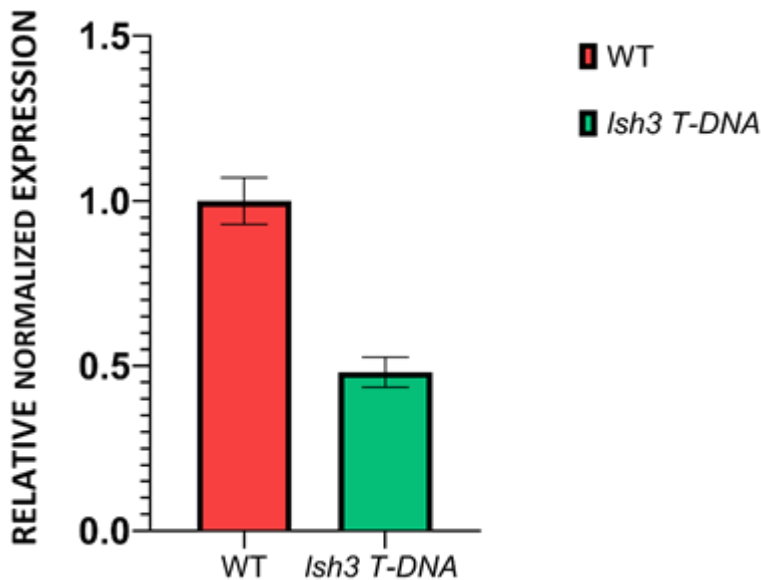
Figure 20. *LSH3* **expression in** *lsh3 T-DNA* **line compare to the WT.**

In parallel, we also performed crosses using the *lsh3* and *lsh4* homozygous T-DNA insertion line to generate the *lsh3 lsh4* double mutants. F1 plants were self-crossed and by PCR double mutant F2 plants were selected and subsequently analysed in the T3 generation for main traits such as length of the primary shoot, number of secondary shoots, number of siliques on the primary shoot. The double mutant didn't show any phenotype when compared to the WT **[Figure 21]**. The graphs were made using Graphpad Prism 8 (https://www.graphpad.com/scientific-software/prism/) and statistical analysis was performed by T-test considering p-value < 0,05.
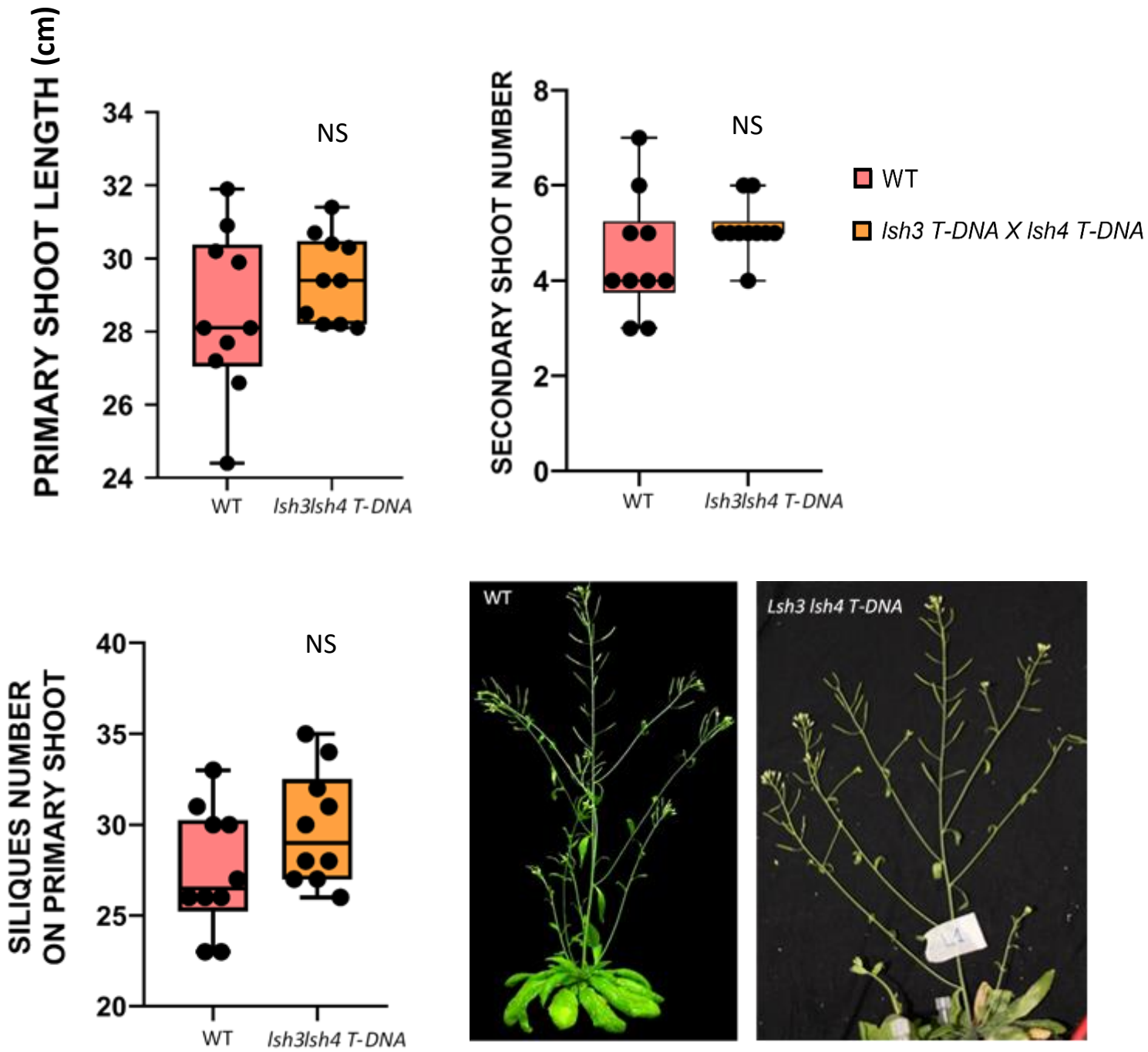
Figure 21. Phenotypical analysis performed on *lsh3 lsh4* double mutant T-DNA line compare to WT.

2.3.2 CRISPR-Cas9 genome edited *lsh* mutants

Since none of the T-DNA insertion lines seemed to be full knock-out mutants and for *LSH1* there is no insertion mutant available we decided to generate mutant alleles using the CRISPR-Cas9 genome editing system. Specific protospacers for these genes were designed to avoid off-targets, and to create mutations close to the ATG start codon (*LSH1* at 53 bp from translation start site, *LSH3* at 24 bp from translation star site and *LSH4* at 121 bp from translational start site) to disrupt the functional ALOG domain and hence obtain a non-functional protein **[Figure 22]**. Each protospacer was cloned first in an entry clone and then in the destination vector *pDeCas9* [179], and the final construct was used to transform *A. thaliana* Col-0 by Agrobacterium-mediated floral dipping [10].
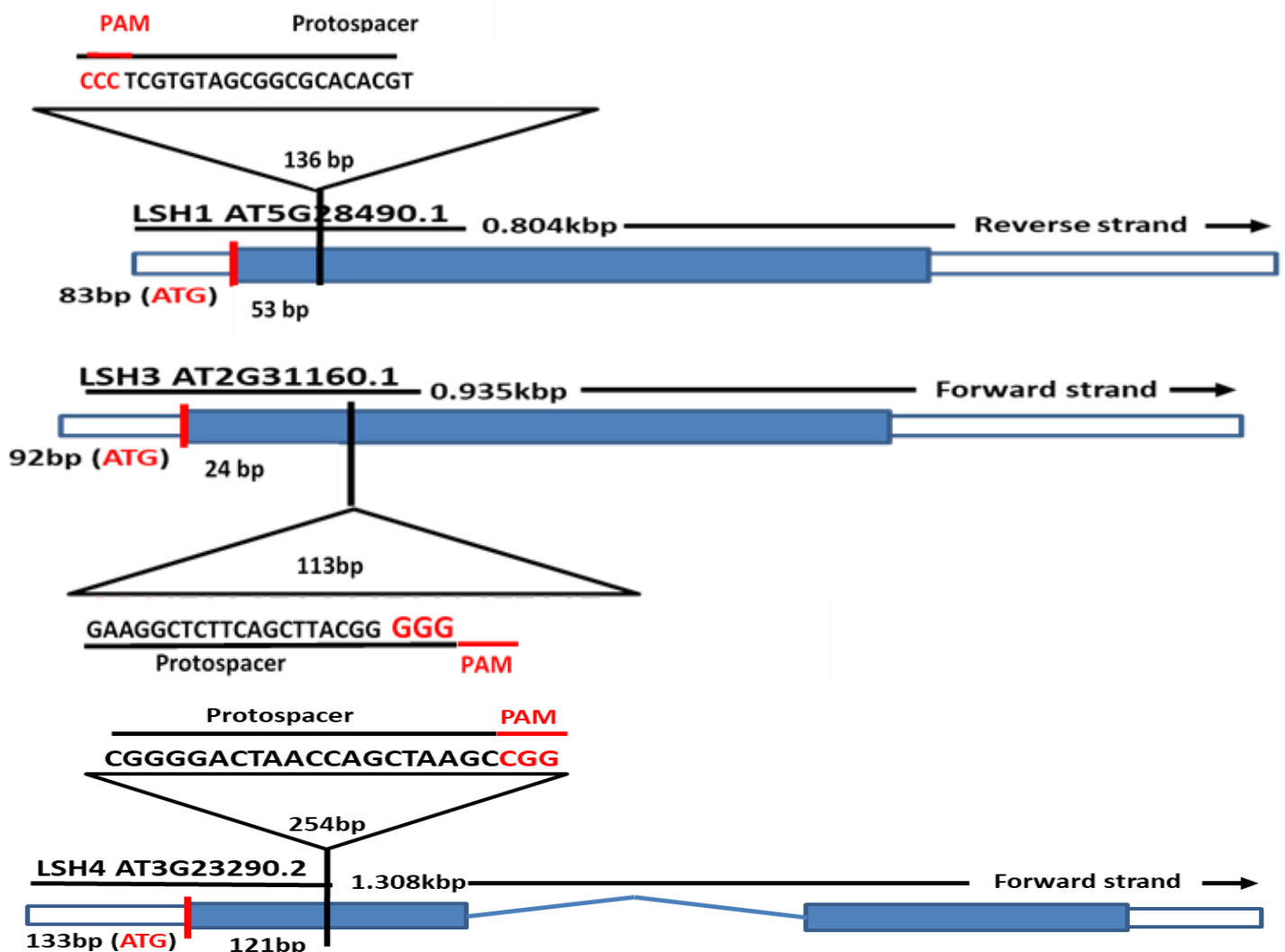
Figure 22. Protospacers designed for *LSH1, LSH3* and *LSH4*

The single *lsh4* mutant was the first mutant obtained. We sowed the T1 generation in soil and through BASTA selection we obtained 6 resistant plants. By sequencing analysis, we identified plant #2 mutated in heterozygosity. The Cas9 produced an A insertion at 3 bp from the PAM site and 138 bp

from the ATG resulting in a frame-shift mutation that led to conversion of an AAG codon instead of an AGC codon and formation of a premature stop codon at 247 bp from ATG resulting in a truncated protein of 82 a.a. **[Figure 23]**. Plant line #2 was taken to the T2 generation to segregate the CRISPR-Cas9 construct and to obtain a homozygous mutant. Plant #2.33 by sequencing resulted in homozygous and without Cas9 **[Figure 23A]**. This line was taken to the T3 generation with WT to perform phenotypical analysis.

Protospacer starting point

A insertion at 3bp from PAM site AGG
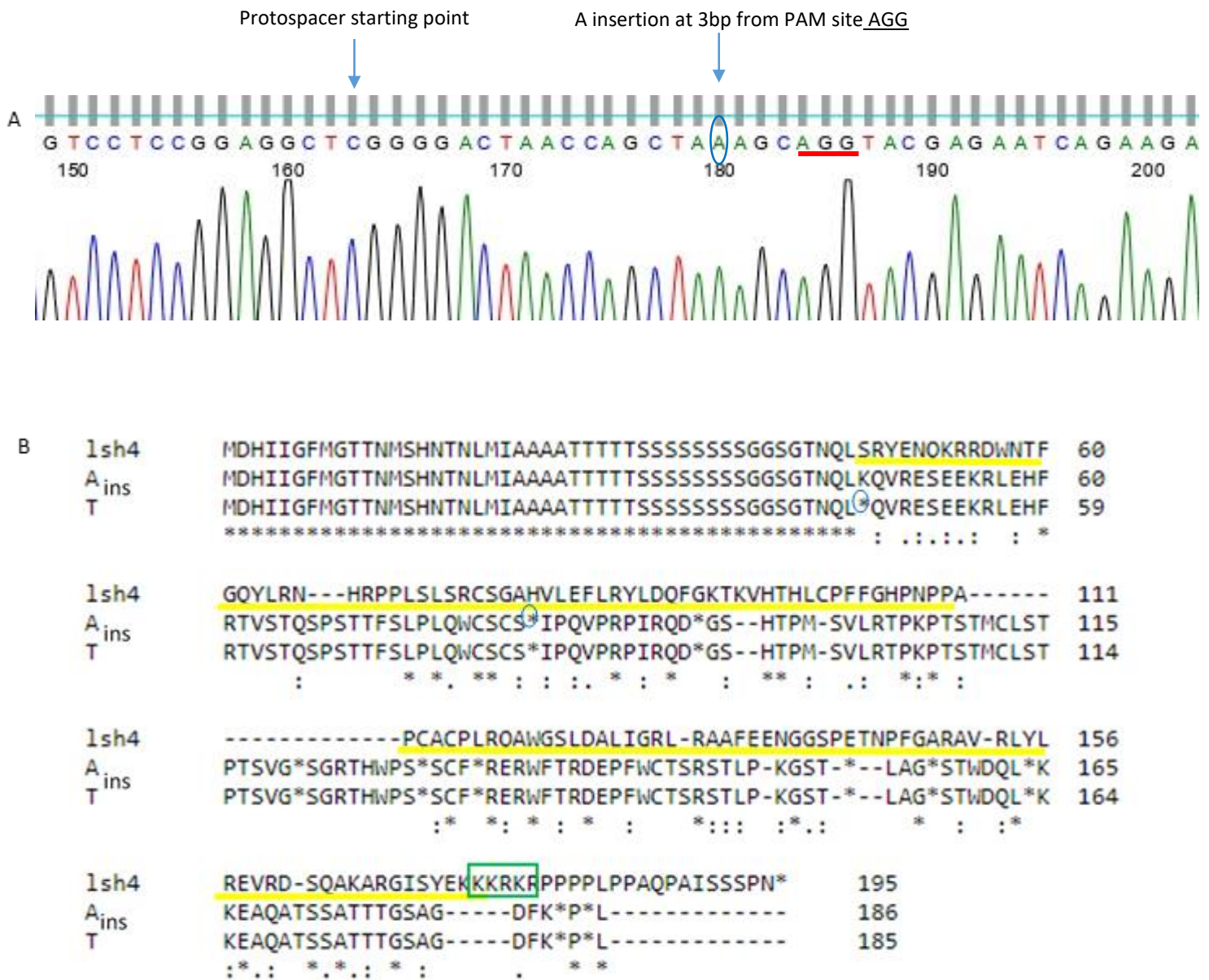
Figure 23. A. *lsh4* **#2.33 chromatogram. B. WT and Mutant protein alignment. In evidence the ALOG domain (▬), stop codon (○) and NLS(▭)**

By transforming Arabidopsis plants with a CRISPR-Cas9 construct specific for *LSH3* and BASTA selection we obtained 21 T1 plants. We identified a homozygote plant, #21, that had a biallelic

insertion at 3 bp from the PAM site and at 41bp from the ATG. In one of the *LSH3* loci an A was inserted whereas in the other *LSH3* locus a T. An A insertion transformed a TAC codon (encoding for the amino acid tyrosine) into a premature stop codon (TAA) at that position whereas T insertion led to formation of premature stop codon at 108 bp from the ATG. In both cases, premature stop codons hampered the translation and lead to a truncated protein length of 13 or 36 a.a without putative NLS (nuclear localization signal) **[Figure 24]**. Plant line #21 was taken to the T2 to segregate the Cas9 construct. Line #21.8, that had a biallelic A/ T insertion, was taken to the T3 generation to perform phenotypical analysis.
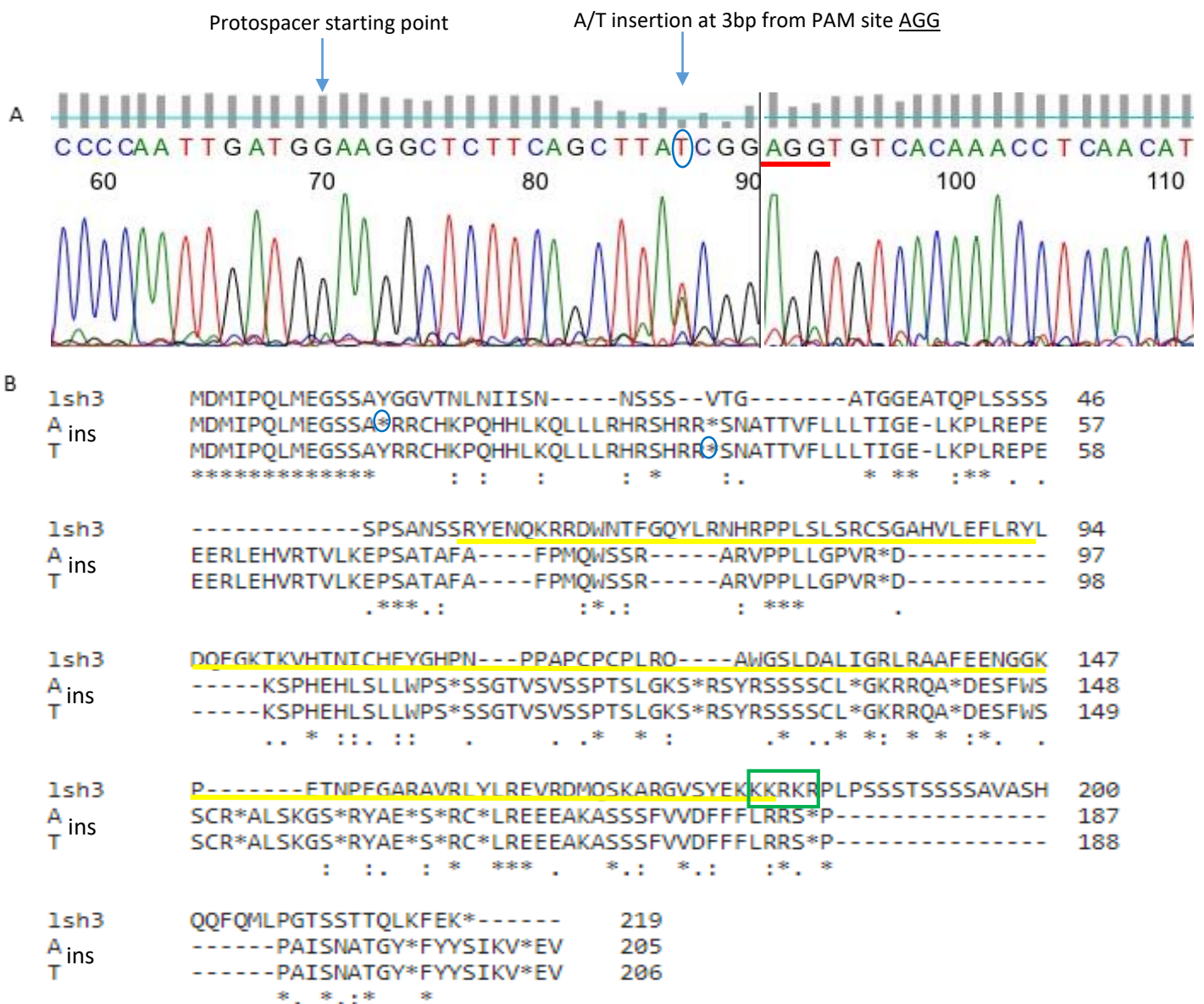
Figure 24. A. *lsh3 #21* **chromatogram. B. WT e Mutant protein alignment. In evidence the ALOG domain (━), stop codon (○) and NLS (▢)**

The *lsh1* mutant was the last single mutant obtained since the first designed protospacer didn't produce mutations. We designed a new protospacer, transformed plants and analyzed the 30 T1 plants resistant to BASTA selection. No mutated plants were found in the T1 generation despite the presence of the Cas9 construct. Therefore, we decided to take a couple of lines with the construct to the T2 generation from which one plant, line #3.4, was selected that resulted to be biallelic. This mutant had a C/A insertion at 3bp from PAM site and at 156 bp from the ATG. Either C or A insertion leads to the formation of a premature stop codon at 159 bp from the ATG that results in a truncated protein of 52 a.a. This mutation transformed indeed a Cysteine codon TGT into a methionine codon, ATG and immediately after a Stop codon TAG **[Figure 25].**

We took this *lsh1* mutant line to the T3 generation in order to segregate the Cas9 construct and to obtain a homozygous line. We first genotyped plants for the Cas9 construct and subsequently the PCR products of plants without Cas9 were sequenced to check for the mutation. 11 /72 plants resulted without Cas9 and among these, 5 plants were heterozygous for an A or C insertion. We self-crossed line #3.4.5 to obtain the lsh1 homozygous single mutant. Analyzing 20 plants we obtained 6 WT plants, 13 heterozygote plants and only one homozygote plant with A insertion. The plants have been genotyped using restriction enzyme analysis but the mutation was also confirmed by sequencing [Figure 26 A]. Line #3.4.5.7 was taken to T5 generation together with WT plants to perform phenotypical analysis.

```
B  lsh1    MDLISHQPNKNPNSSTQLTPPSSSRYENQKRRDWNTFCQYLRNHRPPLSLPSCSGAHVLE   60
   c ins    MDLISHQPNKNPNSSTQLTPPSSSRYENQKRRDWNTFCQYLRNHRPPLSLPSL*RRTRAR   59
   a        MDLISHQPNKNPNSSTQLTPPSSSRYENQKRRDWNTFCQYLRNHRPPLSLPSM*RRTRAR   59
            *********************************************************    .

   lsh1    FLRYLDQFGKTKVH-HQNCAFFGLPNPPAPCPCPLRQAWGSLDALIGRLRAAYEENGGPP   119
   c ins    VPPLP*PVRENKSSPPELCLLWP---P*PSCSLSLS-----SPASLGLTRRSYRPPPRRL   109
   a        VPPLP*PVRENKSSPPELCLLWP---P*PSCSLSLS-----SPASLGLTRRSYRPPPRRL   109
             .       . :.*      : * ::     *    *    *      * :*   * :*.

   lsh1    EANPFGSRAVRLFLREVRDFQAKARGVSYEKKRKRVNRQKPQTQPPLQLQQQQQQPQQGQ   179
   c ins    RGERWPT*S*PIWLTRRQVIPP*SQRLSSQSSRC--------------*L*EEEEESQQAE   151
   a        RGERWPT*S*PIWLTRRQVIPP*SQRLSSQSSRC------------*L*EEEEESQQAE   151
            ..: : : :   ::* . : :    :: :* :..*            * :::::  **.:

   lsh1    SM---------------MANYSGATV*----                190
   c ins    TANAAASTASATATAATTRSVYDG*LLGCNSM               182
   a        TANAAASTASATATAATTRSVYDG*LLGCNSM               182
            :                  : *.*   :
```

Figure 25. A. *lsh1 #3.4.5.7* **Chromatogram (reverse strand). B. WT e Mutant protein alignment. In evidence the ALOG domain (▬), stop codon (◯) and NLS(▭)**

2.3.3 Generation of multiple *lsh* mutant combinations

A *lsh3* CRISPR T2 mutant line, #21.11 with an A insertion in homozygosity and without the Cas9, was used for reciprocal crosses with the *lsh4* CRISPR mutant line to obtain the *lsh3 lsh4* double mutant. Some plants of the F1 of this cross was checked by sequencing to verify that crossing occurred and were subsequently self-crossed to obtain the double homozygous mutant. Knowing the mutation for *lsh3* and *lsh4* we decided to genotype plants by restriction enzyme analysis (M&M). We chose enzymes that can cut only the WT allele of *LSH4* and cut in a different way WT and mutant alleles of *LSH3*.

We genotyped some plants first for the *LSH3* allele and then for *LSH4*. Unfortunately, of the 45 plants that we genotyped none of them resulted homozygous for both genes. Therefore, two *lsh3 lsh4/+* lines were taken to the F3 generation and genotyped to find a *lsh3 lsh4* double mutant. Due to segregation all different genotypes were found in this generation: *lsh3*, *lsh3 lsh4/+* and *lsh3 lsh4*. Ten plants, in total, for each genotype were randomly selected to perform phenotypical analysis comparing to WT.

We crossed heterozygous *lsh1* plants with the *lsh4* mutant to obtain the *lsh1 lsh4* double mutant We started to genotype F1 generation plants for the *lsh1* allele since parental line was heterozygous. 6 out of 12 plants resulted heterozygous for both genes and line #30.10 was used for self-pollination to

obtain the homozygous double mutant. One out of 35 F2 plants genotyped, #30.10.34 resulted homozygote for both genes and it was grown together with WT and the *lsh1* and *lsh4* single mutants to perform phenotypical analysis.

Subsequently also a cross between lsh1 to lsh3 lsh4 has been done to obtain the triple mutant. These experiments are in progress.

2.4. PHENOTYPICAL ANALYSIS OF *lsh* mutants

The *lsh1, lsh3* and *lsh4* complete K.O mutants have not been described yet, hence, we performed a phenotypical analysis on them. We took in consideration at least ten plants for each genotype and we measured length of the primary shoot, number of secondary shoots, number of siliques on the primary shoot. The data are represented using Graphpad Prism 8 and the p-value was calculated by T-test (confidence in threshold: $p < 0.05$).

We analysed 11 T3 *lsh4* plants and 11 WT plants. This analysis revealed that the *lsh4* mutant was not significant different from the WT plants **[Figure 26]**.
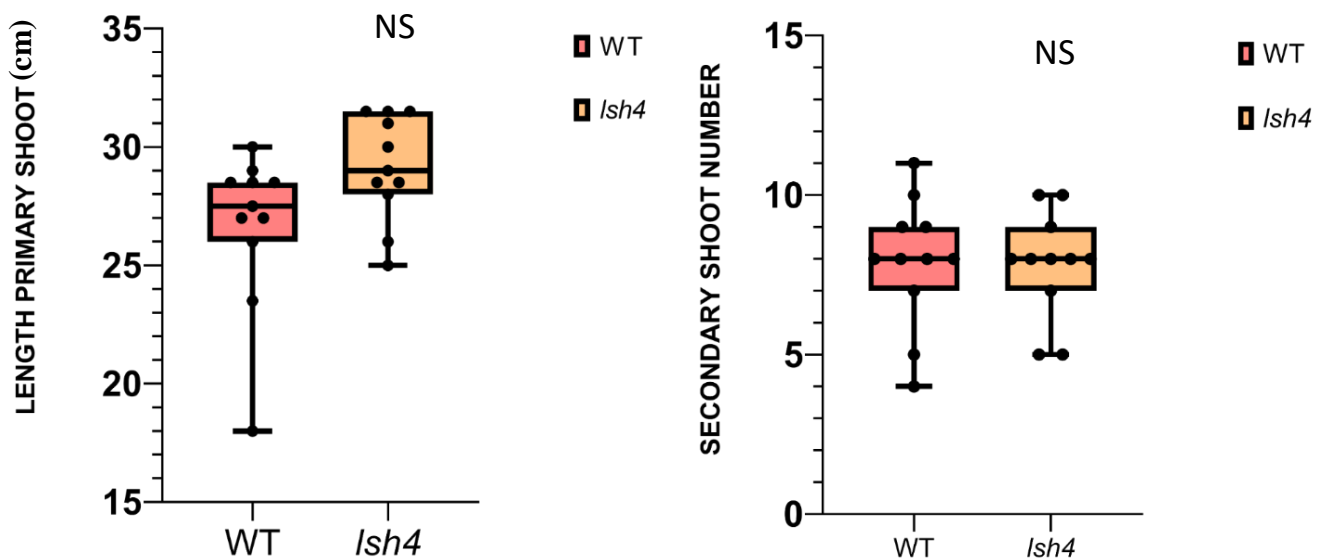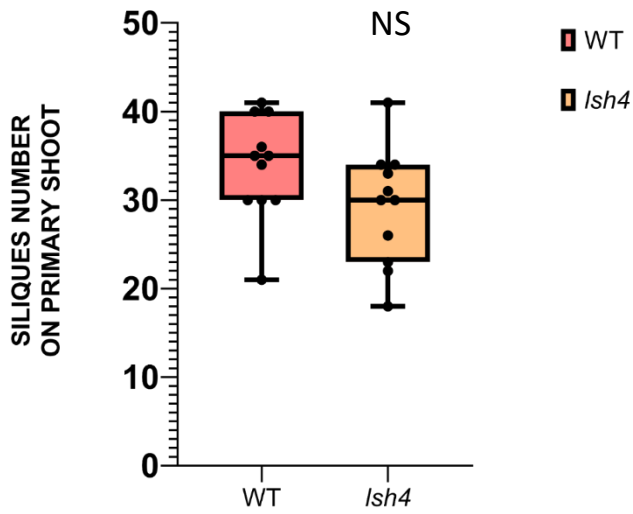
Figure 26. Phenotypical analysis performed on *lsh3 lsh4* T-DNA line compare to WT.

For the *lsh3* mutant 10 T3 plants were analysed **[Figure 27]**. The *lsh3* mutant develops a longer primary shoot longer than WT but didn't show any other defects in terms of number of secondary branches and number of silique produced on the primary shoot.
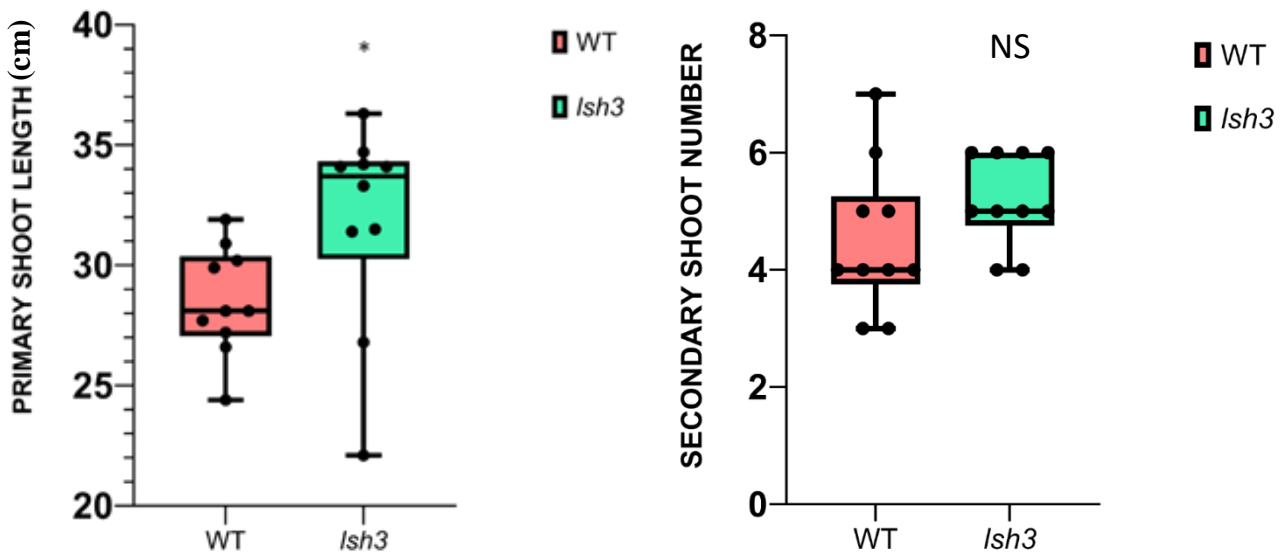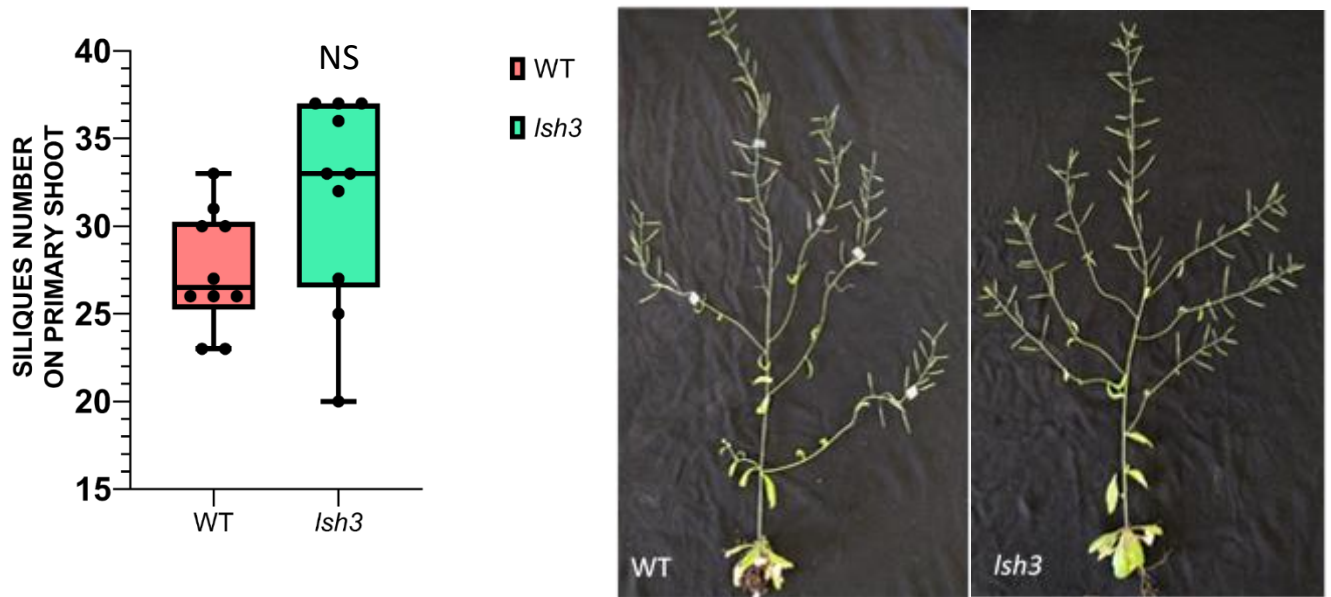
Figure 27. Phenotypical analysis performed on *lsh3* compare to WT; * *p< 0,05*

For *lsh1* instead we took 10 T5 plants and 10 WT to performed phenotypical analysis **[Figure 28]**. *lsh1* produced less secondary shoots when compare to WT whereas other traits were similar to WT or not statistical significantly different.
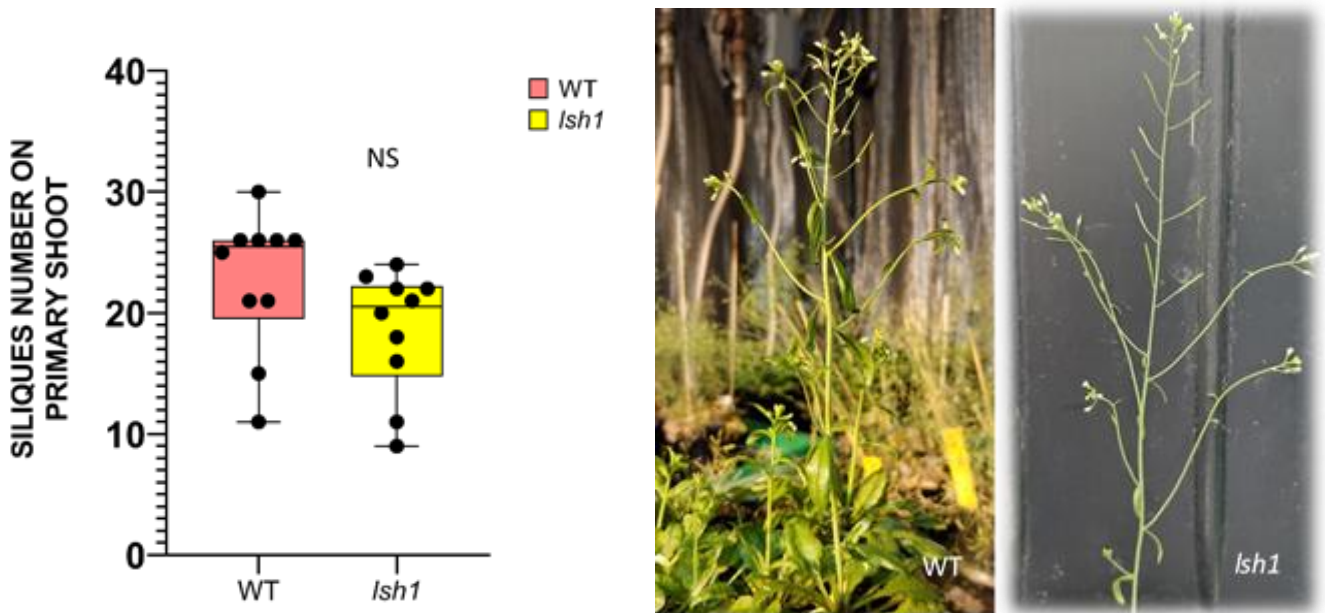
*Figure 28. Phenotypical analysis on WT and lsh1; ** p< 0,01*

As mentioned before ten plants for each genotype (*lsh3, lsh3 lsh4/+)* and *lsh3 lsh4)* were selected randomly by mutant segregation in order to perform the phenotypical analysis. These data are represented by Graphpad Prism 8, and statistical analysis was performed with One-Way ANOVA followed by the Tukey Test (http://vassarstats.net/anova1u.html) **[Figure 29]** sin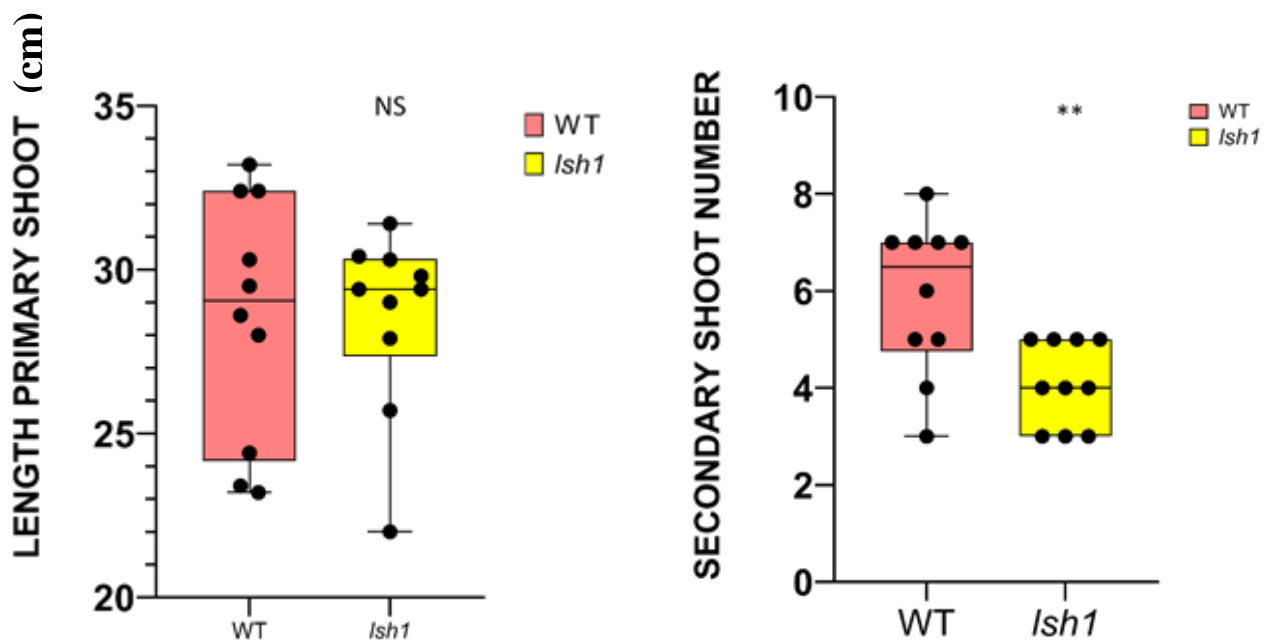ce the genotypes were more than two. The p-value threshold was p< 0,05. The phenotypical analysis didn't show any difference for all genotype compare to WT; but according with previous analysis, primary shoots of *lsh3* seem to be longer than WT and other mutants, although it was not statistical significant. Furthermore, it seems that the length gets closer to the median value of WT primary shoot length when *lsh3* was combined with *lsh4*.

The absence of a statistical sound inflorescence phenotype in all single mutants and the *lsh3 lsh4* double mutants suggests a functional redundancy between these genes, therefore the triple mutant *lsh1 lsh3 lsh4* will have to be generated to understand better the redundancy between these *LSH* genes.

Figure 29. Phenotypical analysis performed on *lsh3*, *lsh3 lsh4(+/-) and lsh3 lsh4* mutants compare to WT.

2.5. PROTEIN-PROTEIN INTERACTION
2.5.1 Yeast Two Hybrid (Y2H)
In collaboration with Prof. Stefan De Folter, LANGEBIO institute (Mexico), and Francesca Caselli (Unimi), we performed a Yeast two-hybrid assay to investigate the interaction between LSH factors and a subset of transcription factors involved in auxin and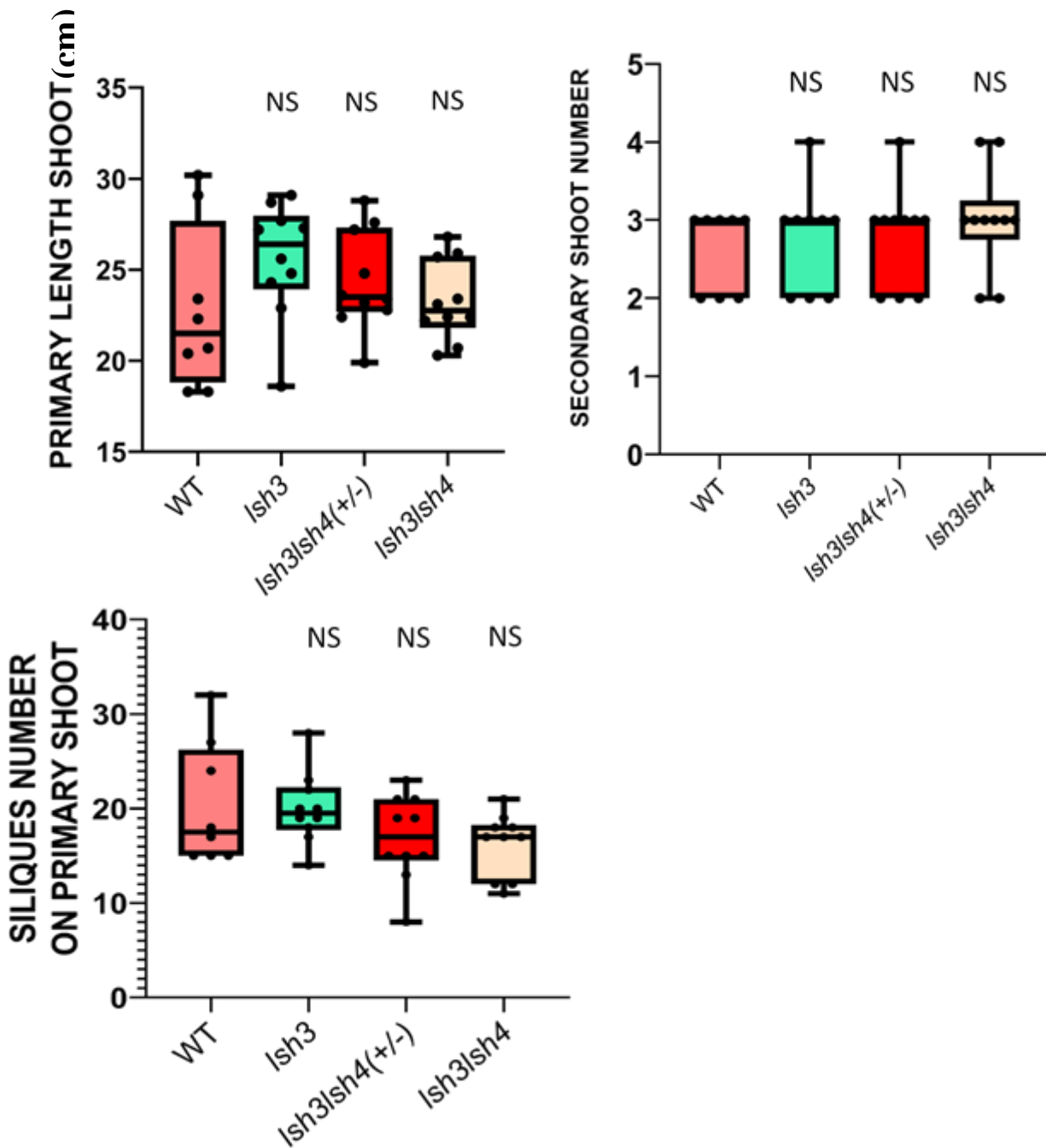 cytokinin control **[Table 1]** since they play a role in inflorescence development The Yeast two-hybrid assay is a technique that allows to detect protein interaction in living yeast cells. Basically, the protein of interests was fused to the DNA binding domain (BD) or activation domain (AD) of GaL4 resulting respectively in a bait and prey construct. When the interaction reconstitutes the functional GaL4 transcription factor it will be able to bind the upstream activator sequence (UAS) of the *GaL1* promoter and activate the expression of a reporter gene downstream such as *LacZ* encoding the enzyme beta-galactosidase which labels the yeast cell when using a colorimetric substrate or reporter genes that enable growth on specific media (HIS3, ADE2). Therefore, to performed this experiment we generated bait and prey constructs in which the CDSs of *LSH1, LSH3* and *LSH4* were fused respectively to the BD and AD domains; the BD-LSHs constructs were used to screen against a matrix containing 94 AD-constructs including AD-LSHs **[Table1].** Three different reporter genes were used in this experiment in order to increase the accuracy of the Y2H screens, such as LacZ, ADE2 and HIS3 **[Figure 30A]**. The most common problems are indeed false positive. The LSH factors didn't interact with them self, however, the assay identified only TCP15, among 94 genes tested, as putative interactor of LSH1 and LSH4 [Figure 30B].

SCR1	CUC1	CUC2	HEC1	WUS	YAB1	CRC	BP	KNAT6	STM	KNAT2	
REM13	PHV	ALC	AS2	BEE1	ARR4	ARR16	TCP15	REV	LSH1	IAA27	ARR15
NGA1	BEL1	RPL	STY1	STY2	ARF19	LSH3	ARF8	IAA27	PHB	BHL14	
NIN	JAG	REM11	ARR10	SEU	WIP3	KAN2	LUG	PNF	ARR12	GIK	TPL
AS1	AG	ARF18	LSH4	ARF4	MSI1	ETT	FIE	NGA2	KAN1	HEC2	ARF17
ARR14	YAB3	mpWIP	LEP	ARR7	HEC3	NGA3	WIP6	DRN	JABC	JABM	JABL
ARF1	VDD	ANT	ZIP30	SHP2	STK	AG	SHP1	AGL14	FUL	SEPA3	AGL63
BPC1	BPC2	BPC3	BPC6	EMF2	VRN2	SWG	LHP1	REM34	REM35	REM36	BPC4

Table 1. Matrix of AD-constructs containing a subset of Transcription factor involved in hormonal control screened against BD-LSHs construct.

A

	ADE	HIS
LSH1	WIP6 (2/4)	TCP15 (4/4)
LSH3	//	//
LSH4	//	TCP15 (3/4)

* LacZ positive colonies

B
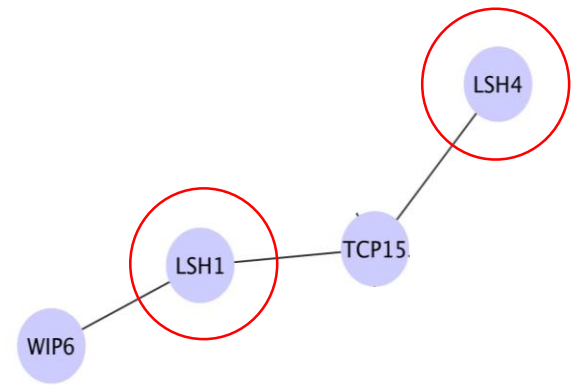
Figure 30. Y2H screening result [A] A table containing a list of *LSHs* genes screened using three different reporter genes (ADE, HIS and LacZ) against a matrix containing 94 genes involved in hormonal control. [B] Y2H assay highlighted TCP15 as putative interactor of LSH1 and LSH4

2.5.2 BiFC assay

To confirm the interaction of LSH1 and LSH4 with TCP15, we decided to perform a BiFC assay in *Nicotiana tabacum* leaves. We performed this experiment in collaboration with the lab of Prof. Marouane Baslam at Niigata University, Japan. We generated constructs in which the CDSs of *LSH1, LSH4* and *TCP15* were fused to the N-terminal or C-terminal part of the fluorescent protein YFP. The concept of the BiFC assay is that, when the YFN and YFC are sufficiently close, the functional YFP recomposes and emits fluorescent light at a wavelength of 527 nm. We used as positive control the already published VAL-VDD interaction [180] while the LSH1-LSH4 interaction, which was not observed in the Y2H assays, was used as negative control. The interactions were analysed with a confocal microscope. **Figures 31-32-33** show the YFP fluorescence (520-550 nm emission filter) and the merge of bright field (BF) and YFP channel.

Both the interaction LSH1/TCP15 and LSH4/TCP15 were confirmed and the localization of fluorescence was in the nucleus **[Figure 31-32]**. The positive control VDD-YFN/VAL-YFC retrieved a fluorescent signal with nuclear localization and in the negative control LSH1-YFN/LSH4-YFC, the YFP fluorescence was undetectable **[Figure 33]**.

TCP15-YFN
/LSH4-YFC

LSH4-YFN /
TCP15-YFC

YFP

BF

BF + MERGE
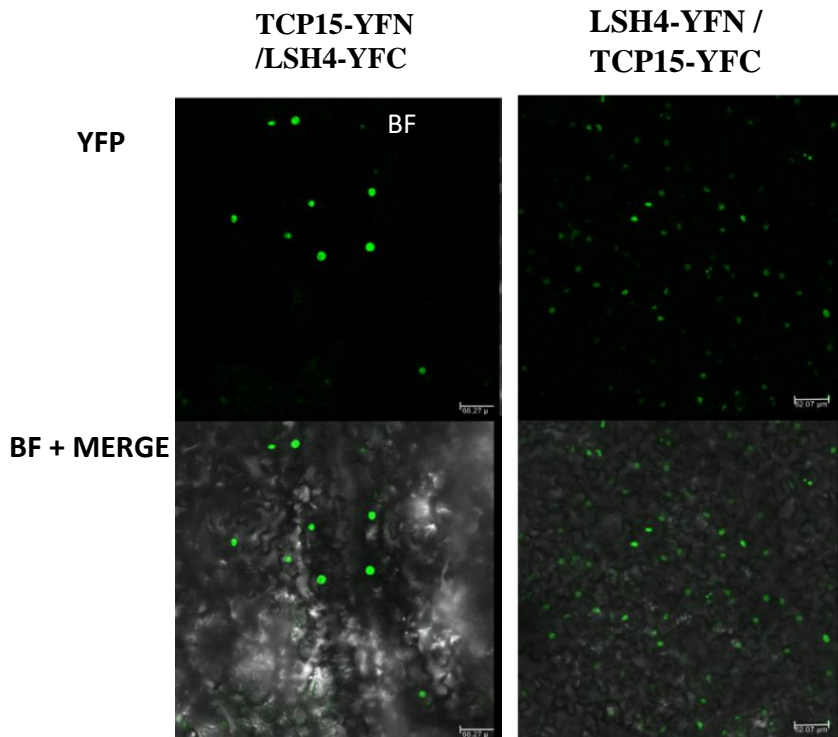
Figure 31. Figure 31. BiFC experiments in tobacco leaf cells showing the reconstitution of YFP activity (green). The interaction between TCP15 and LSH4, fused to the C- and N-terminal fragments of YFP respectively, revealed a clear signal in the nucleus. The YFP and bright field (BF) merged images are shown at the lower part of the panel (BF+ Merge) (bar = 66.27 μm and 62.07 μm).

TCP15-YFN
/LSH1-YFC

LSH1-YFN
/TCP15-YFC

YFP

BF + MERGE
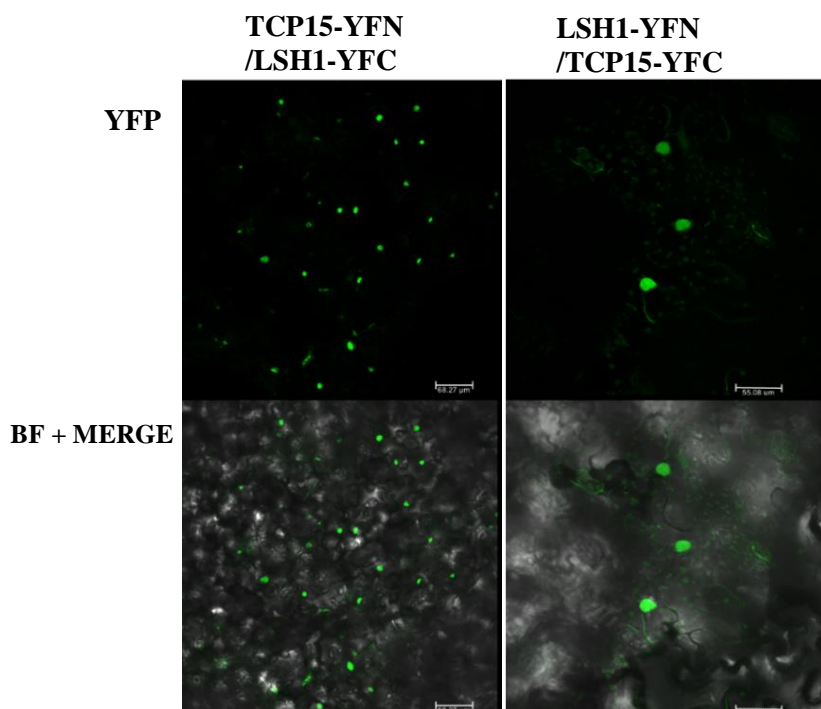
Figure 32. Figure 32. BiFC experiments in tobacco leaf cells showing the reconstitution of YFP activity (green). Interaction between TCP15 and LSH1 fused to the C- and N-terminal fragments of YFP respectively, revealed a clear signal in the nucleus. The YFP and bright field (BF) merged images are shown at the lower part of the panel (BF+ Merge) (bar = 66.27 μm and 55.08 μm).

A POSITIVE –
VDD-YFN/ VAL-YFC

B NEGATIVE –
LSH1-YFN/ LSH4-YFC

YFP

BF + MERGE

Figure 33. BiFC experiments in tobacco leaf cells showing the reconstitution of YFP activity (green). (A) The positive control VDD –VAL showed a clear nuclear signal whereas no signal was detected when (B) LSH1-YFN and LSH4-YFC interaction was tested as negative control. The YFP and bright field (BF) merged images are shown at the lower part of the panel (BF+ Merge) (bar = 100.26 μm and 80.01 μm
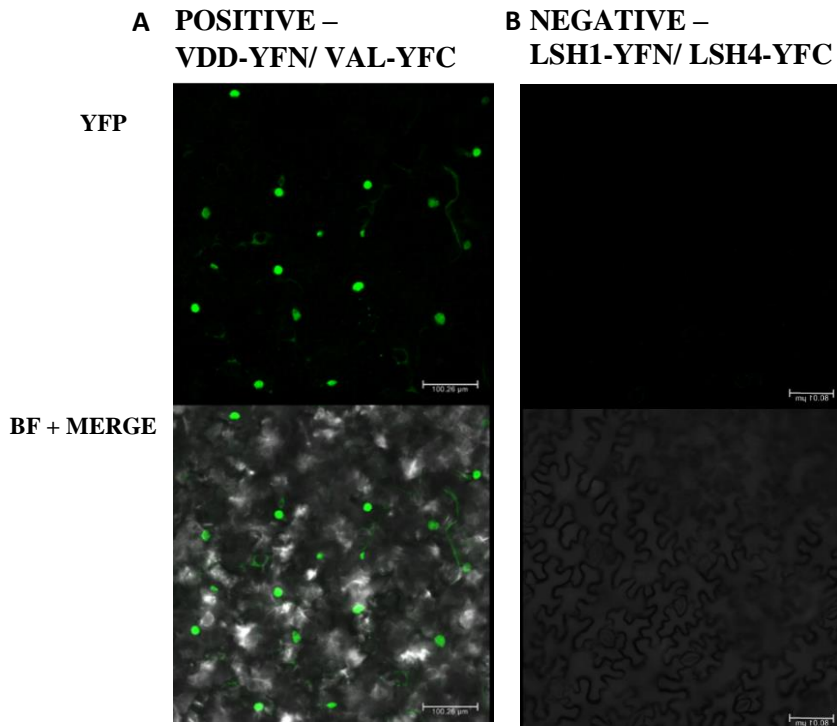
2.6. GENOMIC LOCATION AND DOMAIN CONSERVATION OF *ALOG* GENES IN RICE

The ALOG family in rice is composed of 14 members. They are located on several chromosomes except of Chr.3, Chr.9, Chr.11 and Chr.12 as is shown in **Figure 34**. These genes encode proteins varying from 202 to 284 amino acids with a mass range from 21.673 to 29.165 Da and a highly conserved domain in the middle of the protein sequence corresponding to the ALOG domain shown in **[Figure 35]** although, the novel four genes, *G1L10, G1L11, G1L12* and *G1L13*, don't show very high similarity in functional domain.
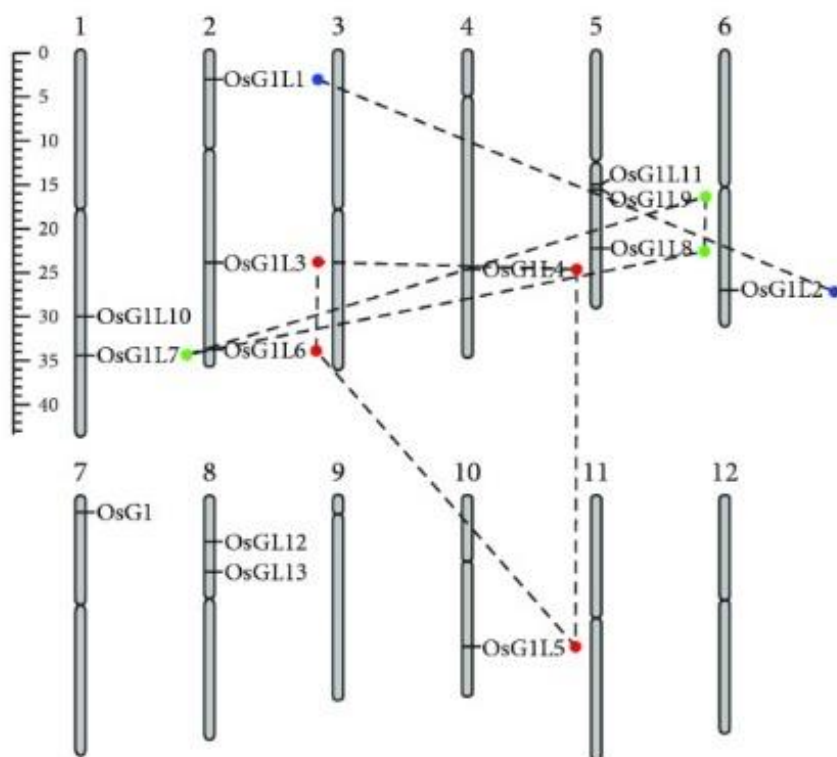
Figure 34. Genomic location of ALOG in rice.

```
G1      1    ------------------------------------------------------------    0
G1L1    1    ------------------------------------------------MD-MIGM         6
G1L2    1    --------------------------------------------------MQGG          4
G1L3    1    --------------MR-GEEEPAVAAAAYTTASKAGLLMELSPP-NHESSPPTAGGGGG      43
G1L4    1    ------------------------------------MDLSPN---PDSPPSGGGNGG        18
G1L5    1    ----------------------------------MEFVAHAAAPDSPHSDSG-GG          20
G1L6    1    MDRHHHHHHHHHHHMMSGGGQDPAAGDGGAGGATQDSFFLGPAAAAMF------------    48
G1L7    1    --------------------------------MDPS----------------G           5
G1L8    1    --------------------------------MEGG----------------G           5
G1L9    1    --------------------------------MEPSPD-----APRAGAAEEQ           16
G1L10   1    ------------------------------------------------------------    0
G1L11   1    MAKH---------------------------TRK-SFISFEPDYARFMHHHMK---N-       26
G1L12   1    ------------------------------------------------------------    0
G1L13   1    ------------------------------------------------------------    0
```

```
                                                                              _____
G1      1    -------MSSS-----SAA-----------------ALGSDDGCSPAELRPSRYESQKRRD    32
G1L1    7    AS-P------------AES-------------PG----------GGGTARPSRYESQKRRD    31
G1L2    5    GGGD------------SSG--------GG----------GGEAPRPSRYESQKRRD       30
G1L3   44    GGGDGAGGSSSAGASSSAG--------GG----------AATPQTPSRYEAQKRRD       81
G1L4   19    GGGS-----SSS--NSSPS-----------MG----------AGAPQSPSRYEAQKRRD    49
G1L5   21    GGGMATGATS--------------------A---------SAAGASPSRYESQKRRD      48
G1L6   49    ----SGAGSSSSGAGTSAG--------GGGG----GPSPSSSSPSLSRYESQKRRD       88
G1L7    6    P-GPSSAAAGG--------------APA-----VAAAPQPPAQLSRYESQKRRD         39
G1L8    6    G-GADG-QAQP--------------------VAQ-----APPAMQPMQQLSRYESQKRRD   38
G1L9   17    P-GPSSSASAPAPAASSNEEEGRHQSQAQQQVQEAPQPLAQQAPAAAGLSRYESQKRRD    75
G1L10   1    ----------------------------------------------------------     0
G1L11  27    --ASCTS---------------FHSLTYT-----TRMGDTPGYEQKVYVVCFYHSVNYRV    64
G1L12   1    ----------------------------------------------------------     0
G1L13   1    ----------------------------------------------------------     0

            Helix-1                      Helix-2              Zinc ribbon insert
            _____              _____        <---------------
G1     33    WQT-FTQYLAAHRPPLELRRCSGAHVLEFLRYLDRFGKTR---V-----HEPPCPSYGG    82
G1L1   32    WQT-FGQYLRNHRPPLELSRCSGAHVLEFLRYLDQFGKTK---V-----HAHGCPFFGH    81
G1L2   31    WHT-FGQYLRNHRPPLELSRCSGAHVLEFLRYLDQFGKTK---V-----HAAGCPFFGH    80
G1L3   82    WNT-FGQYLRNHRPPLGLAQCSGAHVLEFLRYLDQFGKTK---V-----HTAACPFFGH   131
G1L4   50    WNT-FGQYLRNHRPPLSLAQCSGAHVLEFLRYLDQFGKTK---V-----HTAACPFFGH    99
G1L5   49    WNT-FGQYLRNHRPPLSLARCSGAHVLEFLRYLDQFGKTK---V-----HAPACPFFGH    98
G1L6   89    WNT-FGQYLRNHRPPLSLSRCSGAHVLEFLKYMDQFGKTK---V-----HTPVCPFYGH   138
G1L7   40    WNT-FLQYLRNHRPPLTLARCSGAHVIEFLRYLDQFGKTK---V-----HASGCAFYGQ    89
G1L8   39    WNT-FLQYLKNHRPPLTLARCSGAHVIEFLKYLDQFGKTK---V-----HASGCAYYGQ    88
G1L9   76    WNT-FLQYLRNHKPPLTLPRCSGAHVIEFLKYLDQFGKTK---V-----HADGCAYFGE   125
G1L10   1    ---------MPLGPHISSISCLSP--HLSFLSQMARTAAGRVERGGGRGGRACGHRSH     47
G1L11  65    FQGNTLQQLLLRSVHLEHWGTPGY----WSITLANMARTAAGRVERGGGRGGRACGRRSH  120
G1L12   1    -----MSVLSPISL-----LISLF----SLSFLSQMARTAAGGVERGSGSGGRVRSRRSH   46
G1L13   1    ------------------------MARTVAGGVERGGGGGGGRARGRRSH            25
                                                :.:*          *              .

                                        Helix-3
            --------------->        _____
G1     83    RSPSAAGPVAAAAAACQCPLRQAWGSLDALVGRLRAAYDERHGRAGEPDAVAGAGAVATD  142
G1L1   82    PSPP---------APCPCPLRQAWGSLDALVGRLRAAFEEHGGRP--------------   117
G1L2   81    PSPP---------APCPCPLRQAWGSLDALVGRLRAAFEEHGGRP--------------   116
G1L3  132    PNPP---------APCPCPLRQAWGSLDALVGRLRAAFEENGGRP--------------   167
G1L4  100    PSPP---------APCPCPLRQAWGSLDALVGRLRAAFEENGGRP--------------   135
G1L5   99    PAPP---------APCPCPLRQAWGSLDALVGRLRAAYEENGGRP--------------   134
G1L6  139    PNPP---------APCPCPLRQAWGSLDALIGRLRAAYEENGGTP--------------   174
G1L7   90    PSPP---------GPCPCPLRQAWGSLDALIGRLRAAYEESGGTP--------------   125
G1L8   89    PSPP---------APCPCPLRQAWGSLDALIGRLRAAYEESGHAP--------------   124
G1L9  126    PNPP---------APCACPLRQAWGSLDALIGRLRAAYEESGGRP--------------   161
G1L10  48    PSPP---------TLCPCPLRQAWGSLDTLVGRLCTAFDEHGGHP--------------    83
G1L11 121    PSSP---------APWPCPLRQAWGSLDVLVGRLRTAFDEHGGHP--------------   156
G1L12  47    PSPL---------APCPCPLRQAWGSLDVLVGHLRAAFEEHGGHP--------------    82
G1L13  26    PSLP---------VPCPCLLRQAWGSLNALVGRFRAAFEEHGGQP--------------    61
             *  ********:.*:*::  :*::*

                  Helix-4
                  _____
G1    143    STSSSSAAAANPFAARAVRLYLRDVRDAQAMARGISYHKKKKRRGGNMNGARGGGGGGAR  202
G1L1  118    ---------ESNPFGARAVRLYLRDIRDTQSKARGIAYEKKRRKRAAASHTKQKQQQ----  165
G1L2  117    ---------EANPFGARAVRLYLREVRDSQAKARGIAYEKKRRKRPPTSSSSSQAAA-AAA  167
G1L3  168    ---------ESNPFAVRAVRLYLREVREHQARARGVSYEKKKRKKPQPADTSGG------G  213
G1L4  136    ---------ESNPFGARAVRLYLREVREHQARARGVSYEKKKRKKPQQQQLQGGDSS-GLH  186
G1L5  135    ---------ENNPFGARAVRLYLREVREHQARARGVSYEKKKRKKPPHPSSAAAAHD-DAA  185
G1L6  175    ---------EMNPFGARAVRLYLREVRETQARARGISYEKKKRKKPSSAGAGAGPSS-E--  223
G1L7  126    ---------ESNPFAARAVRTLYLREVRDSQAKARGIPYEKKKRKRSQAAQPAG--------  169
G1L8  125    ---------ESNPFAARAVRLYLREVRDAQAKARGIPYEKKKRKRTQQQQPPP--------  168
G1L9  162    ---------ESNPFAARAVRIYLREVREAQAKARGIPYEKKKRGAAAAAAAPP-------  206
G1L10  84    --------EANPFGARVVRLYVR---DSQAKVRGIAYEKKRRKRPPTSFSHSQAAAA---  129
G1L11 157    --------EANPFGARVVRLYLREVCDSQAKVRGIAYEKKRRKRPPTSSSHSQDGTA---  205
G1L12  83    --------EANPFSARAVRLYLHEVRDS*-------------------------------  103
G1L13  62    --------EANPFGARAVRLYLHEVYDCQAKARGIAYEKKRWKRPPTSSSHSQAAAA---  110
             ***..*.**:*::       :
```

```
G1      203  AGVNDGDATAPPVAVTPGLPLPPLPPCLNGVPFEY-----------C-----DFGS----    242
G1L1    166  ------------------------------------------------------------    165
G1L2    168  AA------TSPASPAASP--TPPPPPPTERSAD--VRPMPPEGHFFI--PHPHFMHGHFL    215
G1L3    214  G-----------HPHPPP--PPP-PPPSAGAAC---------------------------    232
G1L4    187  G-----------HQHHPP------PPPPAGAAC---------------------------    202
G1L5    186  NG------A---LHHHHH--MPP-PPPGAAA-----------------------------    204
G1L6    224  --------------------GSP-PPPGGSASG--GGDTSASPQFII--P----------    248
G1L7    170  ----------------------VEPSGSSSAAAAAAGG----------------GDA---    188
G1L8    169  ---------------------PPPPPPQHQPGAAAGEAS---SSSS-AAAAAVAAE---    199
G1L9    207  --------------------VVVAPPPVVTAPDDATGTSGGAGEDDDDEATHSGEQQDT    246
G1L10   130  -------ATCPASPAAS---PT-----PERSADMGACVA----------IAVAVGCTPLS    164
G1L11   206  -------ATCPASPAAS---PTPLPPPPERSADMGACVA----------IVVAVGCTPLS    245
G1L12   104  ------------------------------------------------------------    103
G1L13   111  -------ATSSASQPLA---RCRHRRCRRDQPTWLTVPD----------SLMVVLCAQVQ    150


G1      243  -----------------VLGGAHGA---HGGHGGGGGGF------------YGAGVYLPF    270
G1L1    166  -------------------------------------QQLVEQAAAAAEAHAAGCMMPL    187
G1L2    216  VPG--GDADHHHQVSNAGNGGNTNTNTNTGGGGGNGDEMAVAMAAVAEAHAAGCMLPL    273
G1L3    233  ----------------------------------------------------------    232
G1L4    203  ----------------------------------------------------------    202
G1L5    205  ----------------------------------------------------------    204
G1L6    249  ----------------------------------------------------------    248
G1L7    189  ----------------GSGGGA-AATTTAQPGGSGTAPS----AS--------------    212
G1L8    200  ----------------GSGSSAAAAAATSQTGGGGGGGSTTTTTASAAAPTTATRV----    238
G1L9    247  TPA--A---SPTTPPATSVGTTTAAATAAAAKGSAAKGSATSS---------------    284
G1L10   165  LAARRG--CSYCA---------LAYRR*------------------------------    181
G1L11   246  LAARRG--CSYCA---------LARRR*------------------------------    262
G1L12   104  ----------------------------------------------------------    103
G1L13   151  IKSKAERKRLWMLPSDSPSTGTHLTLKDS---------SE-----------------I    182


G1      271  LYNTFS--    276
G1L1    188  SVFN----    191
G1L2    274  SVFN----    277
G1L3    233  --------    232
G1L4    203  --------    202
G1L5    205  --------    204
G1L6    249  --------    248
G1L7    213  --------    212
G1L8    239  --------    238
G1L9    285  --------    284
G1L10   182  --------    181
G1L11   263  --------    262
G1L12   104  --------    103
G1L13   183  SENTISW*    190
```

Figure 35. ALOG protein sequence alignment; in evidence highly conserved ALOG domain with 4 helix and zinc ribbon insert.

2.6.1 Gene structure of *OsG1L1* and *OsG1L2*

As mentioned before we focused our attention on *G1L1* and *G1L2* since phylogenetic analysis revealed that they are closely related to *G1L5* [Figure36]. Transcriptomic analysis performed on meristematic tissues in rice also showed that they have a similar pattern of expression. This means that these genes might have a role in the same pathway such as *G1L5* and regulate inflorescence architecture.
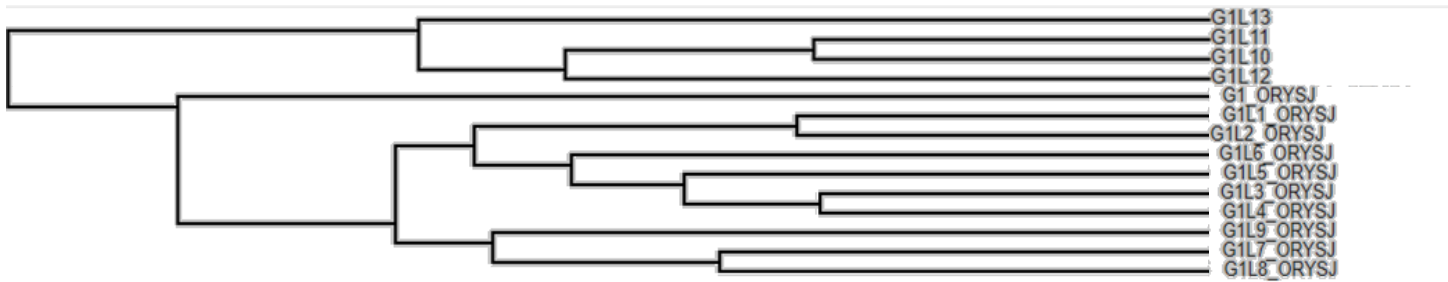

Figure 36. Phylogenetic tree of ALOG protein in rice

OsG1L1 (LOC_Os02g07030) has two exons and one intron. CDS is 813 nucleotides long and the protein consist is 271 a.a with a mass of is 28.628 Da [Figure 37 A]. *OsG1L2 (LOC_Os06g46030)* has also 2 exons and 1 intron and its CDS is 834nucleotides long that encode protein consist of 277 a.a with a mass of 29.165 Da [Figure 37 B].
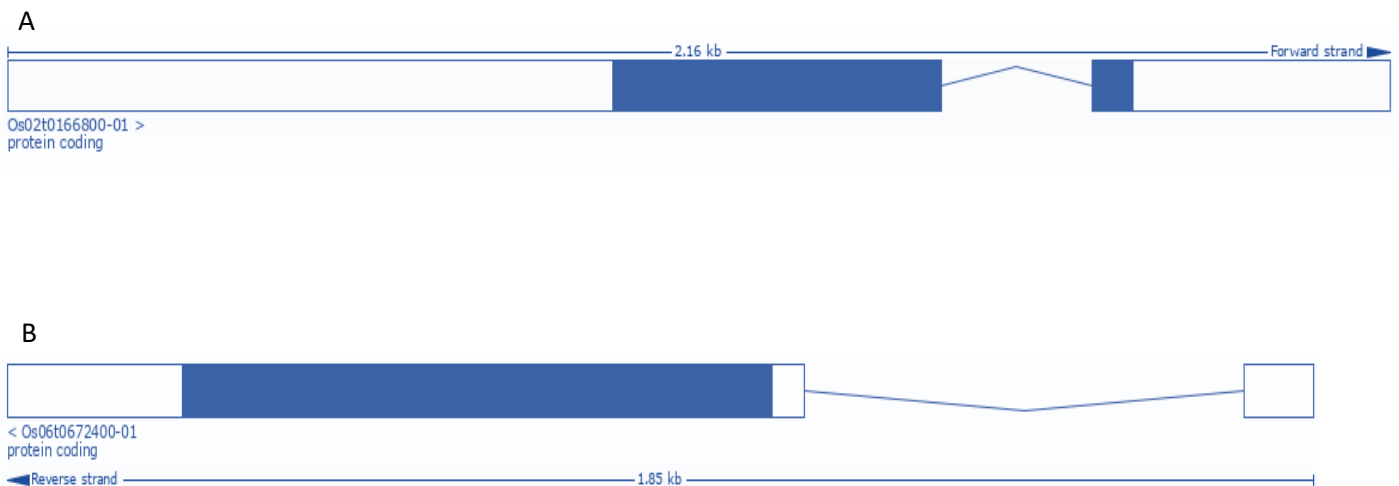
Figure 37. Structure and orientation of *OsG1L1* and *OsG1l2* in rice genome. The white boxes represent the 5' and 3' UnTranslated Regions (UTRs), the blue box indicates the translated region whereas lines indicate the intron.

57

2.7 EXPRESSION ANALYSIS ON GENES OF INTEREST IN RICE

2.7.1 *G1L1, G1L2* and *G1L5* expression analysis by qRT-PCR of across plant tissues

An expression analysis on all plant tissues has been performed in order to confirm the RNAseq data but also to investigate, in more detail, the expression of the *G1L1, G1L2* and *G1L5* genes across plant development **[Figure 38]**. We sampled several vegetative tissues such as roots tips where there is a meristem and whole roots, leaves (young and mature), SAM; all reproductive meristems, like RM, BMs, SMs and FMs; and seeds, such as milk seeds and mature seeds, respectively at 8 and 30 days after fertilization. The genes showed a high expression level in meristem tissues, both vegetative and reproductive like SAM, IM, BM and SM. We used the expression of *G1L5* as control since the expression profile was already characterized [5].

G1L1 was low expressed in vegetative tissues but showed a high expression in milk seeds and mature seeds. *G1L2* instead was more widely expressed, it showed high expression also in vegetative tissues including root tips, whole roots, young leaves and seed tissue i.e mature seeds. *G1L5* was also expressed in root tips, in mature seeds and showed a mild expression in whole root, young leaves and milk seeds. These results confirmed the preferential expression of these genes in reproductive meristems suggesting their function in the regulation of panicle architecture (Ud In, unpublished).
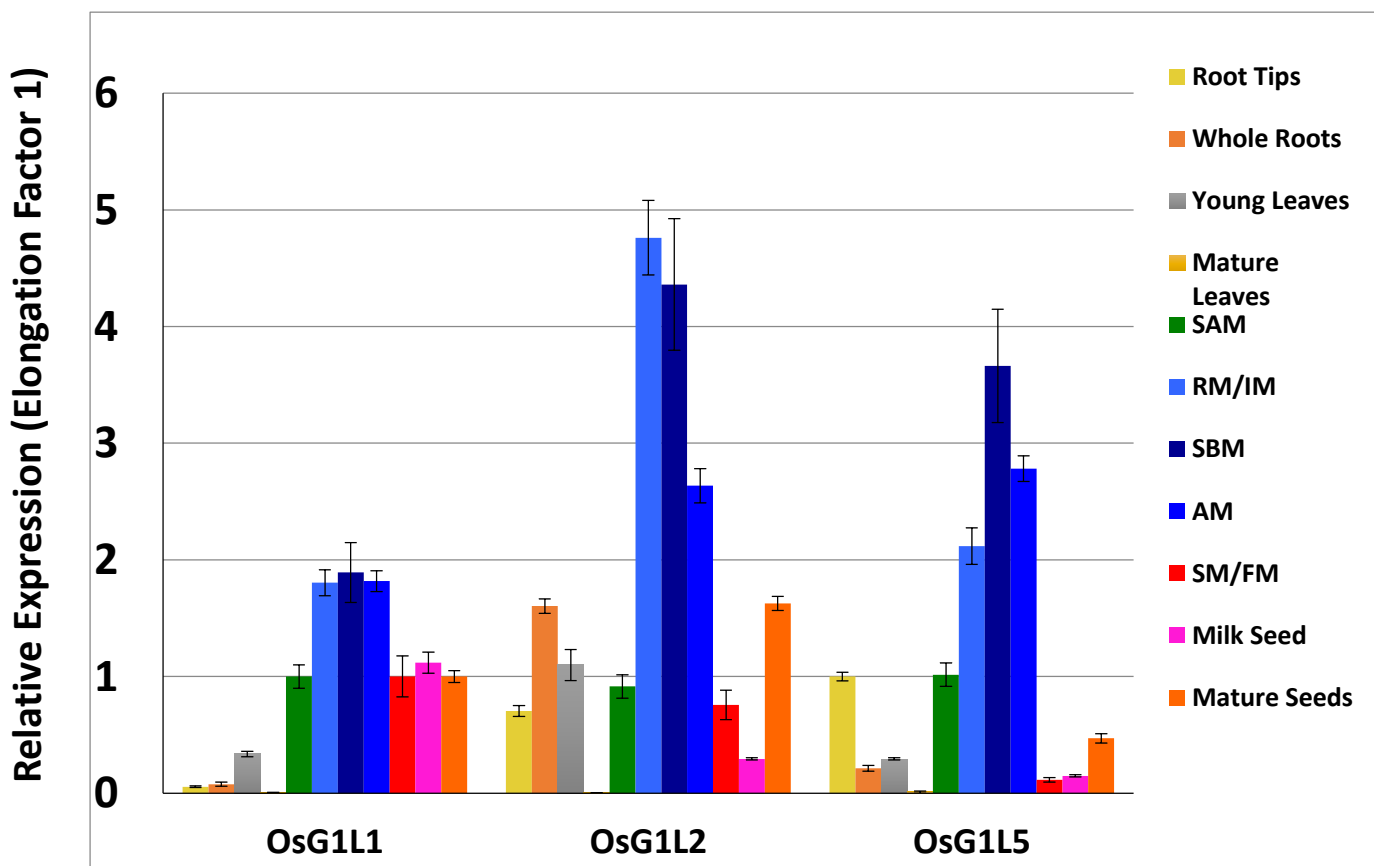

Figure 38. Expression analysis of the *G1L1, G1L2* and *G1L5* across different tissues including vegetative, reproductive and fruit tissues.

2.7.2 Expression analysis of *g1l1* and *g1l2* by *in situ* hybridization across reproductive meristems

To Further investigate the spatial and temporal expression of *G1L1* and *G1L2* during early panicle development we performed an RNA *in situ* hybridization on 4 different meristem samples: RM, PMB, SBM and SM. We used a highly specific antisense digoxigenin- labelled RNA probes for *G1L1, G1L2* and *G1L5*. Both *G1L1* and *G1L2* genes showed a similar expression as *G1L5* in all the meristem types including IM, BMs and SM as shown in [**Figure 39**]. In particular, they were expressed at the tip of the primordia, where the pool of meristematic cells is maintained (Ud In, unpublished).
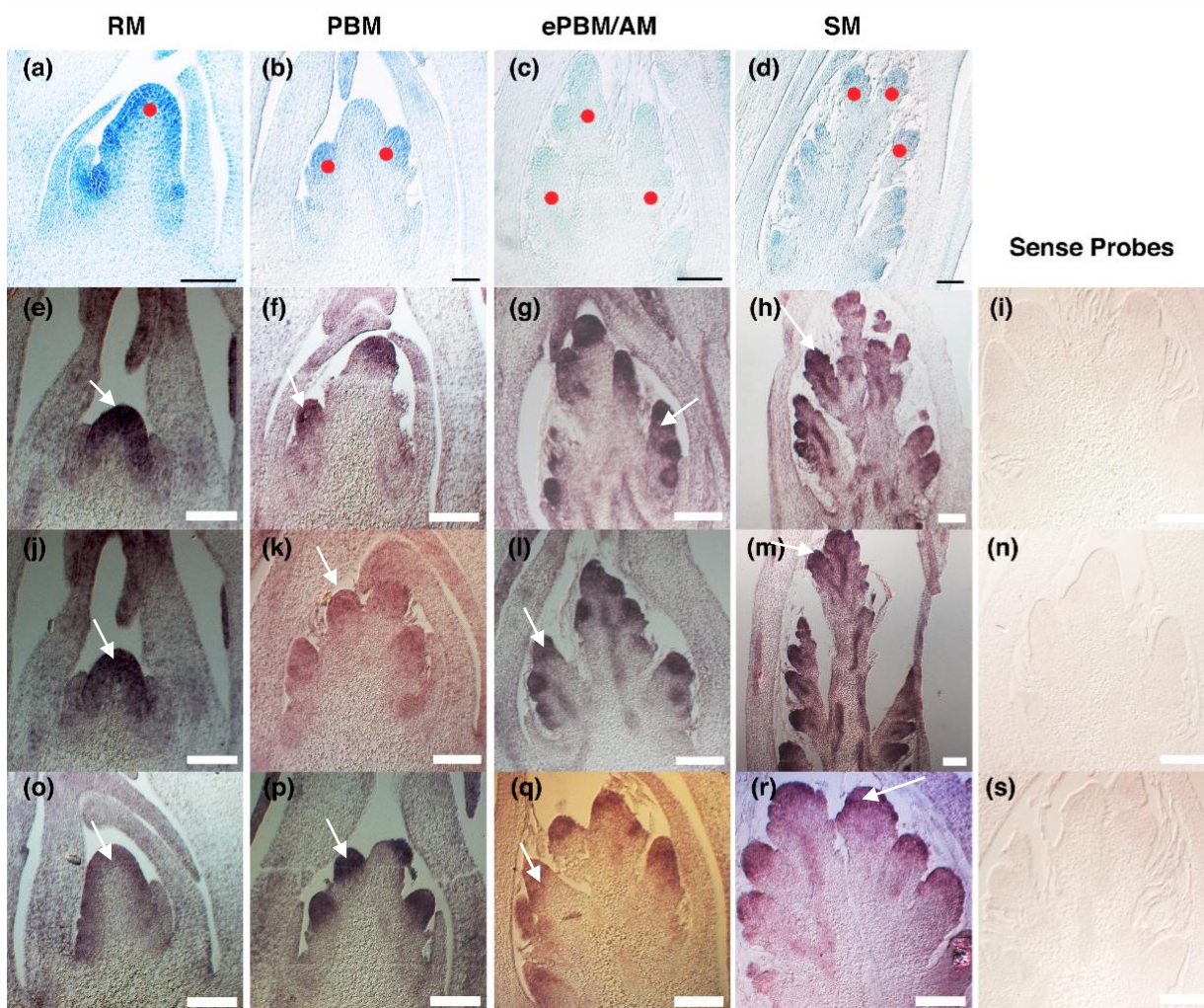

Figure 39. Expression pattern of G1L1, G1l2 and G1l5 analysed by *in situ* hybridization at four stages. Representation of four meristematic stages analysed (a-d) where red dots (●) indicate respectively the different meristematic tissues: RM (a), PBM (b), e PBM/AM (c) and SM (d). *G1L1* Antisense probe (e-h), *G1L1* sense negative control probe (i), *G1L2* antisense probe (j-m), *G1L2* sense negative control probe (n), *G1L5* antisense positive control probe (o-r), *G1l5* sense negative control probe (s). The signal is restricted in each meristematic tissue for each gene in exam (↘). Scale bars represent 50 μm (a-c) and 100 μm (d-s).

2.8. GENERATION OF MUTANT LINES
2.8.1 Generation of K.O mutants by CRISPR-CAS9 technology

To functional characterize *G1L1* and *G1L2* we generated knock-out mutants by CRISPR-Cas9 technology. Specific gRNAs were designed for both genes, cloned in single and multiple CRISPR-Cas9 constructs [181,182] and then used to transform rice plants by *Agrobacterium tumefaciens* to generate single and double mutants. In particular, the *G1L1* protospacer was designed to target the first exon at 397 bp from the ATG, in the last 50 nucleotides that translate the ALOG domain. sgRNA for *G1L2* (*OS06G0672400*) was designed to target a region at 131 bp downstream from the ATG start codon **[Figure 40]**. Also in this case, the mutation is expected to be located at the beginning of the ALOG domain and will produce a none functional protein. The same gRNAs was cloned in two different constructs, single and multiplex in order to obtain single and double mutants.
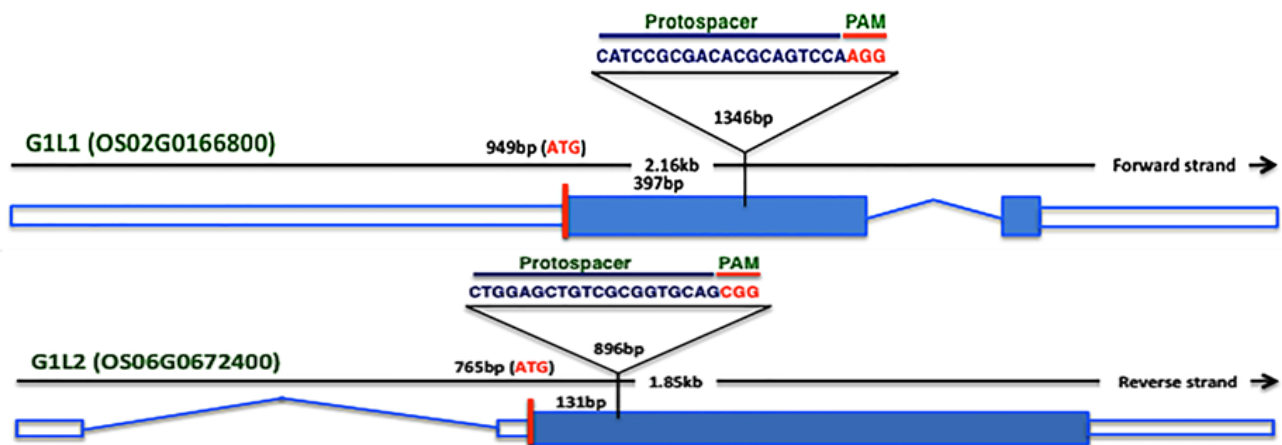

Figure 40. Protospacer designed for *G1L1* and *G1L2*.

The *g1l2* single mutant was the first mutant obtained. We identified different mutant alleles for *G1l2* across 18 T0 transgenic plants. Cas9 produced a frame shift mutation due to an insertion of one base pair at 3 bp from the PAM site and at 148 bp from the ATG in heterozygosity or that showed a biallelic mutation The A insertion will lead to the formation of a premature stop codon TGA instead of a codon encoding Cysteine (TGC) at 148 bp from ATG resulting in a truncated protein of 49 a.a. without functional ALOG domain and putative NLS. The insertion of other bases instead leads to the formation of longer proteins with a length of 176 a.a but always without ALOG domain and putative NLS **[Figure 41]**. Two alleles, the A and C insertions, were taken to the T1 generation to segregate Cas9; the phenotypical analysis was performed in the T2 generation.

Figure 41. A. *g1l2* chromatogram. B. WT e Mutant protein alignment. In evidence the ALOG domain (➖), stop codon (◯) and NLS(☐)

We obtained only 6 transgenic plants with a sgRNA specific for *G1L1*. One of these resulted WT for the G1L1 gene despite of the presence of the Cas9 construct, the other 5 plants instead resulted in homozygous or biallelic mutants. Two transformant lines showed respectively a deletion of 6 bp GCAGTC at 143 bp from the ATG and a deletion of 3 bp AGT t 145 bp from the ATG. These mutations were in frame and therefore are likely to result in functional proteins missing one or two

a.a.. Two plants instead showed an AG deletion at 145 bp from the ATG that led to frame shift mutation resulting in the formation of a protein without the putative NLS and hence is likely not functional **[Figure 42]**, and the last plant showed a AG/AGT biallelic mutation. This plant, due to environmental condition didn't produce any seeds, therefore, we couldn't propagate it in the next generation.
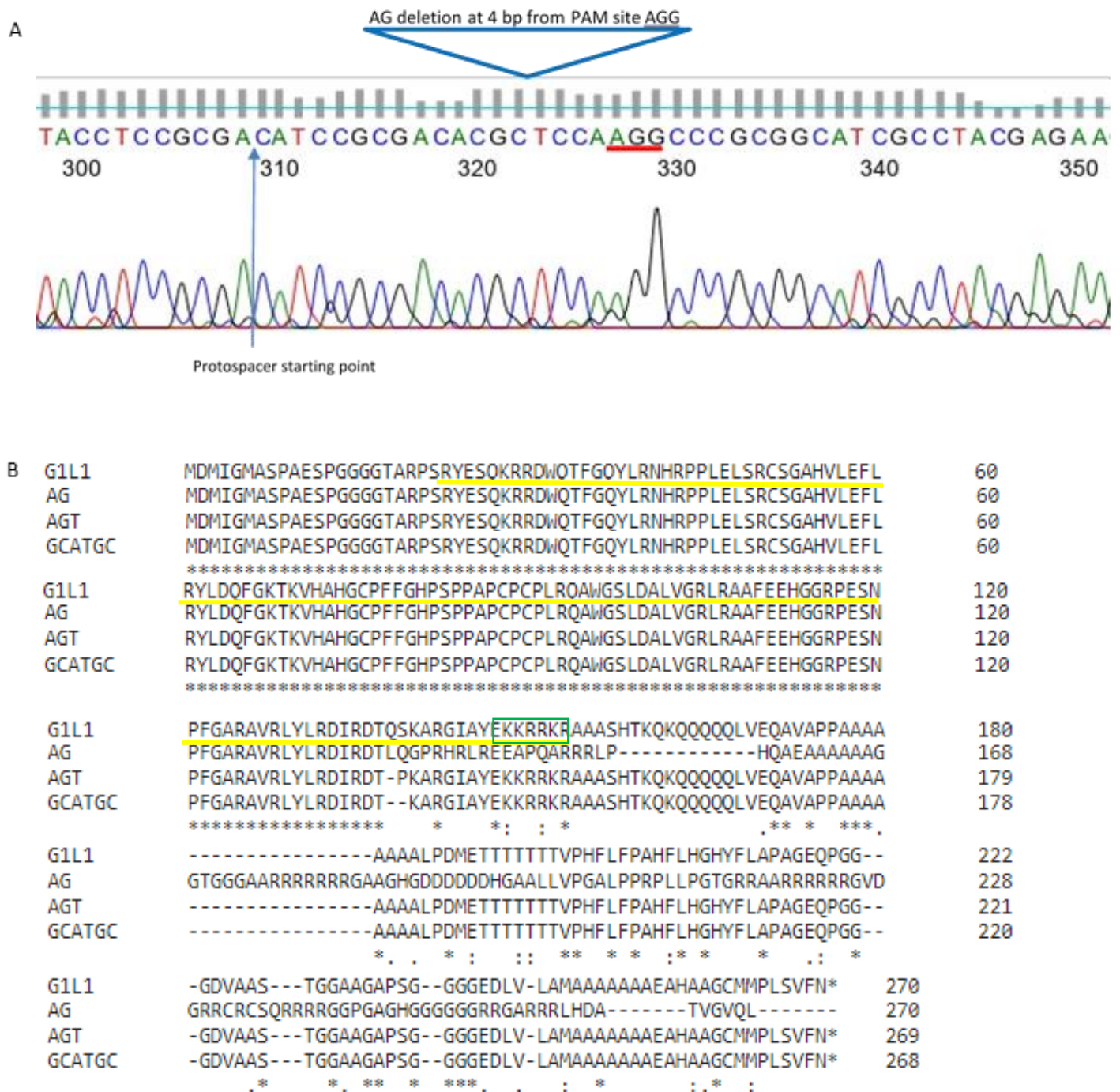

A

AG deletion at 4 bp from PAM site AGG

Protospacer starting point

B

```
G1L1    MDMIGMASPAESPGGGGTARPSRYESQKRRDWQTFGQYLRNHRPPLELSRCSGAHVLEFL    60
AG      MDMIGMASPAESPGGGGTARPSRYESQKRRDWQTFGQYLRNHRPPLELSRCSGAHVLEFL    60
AGT     MDMIGMASPAESPGGGGTARPSRYESQKRRDWQTFGQYLRNHRPPLELSRCSGAHVLEFL    60
GCATGC  MDMIGMASPAESPGGGGTARPSRYESQKRRDWQTFGQYLRNHRPPLELSRCSGAHVLEFL    60
        ************************************************************

G1L1    RYLDQFGKTKVHAHGCPFFGHPSPPAPCPCPLRQAWGSLDALVGRLRAAFEEHGGRPESN   120
AG      RYLDQFGKTKVHAHGCPFFGHPSPPAPCPCPLRQAWGSLDALVGRLRAAFEEHGGRPESN   120
AGT     RYLDQFGKTKVHAHGCPFFGHPSPPAPCPCPLRQAWGSLDALVGRLRAAFEEHGGRPESN   120
GCATGC  RYLDQFGKTKVHAHGCPFFGHPSPPAPCPCPLRQAWGSLDALVGRLRAAFEEHGGRPESN   120
        ************************************************************

G1L1    PFGARAVRLYLRDIRDTQSKARGIAYEKKRRKRAAASHTKQKQQQQQLVEQAVAPPAAAA   180
AG      PFGARAVRLYLRDIRDTLQGPRHRLREEAPQARRRLP------------HQAEAAAAAAG   168
AGT     PFGARAVRLYLRDIRDT-PKARGIAYEKKRRKRAAASHTKQKQQQQQLVEQAVAPPAAAA   179
GCATGC  PFGARAVRLYLRDIRDT--KARGIAYEKKRRKRAAASHTKQKQQQQQLVEQAVAPPAAAA   178
        *****************    *    *:  : *          .** *   ***.

G1L1    ---------------AAAALPDMETTTTTTTVPHFLFPAHFLHGHYFLAPAGEQPGG--   222
AG      GTGGGAARRRRRRRGAAGHGDDDDDDHGAALLVPGALPPRPLLPGTGRRAARRRRRRGVD   228
AGT     ---------------AAAALPDMETTTTTTTVPHFLFPAHFLHGHYFLAPAGEQPGG--   221
GCATGC  ---------------AAAALPDMETTTTTTTVPHFLFPAHFLHGHYFLAPAGEQPGG--   220
        *. .  * :   :: ** * * ;* *      *   .: *

G1L1    -GDVAAS---TGGAAGAPSG--GGGEDLV-LAMAAAAAAAEAHAAGCMMPLSVFN*    270
AG      GRRCRCSQRRRRGGPGAGHGGGGGGGRRGARRRLHDA-------TVGVQL-------    270
AGT     -GDVAAS---TGGAAGAPSG--GGGEDLV-LAMAAAAAAAEAHAAGCMMPLSVFN*    269
GCATGC  -GDVAAS---TGGAAGAPSG--GGGEDLV-LAMAAAAAAAEAHAAGCMMPLSVFN*    268
        .*    *. ** * ***.  .  :  *       :.* :
```

Figure 42. A. *g1l1* chromatogram. WT e Mutant protein alignment. In evidence the ALOG domain (▬) and NLS (▢)

By transformation with the multiplex construct, we obtained 10 regenerant plants with the Cas9 construct. Three of them resulted in WT, line #7 resulted in homozygote for both genes (*g1l1 g1l2*) and the other 6 lines resulted in homozygote for *G1L1* and heterozygote for *G1L2 (g1l1 g1l2/+)* **[Table 2].** With this strategy, we were able to obtain different mutations in the *G1L1* sequence compared to the one obtained with a single gRNA construct, whereas for *G1L2* we obtained the same mutation as in the single mutant **[Table 2]**. All the new mutations in *G1L1* led to a frame-shift mutation **[Figure 43].** These plants were taken to the T1 generation where we obtained the *g1l1* single mutants, and the *g1l1 g1l2/+, g1l1 g1l2* double mutants. Subsequently, we used *g1l1* and *g1l2* single and double mutants for phenotypical analysis although *g1l1 g1l2* mutant produced only a few seeds.

T0	G1L1	G1L2
#1	del 5 bp CGCAG	hetero T insertion
#5	AG deletion	hetero T insertion
#7	G deletion	homo T insertion
#12	AG deletion	hetero T insertion
#13	T/A insertion	hetero T insertion
#19	WT	WT
#21	WT	WT
#22	WT	WT
#25	T insertion/ AGT deletion	hetero A insertion
#28	GCAG del homo	hetero C insertion

Table 2. Genotyping T0 regenerant plants transformed with multiplex CRISPR-Cas9 construct

```
G1L1    MDMIGMASPAESPGGGGTARPSRYESOKRRDWOTFGQYLRNHRPPLELSRCSGAHVLEFL   60
G       MDMIGMASPAESPGGGGTARPSRYESQKRRDWQTFGQYLRNHRPPLELSRCSGAHVLEFL   60
GCAG    MDMIGMASPAESPGGGGTARPSRYESQKRRDWQTFGQYLRNHRPPLELSRCSGAHVLEFL   60
A       MDMIGMASPAESPGGGGTARPSRYESQKRRDWQTFGQYLRNHRPPLELSRCSGAHVLEFL   60
T       MDMIGMASPAESPGGGGTARPSRYESQKRRDWQTFGQYLRNHRPPLELSRCSGAHVLEFL   60
        ***********************************************************

G1L1    RYLDQFGKTKVHAHGCPFFGHPSPPAPCPCPLRQAWGSLDALVGRLRAAFEEHGGRPESN  120
G       RYLDQFGKTKVHAHGCPFFGHPSPPAPCPCPLRQAWGSLDALVGRLRAAFEEHGGRPESN  120
GCAG    RYLDQFGKTKVHAHGCPFFGHPSPPAPCPCPLRQAWGSLDALVGRLRAAFEEHGGRPESN  120
A       RYLDQFGKTKVHAHGCPFFGHPSPPAPCPCPLRQAWGSLDALVGRLRAAFEEHGGRPESN  120
T       RYLDQFGKTKVHAHGCPFFGHPSPPAPCPCPLRQAWGSLDALVGRLRAAFEEHGGRPESN  120
        ***********************************************************

G1L1    PFGARAVRLYLRDIRDTQSKARGIAYEKKRRKRAAASHTKQKQQ-----QQQLVEQAVAP  175
G       PFGARAVRLYLRDIRDTHPRPAASPTRRSAASAPPPPTPSRSSSSSSWWNRRWRRPPPPP  180
GCAG    PFGARAVRLYLRDIRDT-PRPAASPTRRSAASAPPPPTPSRSSSSSSWWNRRWRRPPPPP  179
A       PFGARAVRLYLRDIRDTQYQGPRHRLREEA------PQA----------RRRLPHQAEAA  164
T       PFGARAVRLYLRDIRDTQFQGPRHRLREEA------PQA----------RRRLPHQAEAA  164
        ****************  :        ...                    .::   .

G1L1    PAAAA-----------------AAAALPDMETTT------------------TTTTVP   198
G       PPRR----CRTWRRRRRRPRCRTSCSRRTSSTATTSWHRPASSPAAATSRRRRAALPVLP  236
GCAG    PPRR----CRTWRRRRRRPRCRTSCSRRTSSTATTSWHRPASSPAAATSRRRRAALPVLP  235
A       AAAAGGTGGGAARRRRRR-RGAAGHGDDDDDDHG-------------------AALLVP  203
T       AAAAGGTGGGAARRRRRR-RGAAGHGDDDDDDHG-------------------AALLVP  203
            :.  .     .                              :    :*

G1L1    HFLFPAHFL-HGHYFLAPAGEQPGG---GDVAAS---TGGAAGAPSG--GGGEDLV-LAM  248
G       AAAAGRTWCWPWRRRRRPPRR-TPPAA*CHCRCST------------------------  269
GCAG    AAAAGRTWCWPWRRRRRPPRR-TPPAA*CHCRCST------------------------  268
A       GALPPRPLL-PGTGRRAARRRRRRGVDGRRCRCSQRRRRGGPGAGHGGGGGGGRRGARRRL  262
T       GALPPRPLL-PGTGRRAARRRRRRGVDGRRCRCSQRRRRGGPGAGHGGGGGGGRRGARRRL  262
                      .            .*

G1L1    AAAAAAAEAHAAGCMMPLSVFN*           270
G       ----------------------           269
GCAG    ----------------------           268
A       HDA-------TVGVQL-------           271
T       HDA-------TVGVQL-------           271
```

Figure 43. WT e Mutant protein alignment. In evidence the ALOG domain (▬) and NLS (☐)

2.8.2. Generation of overexpression line for *G1L1* and *G1L2* and expression analysis in leaves by qRT-PCR

In order to check if overexpression of *G1L1* or *G1L2,* like observed for *TAW1*, could delay the SM transition resulting in a higher number of branches, transgenic lines expressing *G1L1* or *G1L2* from the rice Actin 1 promoter (pACT1) were generated. Six regenerant plants (#1, #2, #3, #4, A, B), with *pACT1::G1L1* construct, were obtained by calli transformation whereas unfortunately, after selection, we were unable to regenerate plants from *pACT1-G1L2* calli that, instead of becoming greener and differentiating the shoot organs like the *pACT1-G1L1*, they showed a high proliferation rate and bigger size **[Figure 44]**.

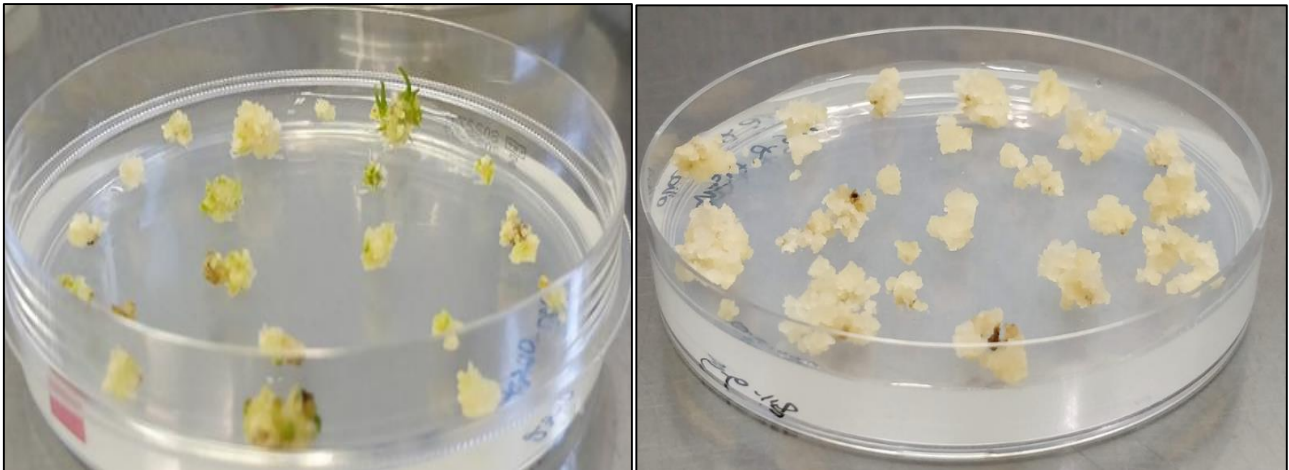*Figure 44. pACT1::G1L1 and pACT1::G1L2 calli in N6-R regeneration medium.*

They were transferred to soil and subsequently young leaves were sampled to perform RNA extraction and cDNA synthesis for the analysis of *G1L1* transcript levels. In WT leaves *G1L1* expression was almost absent whereas the transformants showed high expression of *G1L1* transcripts **[Figure 45]**
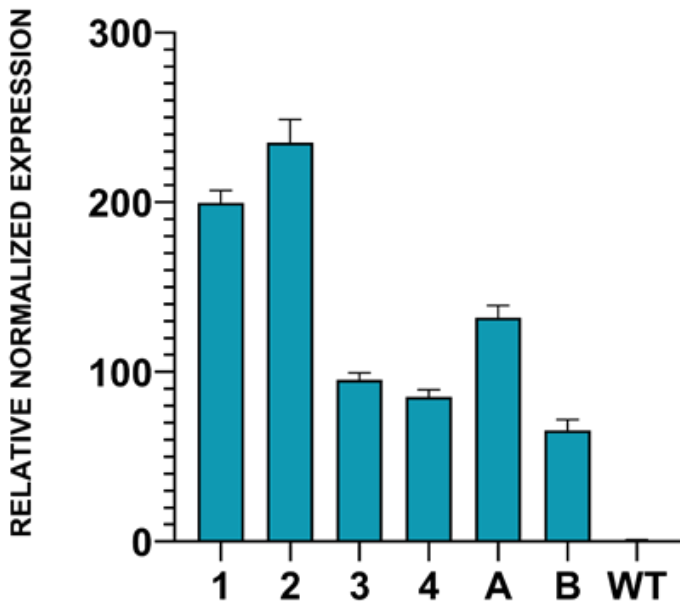
Figure 45 . Transcript level of *G1L1* in WT and *pACT1::G1L1* line normalized on EF1.

Unfortunately, these plants all died. This could be due to the overexpression but might also be influenced by environmental conditions in the green house (like blast disease). To investigate this further, we performed new transformation experiments in which the CDS of *G1L1* and *G1L2* was expressed from the *Ubiquitin* promoter instead of the *ACT1* promoter. 18 regenerant plants containing *pUBI::G1L1* construct and 53 regenerant plant containing *pUBI::G1L2* construct were obtained. Of these one, only 8 pUBI::G1L1 and 16 pUBI::G1L2 were sampled for expression analysis at 15 days **[Figure 46]** after transplanting in soil.
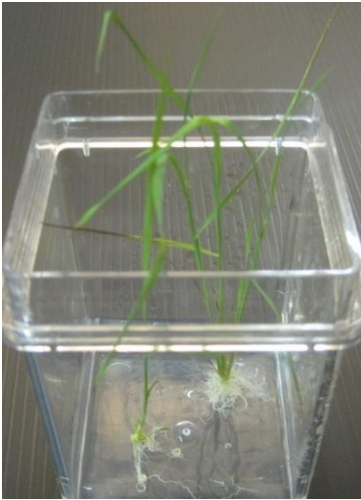
Figure 46. 15 days old-seedling regenerant plant ready to move in soil.

Regenerant plants with the *pUBI::G1L1* construct showed different expression levels of the transcript. Compared to endogenous levels of *G1L1* in WT plants the transformants overexpressing *G1L1* showed a range of expression levels from 10-fold to 5000-fold whereas **[Figure 47]**. Compare to endogenous levels of *G1L2* in WT plants, the transformants overexpressing *G1L2* instead showed a range of expression levels from 2-fold to 16-fold **[Figure 48]**. These plants are flowering and phenotypical analysis will be performed on T1 stable mutants. The T0 plants, indeed, are more variable in phenotype since they came from in vitro culture.
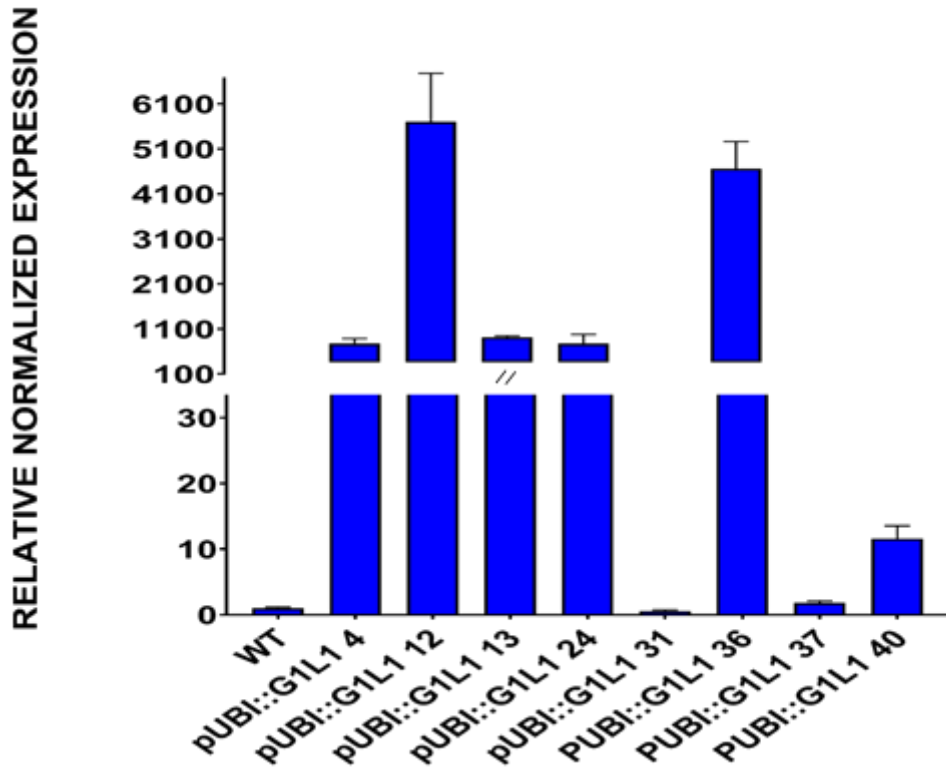
Figure 47. Transcript level of *G1L1* in WT and *pUBI::G1L1* line normalized on EF1
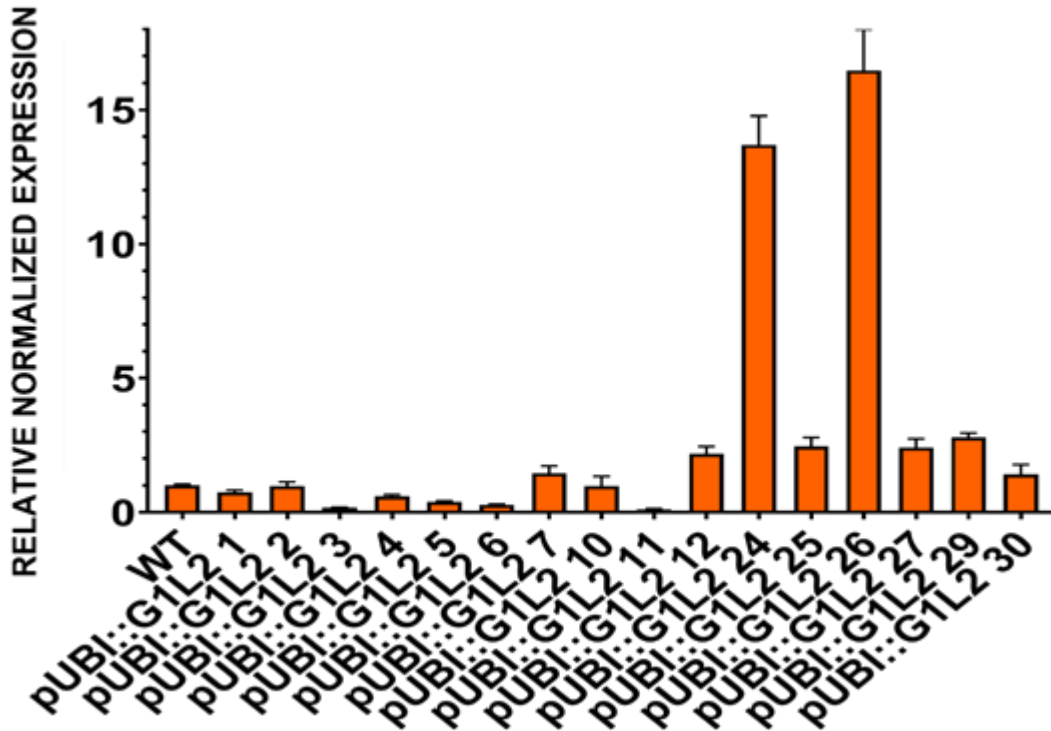
Figure 48. transcript level of *G1L2* in WT and *pUBI::G1L2* line normalized on EF1.

2.9. PHENOTYPICAL ANALYSIS

2.9.1 Preliminary Phenotypical Analysis on *g1l1, g1l2, g1l1g1l2/+* and *g1l1g1l2* plant.

A preliminary phenotypical analysis of the panicle structure was performed on T2 *g1l1, g1l2, g1l1g1l2(+/-)* lines and T1 *g1l1g1l2* double mutant plants. Plants were grown in the phytotron under controlled conditions. The main panicle of each plant was collected at the stage when seeds were mature and by hand, the main panicle traits such as panicle length, number of primary branches, number of secondary branches and number of spikelets were measured. The Graphpad Prism 8 program was used to make box-plots and for statistical analysis we use One-Way ANOVA test followed by Tukey test considering $p < 0,05$ **[Figure 49]**. a total of 58 plants were analysed: 12 were WT, 19 *g1l1* (homo AG deletion mutation), 14 *g1l2* (homo C insertion mutation), 10 *g1l1(-/-) g1l2(+/-)*3 *g1l1 g1l2* **[Table 3].**

g1l1g1l2(+/-) line	*G1L1* mutation	*G1l2* mutation
#28.1.6	Homo GT deletion	Hetero A insertion
#28.1.7	Homo GT deletion	Hetero A insertion
#1.4.3	Homo AG deletion	Hetero T insertion
#1.4.5	Homo AG deletion	Hetero T insertion
#1.4.8	Homo AG deletion	Hetero A insertion
#1.4.10	Homo AG deletion	Hetero G insertion
#1.4.16	Homo AG deletion	Hetero T insertion
#1.4.17	Homo AG deletion	Hetero G insertion
#1.4.19	Homo AG deletion	Hetero A insertion
#12.3.8	Homo AG deletion	Hetero A insertion
g1l1g1l2 line	*G1L1* mutation	*G1l2* mutation
#28.4	Homo GT deletion	homo A insertion
#28.10	Homo GT deletion	homo A insertion
#1.4.12	Homo AG deletion	homo A insertion

Table 3. *g1l1g1l2(+/-)* and *g1l1g1l2* mutant lines used for phenotypical analysis.

Unfortunately, a combination of poor growing conditions and an infection by rice blast, caused slow growth, low yield and high variability. We obtained WT plants with around 40 seeds and 7 primary branches instead of 150 seed and 10 PB that they normally produced. The high variability made the data less reproducible. Furthermore, we had only three double homozygous mutants to analyse, a very low number to work with. By this statistical analysis the number of PBs didn't show any significant difference between mutants and WT, even if the median value of *g1l2* and *g1l1 g1l2* is lower than the WT. The *g1l1 g1l2* mutant had significantly less secondary branches; also *g1l2* produced fewer branches compare to WT even if it didn't result in statistical significant. However, the data are very flat towards zero, gathering a non-gaussian distribution, not very much suitable for the statistical analysis. The *g1l2* and *g1l1g1l2* panicles had fewer spikelets even if for the double mutant it was not significant. Furthermore, all the mutant genotypes had a higher percentage of sterile spikelets that didn't undergo grain filling. Sterility seems to be worse in the double mutant, where 2 among 3 panicles didn't produce any seeds. Any significant difference in panicle length was observed between mutants and WT. It could consider this analysis as a preliminar in which *g1l1* and *g1l1(-/-) g1l2(+/-)* plants didn't show significant differences in respect to the WT in any of the traits taken into consideration in contrast to *g1l2* and *g1l1g1l2* that seemed to be affected in branching and spikelets number.
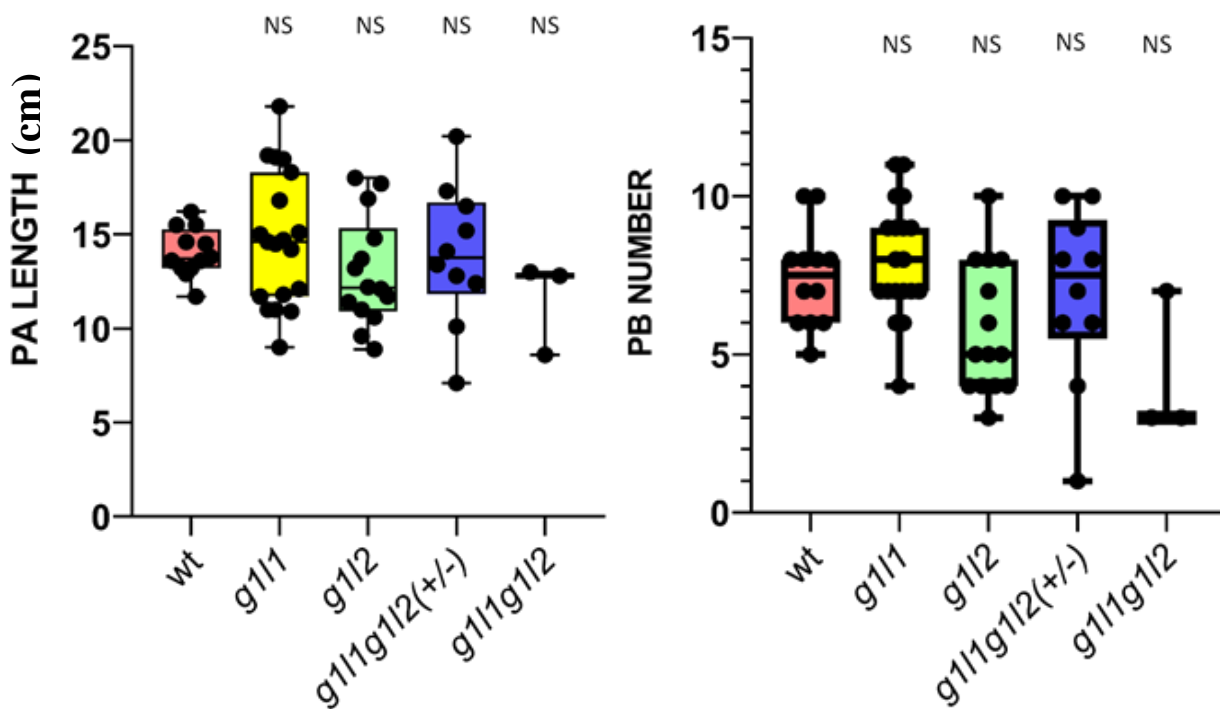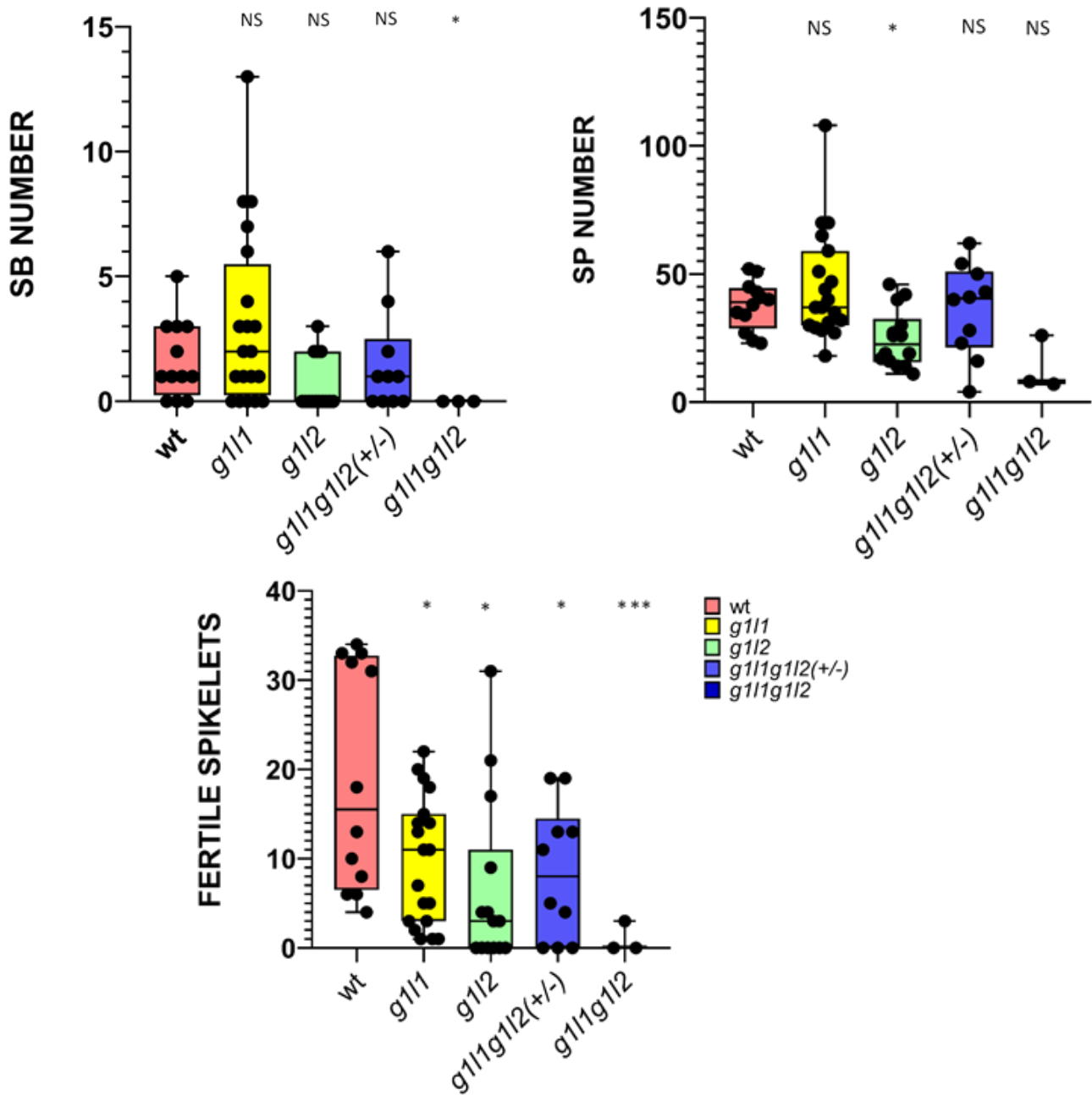
Figure 49. Phenotypical analysis on WT, *g1l1, g1l2, g1l1g1l2* *(+/-)* **and** *g1l1g1l2.* ** p-value < 0,05; *** p-value<0,001*

2.9.1.1 Flowering time

We performed also flowering time analysis on the mutant plants and WT to find possible differences since the floral transition is often connected with flowering time. In particular, we measured the time span between the flower induction (plants moved in SD conditions) and heading, when the first panicle emerges from flag leaf, for a total of 45 plants: 8 WT, 15 *g1l1, 15 g1l2, 6 g1l1 g1l2/+* and *3 g1l1 g1l2*. The *g1l2* mutant flowered on average 5 days later than the WT, while other genotypes didn't show any significant difference **[Figure 50].** There is not much information on flowering time phenotypes attributable to *ALOG* genes; *TAW1* itself doesn't show any difference in flowering time [5] even If K.O mutant of its homolog, *TFM*, is early flowering. Further analysis should be done to elucidate the role of *G1L2* in flowering time.
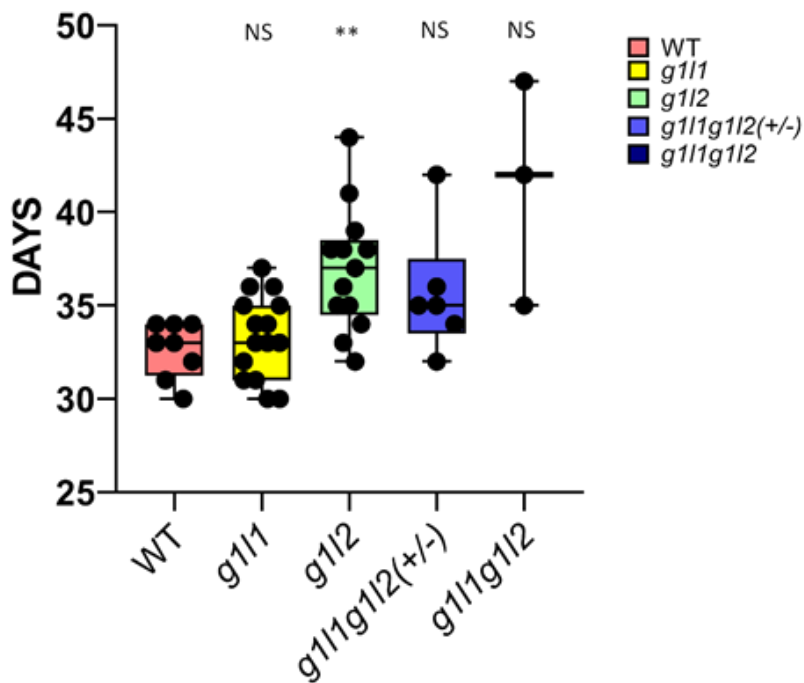
Figure 50. Flowering time in Wt and mutant lines. ** p< 0,01

2.9.1.2 Pollen viability Test

A preliminary experiment was performed on 3 WT and 3 *g1l1g1l2* spikelets to understand whether the sterility of the mutants was related to pollen viability using a variant of Alexander's staining which is less toxic and faster [183]. It is a simplified method that stains with different colour, magenta-red and blue-green, respectively aborted and non-aborted pollen grains. This preliminary analysis didn't show a relevant difference between WT and the mutant **[Figure 51]** suggesting that male gametophyte development is not affected in the double mutant. Further analysis should be done to understand whether the sterility observed in this line is linked to defects during female gametophyte development or embryogenesis.
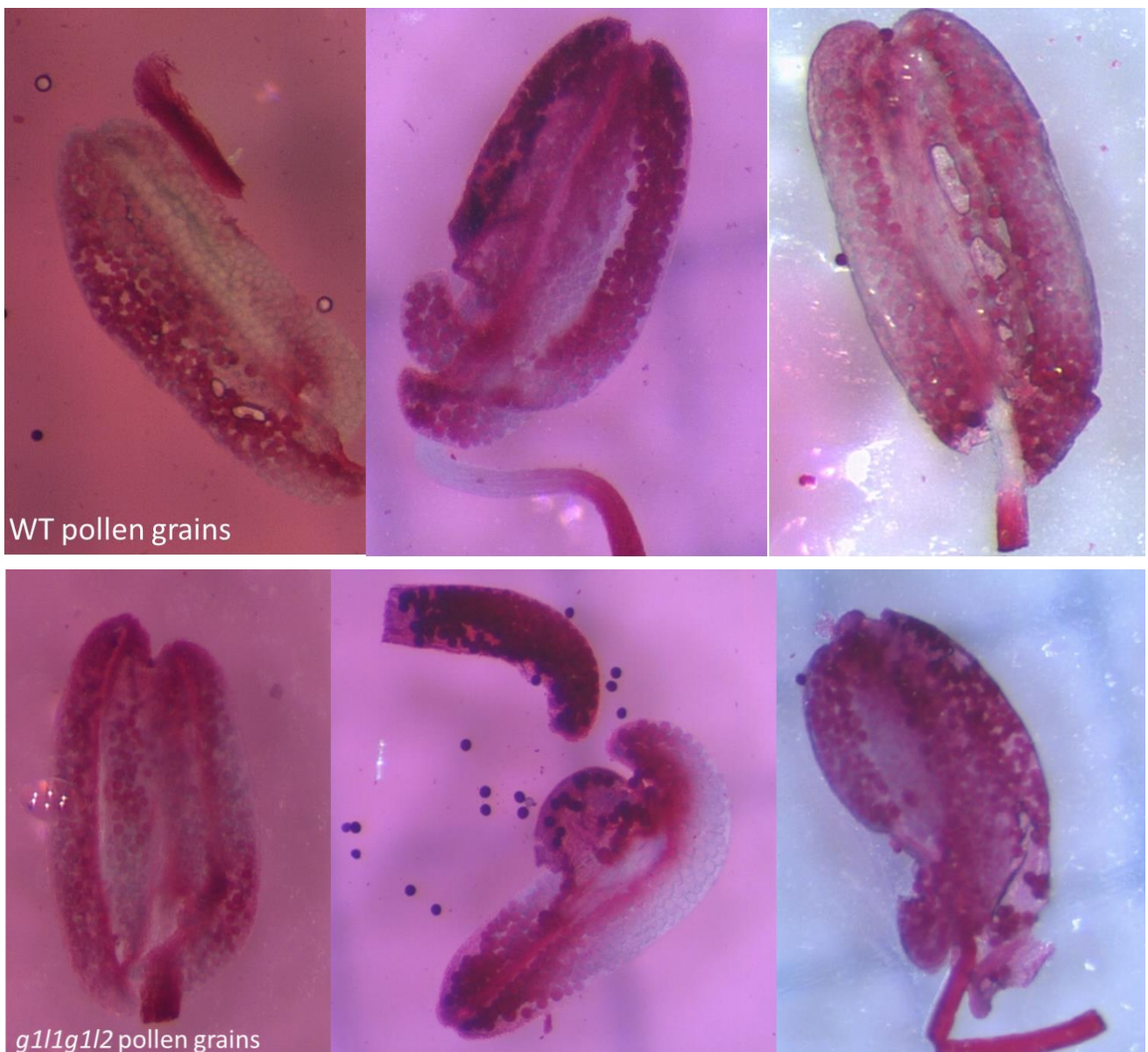
Figure 51. Pollen viability Test on WT and *g1l1g1l2*.

2.9.2 Phenotypical Analysis with P-Trap.

To obtain a more detailed and statistically sound analysis of the mutant panicles we collaborated with the group of Dr. Jouannic at IRD in Montpellier. For the analysis only *g1l1* and *g1l2* line were compared with WT since the number of double mutant seeds was not enough. Twenty plants for each genotype were analysed, to obtain a robust statistical analysis, using P-TRAP software [184]. This software developed by the group of Dr. Jouannic is able to measure all characteristics (like branch and seed numbers, internode length etc.) related to the panicle that with a specific package in R can be graphically visualized. *g1l1* and *g1l2* produced significantly shorter panicles than WT and with fewer PBs, SBs and spikelets. In particular, *g1l1* produced panicles which were on average two cm shorter than WT and with on average 3 PB and 30 spikelets less than WT **[Figure 52]**. *g1l2* instead produced panicles that were on average shorter than 1.5 cm compared to WT and with on average 4 PBs, 8 SBs and 51 spikelets less than WT **[Figure 52]**. Exhaustive analysis revealed also that mutant lines had longer PBs and SBs then WT with longer internodes in PBs **[Figure 52].** In detail, *g1l1* showed PBs and SBs that were respectively on average 1 cm and 0.5 cm longer than WT with internodes in PBs which were on average 0.4 cm longer than WT; *g1l2* instead produced PBs and SBs which were respectively on average 1.6 cm and 1 cm longer than WT with internode in PBs which were on average 0.7 cm longer than WT. A schematic representation of the panicle structure and grain number for each genotype is shown in **Figure 53.** Furthermore, as shown in **Figure 54 t**he topology of the panicle in mutants is different compared to WT. *g1l1* and *g1l2* produced also smaller grains than WT. Both *g1l1* and *g1l2* seeds showed a smaller area than WT, but whereas *g1l1* seeds resulted shorter and narrower than WT; *g1l2* seeds showed a reduction only in seed width compare to WT **[Figure 55].** The mutants didn't show changes in plant height and tiller numbers, suggesting that the vegetative part remained unaffected by the mutation **[Figure 56]**. These data indicate that these genes play a role during the reproductive phase and in particular in branching.
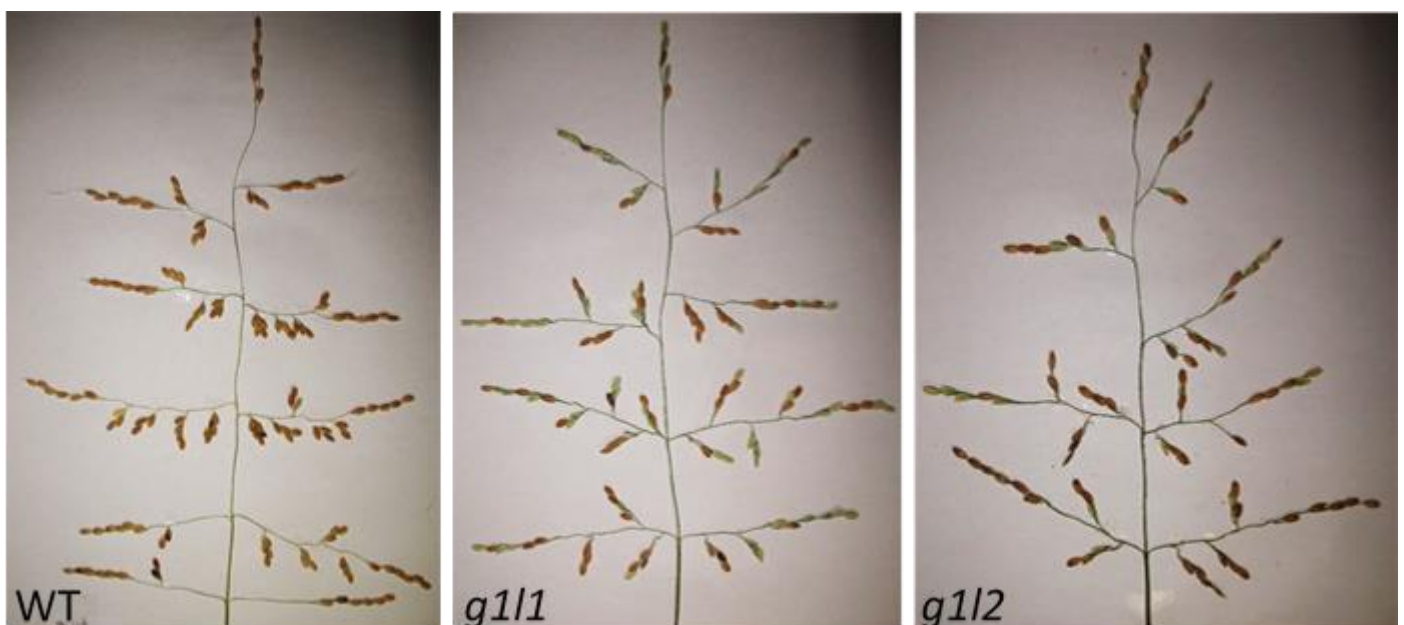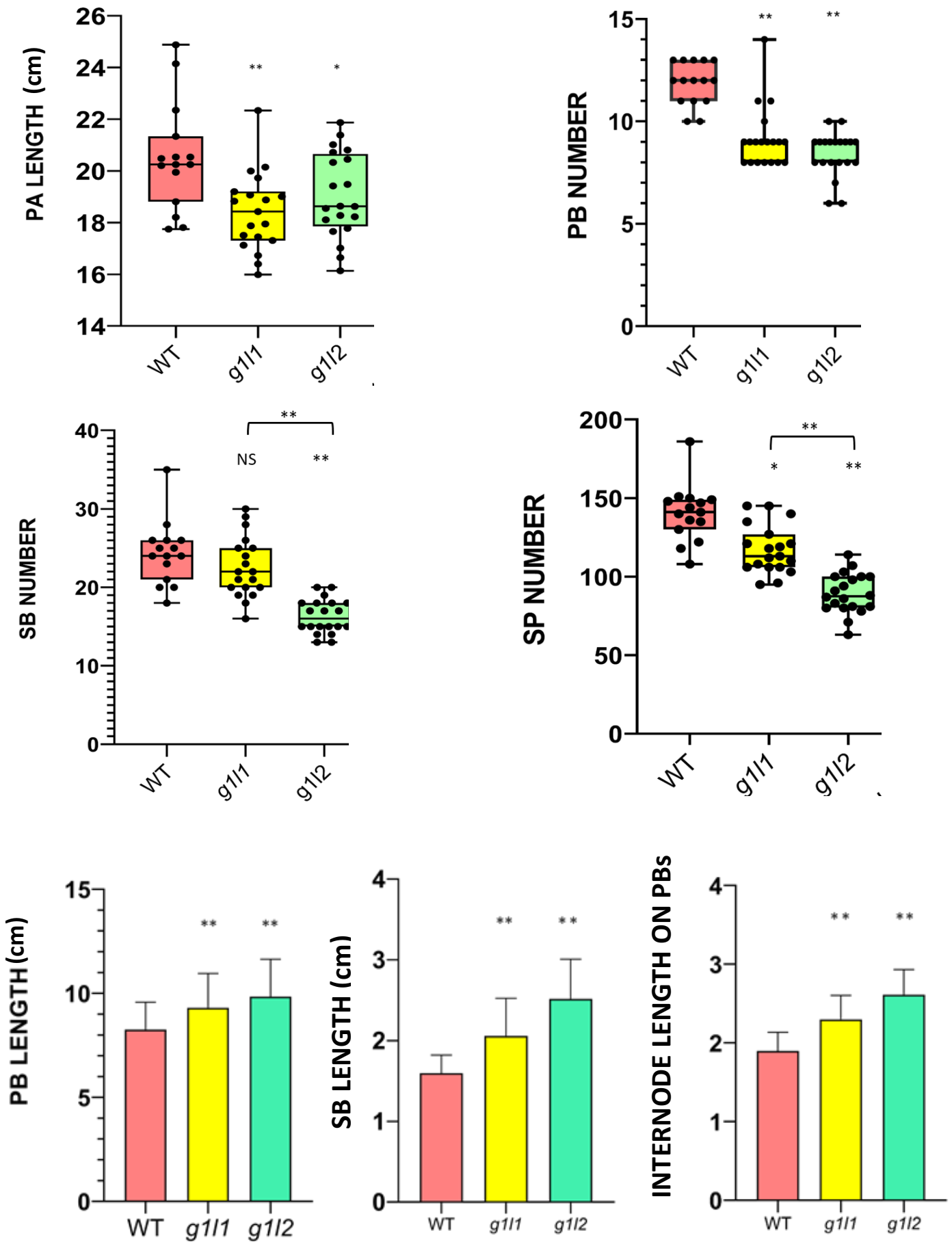
Figure 52. Phenotypical analysis on Panicle structure in WT, *g1l1* and *g1l2*. Graphs obtained using GraphPad Prism 8. One-Way ANOVA with Tukey test; **p<0,01; * p<0,05
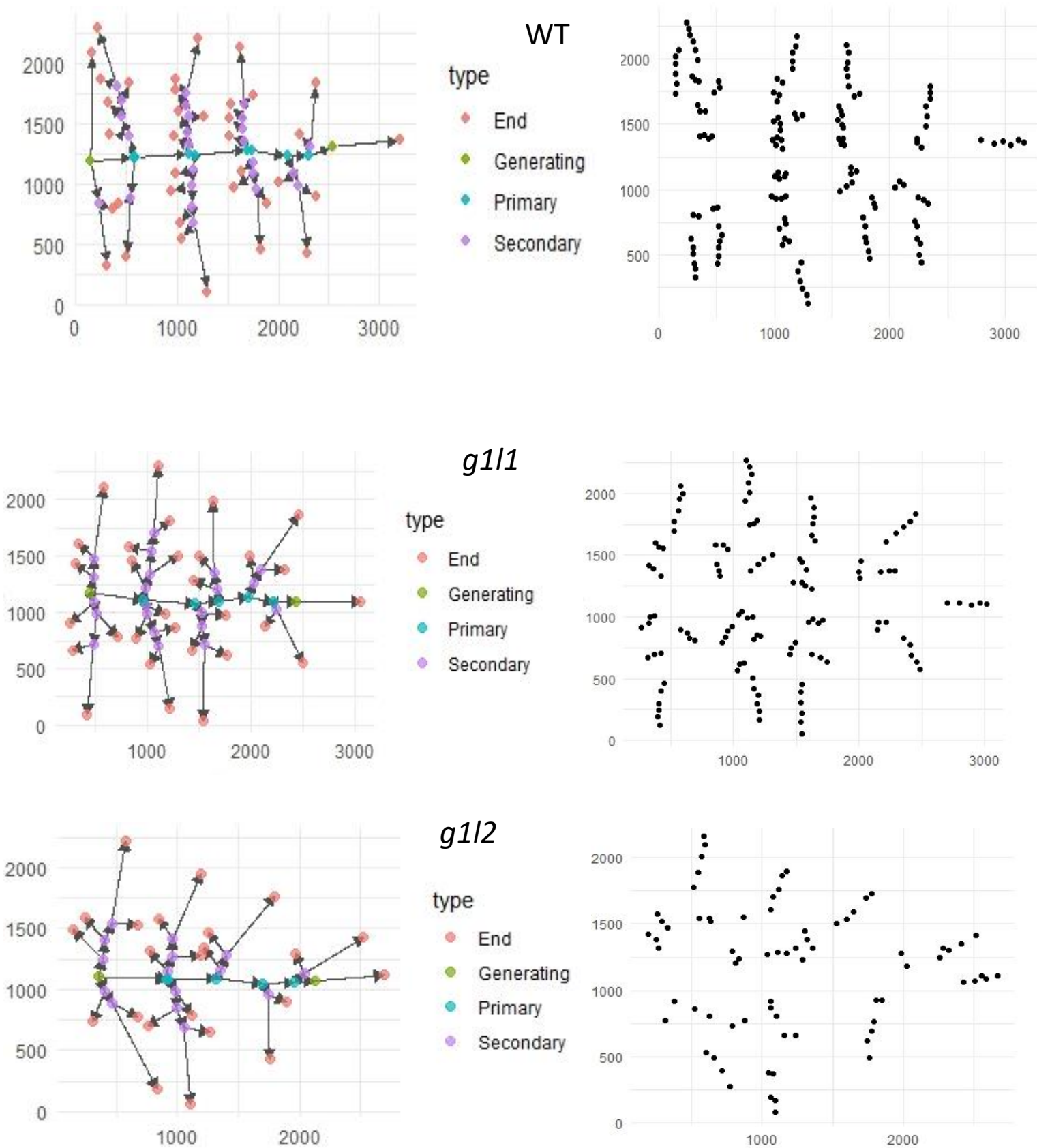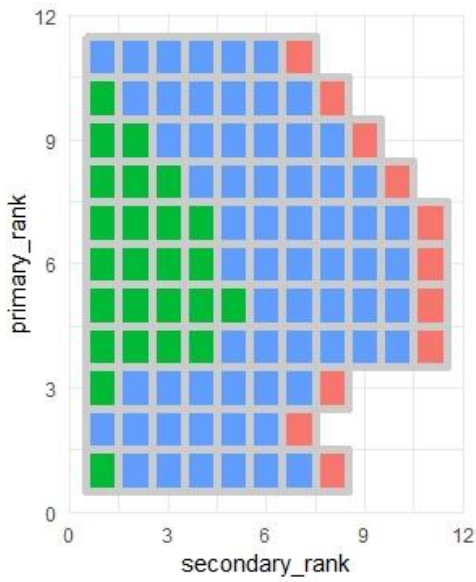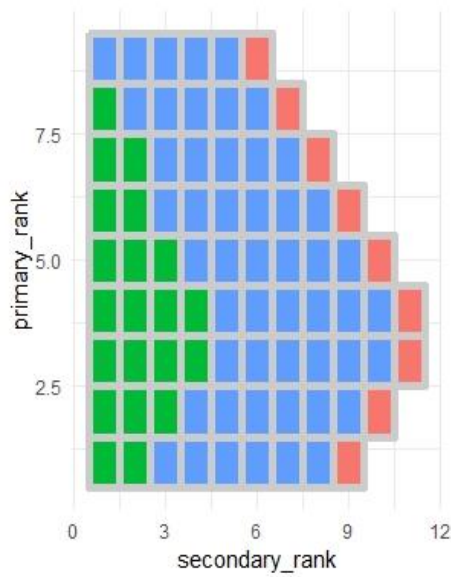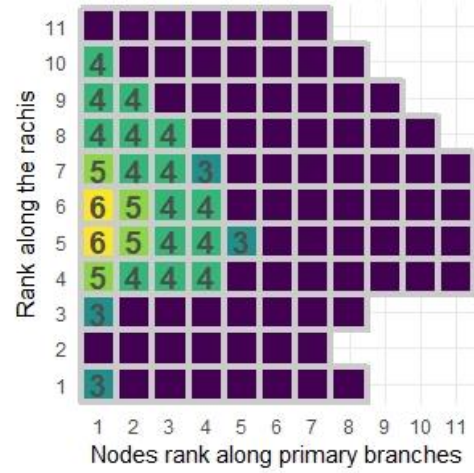
WT

g1l1

g1l2

Figure 53. A schematic representation of panicle structure and grain number of representative plant for each genotype (WT, *g1l1* and *g1l2*).
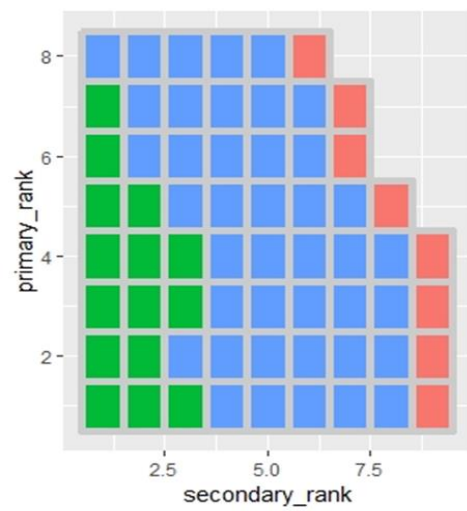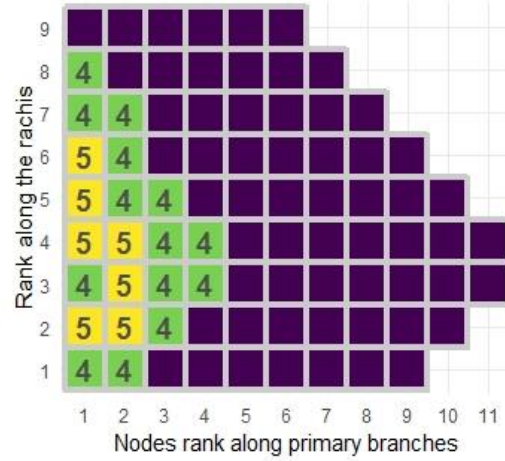
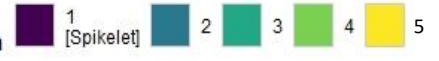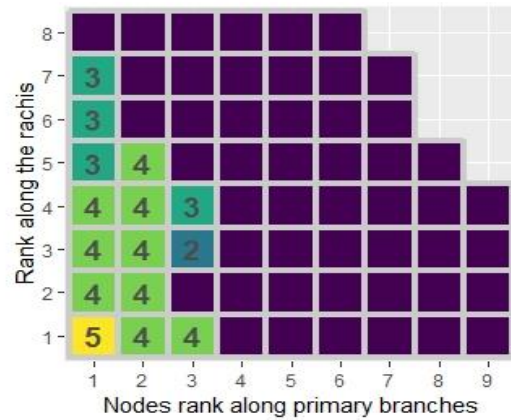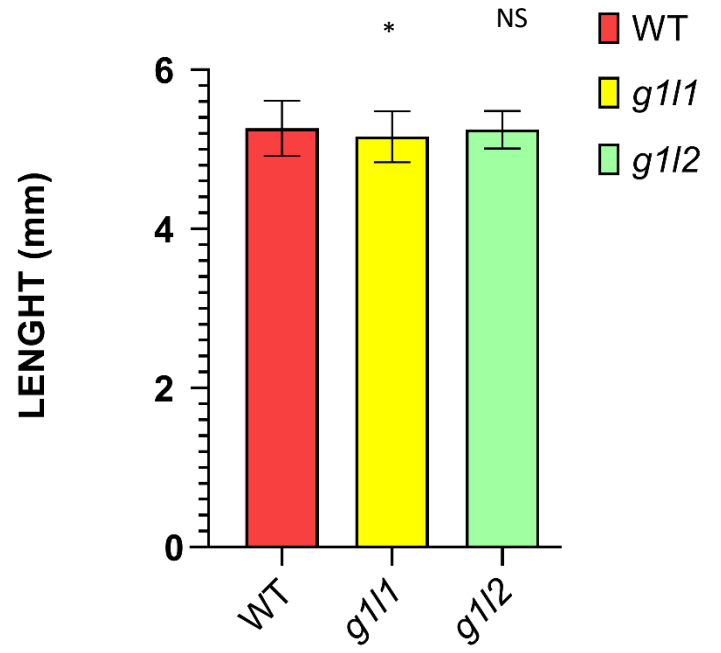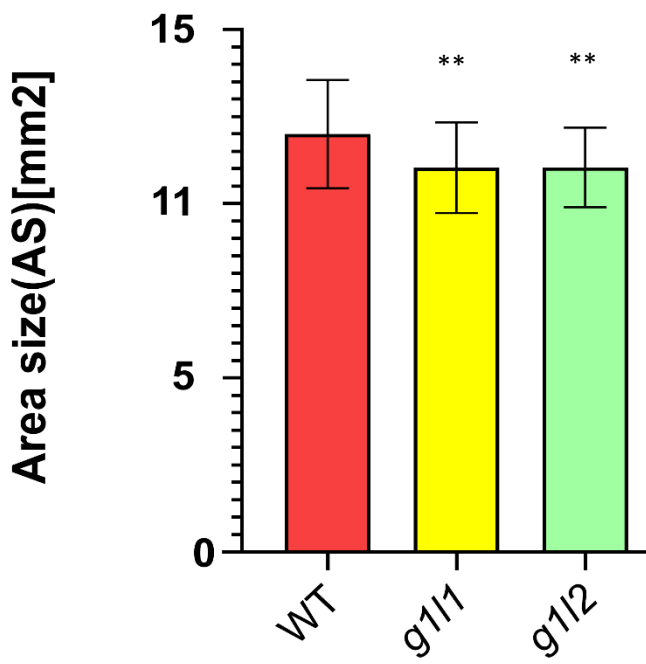**Figure 54. Topology structure of representative plant for each genotype: number of PBs, number of SBs on each PBs and number of Spikelets on Branches.**
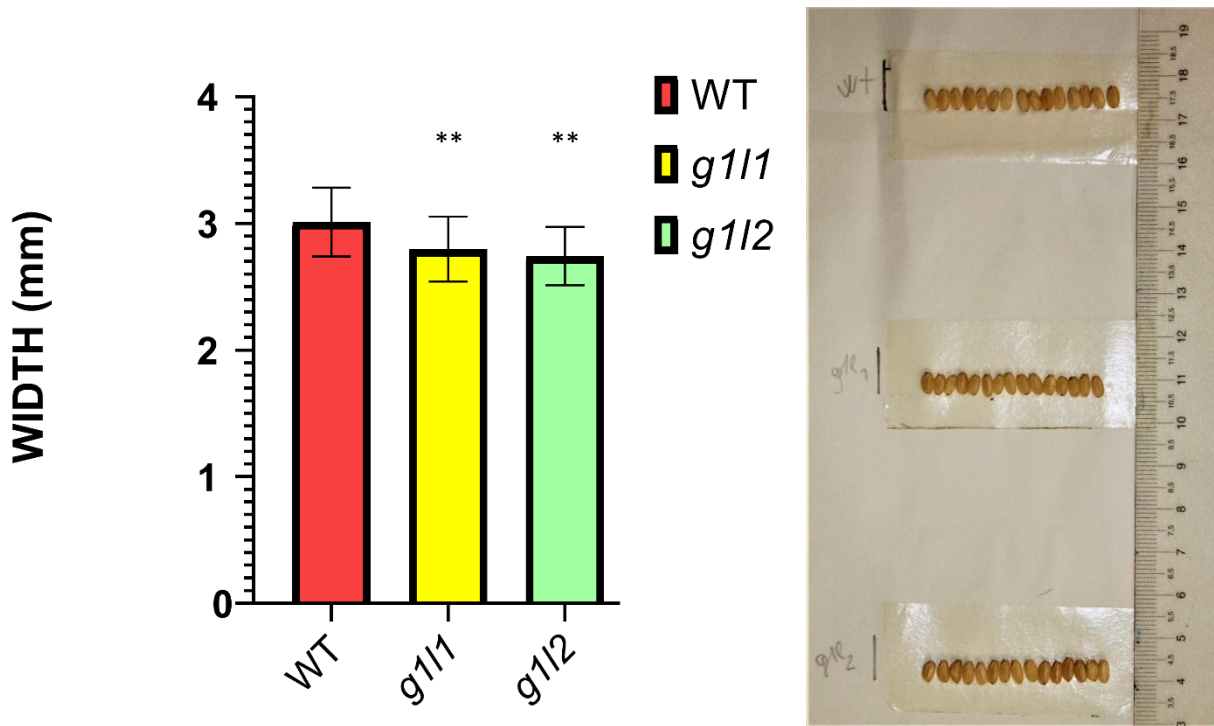
Figure 55. Seeds analysis performed using Smart Grain. One-Way ANOVA with Tukey test; **p<0,01.
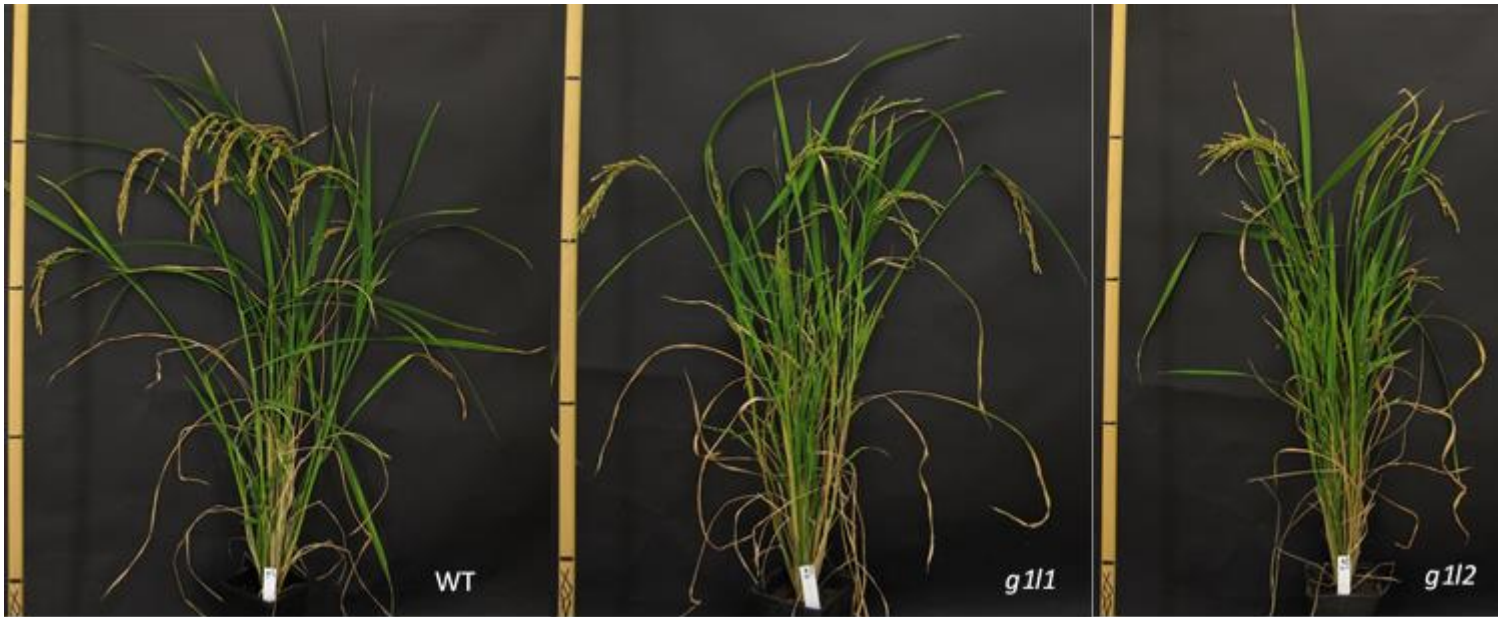

Figure 56. Whole plants of WT, *g1l1* and *g1l2*.

2.10. UNRAVELLING THE ROLE of *G1L2* in INFLORESCENCE BRANCHING

Since the panicle traits seemed to be more severe in *g1l2* respect to *g1l1* we decided to focus our attention on the *g1l2* mutant and to investigate how this gene is involved in inflorescence patterning.

2.10.1 Introgression and generation of transgenic marker lines for phytohormone analysis in rice

The phytohormones Auxin and Cytokinin have shown to play important roles in inflorescence development [13,151,163,185,186]. To elucidate the relation between *g1l2* and these plant hormones we decide to employed transgenic marker lines. *G1L2* might mediate the signalling or transport of them to promote meristem initiation. Auxin marker lines, *DR5::VENUS* and *DII::VENUS*, respectively specific for maximum and minimum of Auxin were provided by Dabing Zhang's laboratory [187]. In order to obtain a *DR5::VENUS* marker line in the *g1l2* background a reciprocal cross between the DR5::VENUS marker line and the *g1l2* mutant has been done. In parallel WT and *g1l2* rice calli were transformed with the *DII::VENUS* construct and T0 transgenic rice plants are now available.

Furthermore, since no Cytokinin marker line was available for rice, a construct in which the Fluorescent protein eGFP is under control of the new version of synthetic responsive CKs promoter Two Component signaling Sensor (TCSn) [188,189] was generated: *TCSn::eGFP* and used to transform WT and *g1l2* calli. A Zeiss microscope with a fluorescent filter was used to confirm GFP activity in WT and *g1l2* transformant calli **[Figure 57]**. We recently obtained the first regenerant calli and other analyses will be done in plant tissues to test whether construct works well and its suitability for phytohormone relate analysis.
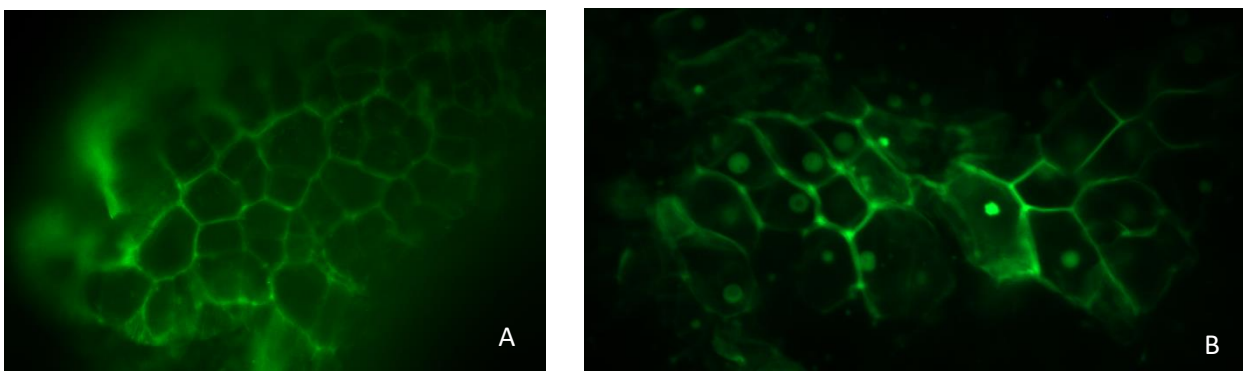

Figure 57. *TCSn::GFP* trasformant calli in WT(A) and *g1l2* (B) background.

2.10.2 Meristem Size Analysis

Branching phenotypes could be related to differences in reproductive meristem size [29,134]. To understand if the branching phenotype of the *g1l2* mutant is related to a change in meristem size a histological analysis was performed, comparing WT with *g1l2* mutant reproductive meristems. Therefore, we sampled WT and *g1l2* meristems at different time points: 12, 14 and 16 Days After Shifting (DAS) from non-flowering inductive long day to flowering inductive short day corresponding to IM (N1), PBM (N2), SBM (N3) stages. We fixed samples in the FAA and we embedded in paraffin. Slide of meristem got on microtome at 8 μm of thickness was stained with toluidine blue, staining that marks a cell wall. We collected at least seven samples for each meristem type and we took a picture at Zeiss Microscopy. According to analysis reported by Kawakatsu et al., (2006)[190] and Ta et al., (2017)[29] we decided to measure the Meristem Area at 40um from the tip of meristems, the width of meristems and the ratio between length and width. This analysis, done with ImageJ, showed that there is no difference in meristem size between WT and *g1l2* **[Figure 58]** therefore the branching phenotype is not related to a smaller meristem size but might depend on its target genes involved in this process.

B
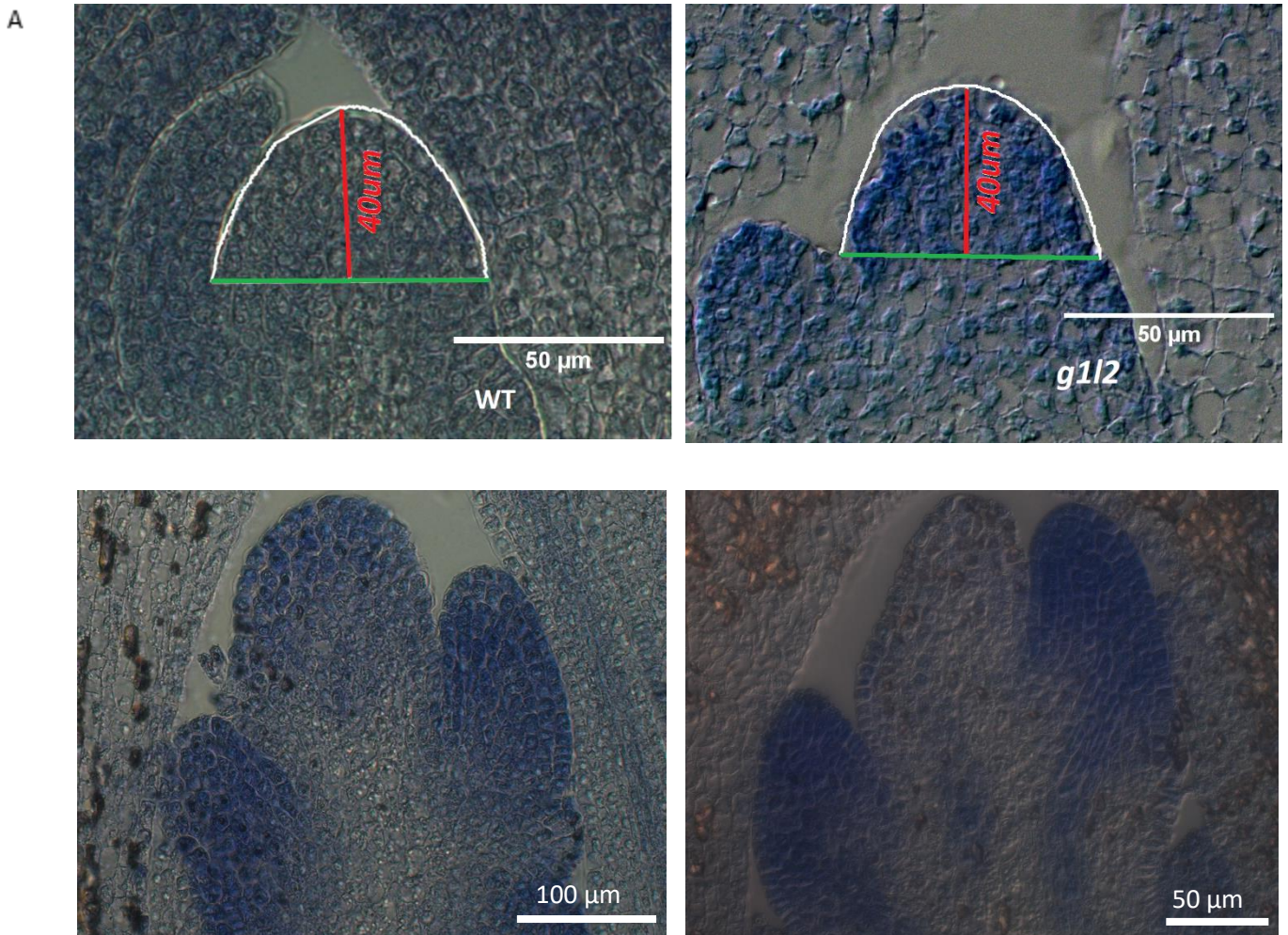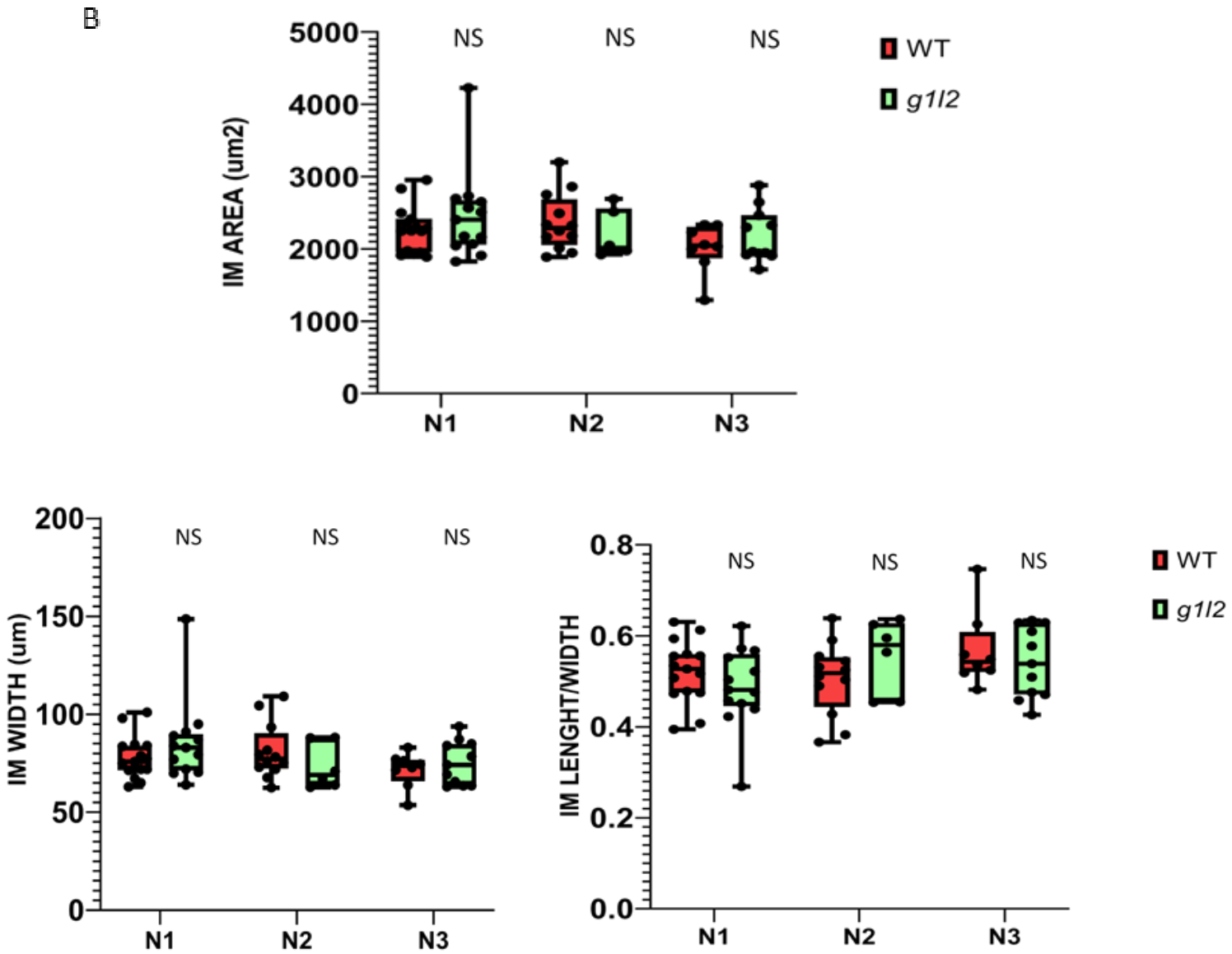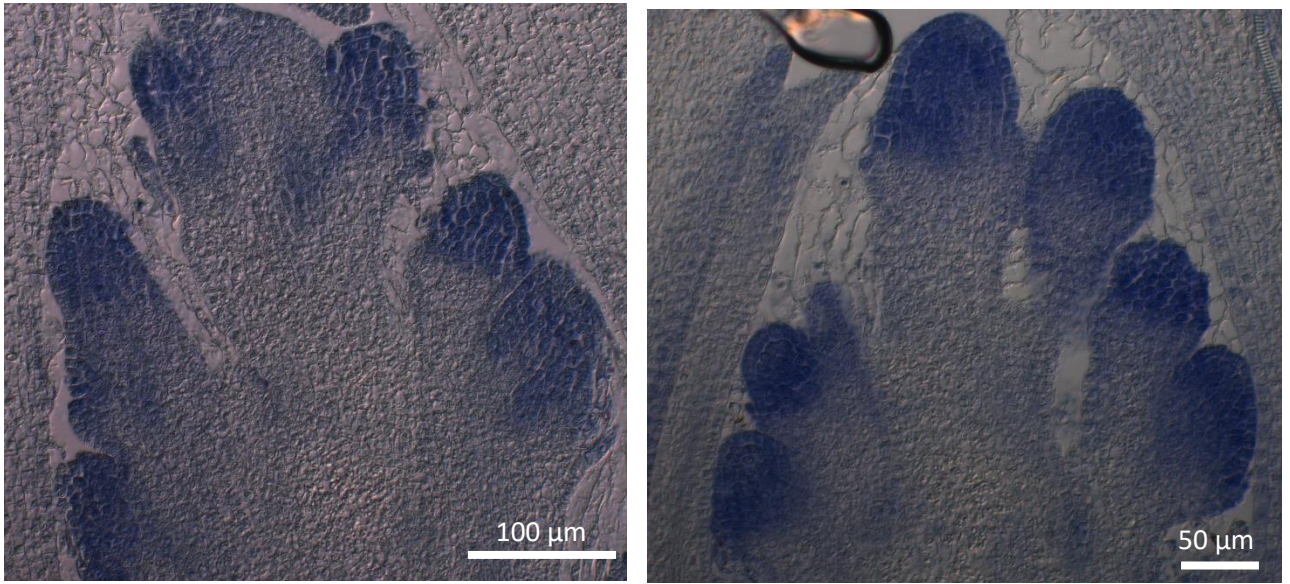
Figure 58. Meristem N1, N2 and N3 stages in WT an *g1l2*(A) and statistical analysis performed (B).

2.11. *g1l2* AND RELATED PHENOTYPE IN ROOTS

A combination of several indications suggested a putative role of *G1L2* also in root development. This gene indeed by qRT-PCR analysis resulted in expressed both in the root tips and in the whole roots **(see 8.1).** Furthermore, a preliminary analysis performed in WT and *g1l2* plants suggested a delay in root growth development in *g1l2* mutant compare to WT **[Figure 59].** To further investigate how this gene regulates this process we decided to perform in parallel a 2D and a 3D root phenotyping analysis [191] on WT and *g1l2* plants in collaboration respectively with Ross Sozzani's lab (NCSU University) and Philip Benfey's lab (Duke University). Twenty plants for each genotype were sown on plates for 2D analysis and in magenta boxes for 3D analysis. These experiments are in progress.

Figure 59. Root growth development preliminary analysis in WT and *g1l2* plants.

3. DISCUSSION

The inflorescence architecture is an agronomical trait that influences plant yield and is finely regulated by genes involved in meristem identity and in the transition of meristems from an indeterminate to a determinate state. Identifying the genes involved in these processes will provide important insights into crop domestication and will deliver tools for biotechnological approaches for yield improvement.

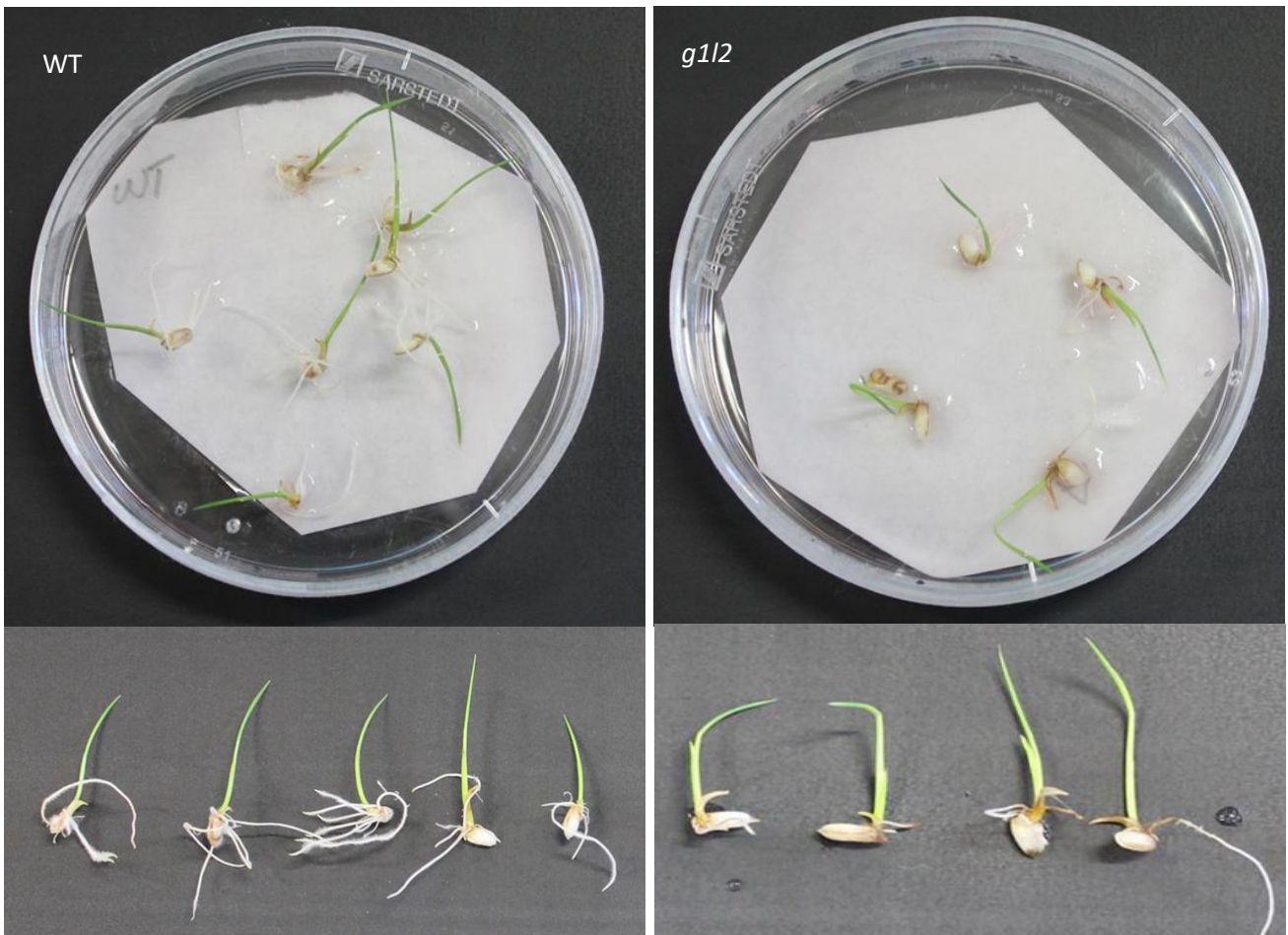In this PhD research project, I focused on the functional characterization of rice and Arabidopsis *ALOG* genes that are likely to play important roles in the regulation of the architecture of inflorescences.

3.1 FUNCTIONAL REDUNDANCY OF *LSH1, LSH3* AND *LSH4* IN INFLORESCENCE DEVELOPMENT

Expression data obtained by RT-PCR highlighted a similar expression profile for *LSH1, LSH3* and *LSH4* throughout the plant, including the inflorescence, although with different expression levels. In particular, RNA *in situ* hybridization experiments showed that *LSH1, LSH3* and *LSH4* were expressed in the IM and in the boundary region between IM and FM, suggesting a possible redundant function for these genes during inflorescence development. *LSH1* might regulate inflorescence meristem identity and its presence in a boundary region suggests also a role, together with other genes, in the promotion of flower meristem specification. The flower meristem identity is specified both by well characterized FMI genes [48] and by the action of the phytohormone auxin [52,185]. Therefore, *LSH1*, together with *LSH3, LSH4* could be involved in one of these pathways. The idea that these genes have a redundant function is also supported by the absence of an inflorescence phenotype in the *lsh1, lsh3* and *lsh4* single mutants and in the *lsh3 lsh4* double mutant. It is likely that *lsh1 lsh3 lsh4* triple mutant will show more severe inflorescence defects.

3.2 PUTATIVE ROLE OF *LSH3* IN STEM ELONGATION

The *lsh3* mutant showed an interesting phenotype in shoot architecture, in particular, it produced a primary shoot that was longer than WT but with the same number of secondary shoots and siliques on the primary inflorescence axis, which suggests a putative role of *LSH3* in primary stem elongation. This phenotype could be due to the presence of longer cells in the stem and therefore could be related to a hormone pathway such as GAs, since this phytohormone is the major regulator of stem elongation [192,193]. For instance, it is known that overexpression of *AtERF11*, a positive regulator of GAs signalling and biosynthesis, causes an increase in plant high. In particular, this phenotype is linked to

an increase in cell length in the internodes [194]. It is possible that the increased length of *lsh3* primary inflorescence can be linked to an increase in cell length. If this is true then it would be possible to speculate that *LSH3,* might regulate genes involved in signalling or in the biosynthesis of GA in a direct or indirect way. Further analysis should be done to elucidate this hypothesis.

3.3 *LSH1* as putative regulator of secondary shoot number

The *lsh1* mutant showed a reduction in secondary shoot number respect to WT. This phenotype could be related to a role of *LSH1* in the regulation of genes involved in AM initiation, such as *REGULATOR OF AXILLARY MERISTEMS1 (RAX1)* [195]. Because of the fact that the other mutants analysed in this study *(lsh3, lsh4, lsh3lsh4)* did not show a reduction in secondary shoot number, this analysis revealed a unique role of *LSH1* in the control of axillary meristem maintenance and organogenesis.

Phenotypical analysis also showed that the *lsh1* mutant seemed to be reduced in size and developed fewer seeds when compared to WT. Even if these data are not statistically significant, because of the fact *LSH1* was found to be expressed also in the FM boundary region, it is tempting to hypothesise that *LSH1* plays a role in FM maintenance, but in this case it likely acts together with *LSH3* and *LSH4*. A deeper analysis should be done to better understanding of how *LSH1* regulates these processes.

Moreover, protein–protein interaction assays indicated a putative role for LSH1 in the regulation of cell proliferation since together with LSH4 it interacted with TCP15. TCP1 is a transcription factor involved in the regulation of the expression of boundary-specific genes such as *LOB, CUC1, and CUC2* through a pathway that affects auxin homeostasis [196] but it is also a regulator of cell proliferation and seed germination; in particular, it represses cell proliferation in the leaf blade, internodes and in specific floral tissues [197,198]. Therefore, the LSH1 complex, which includes LSH4, TCP15 and probably other co-factors, might be involved in the maintenance of undifferentiated cells in the AM and IM meristems, and it promotes respectively, differentiation of the branching shoot and the floral organs. It might regulate not only genes involved in this process but also genes involved in the auxin pathway since as already mentioned before correct transport of auxin is crucial for primordium initiation.

3.4 *G1L1* AND *G1L2* AS PUTATIVE REGULATORS OF INFLORESCENCE ARCHITECTURE IN RICE

Expression data obtained by RT-PCR in rice showed a preferential expression of *G1L1* and *G1L2* in reproductive meristematic tissues, with a similar expression profile, suggesting a role in inflorescence development, like already described for the closely related gene *G1L5/TAW1*. Furthermore, *in situ* hybridization experiments showed, that *G1L1* and *G1L2* as well as *TAW1* are expressed in IM, PBM, SBM and SM. In particular, they are detectable where a pool of meristematic cells is maintained, suggesting a role in meristem maintenance. Expression analysis of meristem marker genes, such as *OSH1,* in the *g1l1* and *g1l2* mutant background might further clarify the role of these genes in this process.

3.5 *G1L1* AND *G1L2* HAVE A ROLE IN BRANCHING FORMATION, SPIKELET NUMBER AND GRAIN SIZE.

The idea that these genes are involved in inflorescence architecture was confirmed by the phenotypical analysis performed on *g1l1* and *g1l2* single mutants that suggested a function in branch formation and in spikelet numbers. Mutant lines didn't show any phenotype in the vegetative phase, they didn't change in high an in a number of the tiller, but showed defects in inflorescence architecture, suggesting that these genes might have a specific role in the reproductive phase. We found that *g1l1* and *g1l2* produced shorter panicles with fewer branches and fewer spikelets compare to WT. Inflorescence branches and grain numbers are determined by reproductive meristems formation, maintenance and differentiation. Therefore, their phenotypical characterization suggests that these genes are likely to be important for the inflorescence architecture, in particular promoting branches initiation and spikelet formation.

The branching phenotype indeed could be related to a defect in AMs initiation and formation. For instance, mutants such as *lax1, lax2,* impaired in this process showed a reduction in branch numbers [199].

In addition, according to the gene co-expression database, which is based on microarray analysis (RiceFREND, http://ricefrend.dna.affrc.go.jp) they also result co-expressed with Homeobox genes like *OSH6* and *OSH15* that are involved in the shoot apical meristem maintenance [128] and are highly expressed in indeterminate AMs suggesting their function also in the promotion of BM identity [2]. It is possible to speculate that *G1L1* and *G1L2* control AMs initiation and formation or are acting with them or regulating their expression. Interestingly, we also found that *G1L1* and *G1L2* are co-expressed with genes involved in Auxin transport and signalling pathway like *OsPIN1D* and *BIF2,* both necessary for a

correct formation and initiation of AMs [153,200]. Therefore, another explanation for the observed branch phenotype could be linked to a putative role of these genes in controlling auxin signalling in the AMs. The defect in branches and spikelets formation also suggests that *G1L1* and *G1L2* might be involved, like *TAW1*, in the timing of the transition from BMs to SMs, regulating the expression of genes that repress FM identity such as *OsMAD22* or *OsMAD34*. This idea is also supported by the fact that *g1l1* and *g1l2* mutants had panicles that were shorter in length compared to WT, like in the *taw1* mutant [5]. In contrast to *TAW1*, *G1L1* and *G1L2* could also be involved in embryo development and in grain size. Our analysis showed that the *g1l1, g1l2, g1l1g1ll2/+* and *g1l1g1l2* mutant lines showed a high level of sterility and smaller seeds than WT. A deeper analysis highlighted that *g1l1* and *g1l2* seeds showed a reduction in seed length and width and hence in seeds area.

Because of the reduced seed sized and the fact that *G1L1* and *G1L2*, by qRT-PCR showed expression in milk seed and in mature seed, they might have a role also in embryo/seed development regulating genes important for embryo formation and grain size such as *GS3, GW2* [201–204]. Furthermore, *G1L1* and *G1L2* result also co-expressed with gene encoding AP2-EREBP transcription factor *AINTEGUMENTA (ANT),* which in Arabidopsis is involved in embryo development [205,206]. However more exhaustive analysis should be done in the future to investigate these aspects.

3.6 A MAJOR ROLE OF *G1L2* IN INFLORESCENCE ARCHITECTURE

The preliminary analysis that we performed, showed that the *g1l1g1l2 (+/-)* double mutant seems to be more similar to *g1l1* than the *g1l2* single mutant, whereas the double homozygous mutant seems to be more severe than both. This confirmed again their role in the determination of inflorescence architecture but suggests a major role for *G1L2* in this process and a putative dose effect in the double mutant even if other analyses with a larger number of plants should be done. The hypothesis that *G1L2* has a major role in inflorescence architecture is also supported by the significant defect in secondary branch formation in the *g1l2* single mutant. Furthermore, *g1l2* showed also a late flowering phenotype. There is not much information about flowering time phenotypes attributable to ALOG genes, *TAW1* itself didn't show any difference in flowering time, even when its homolog in tomato, *TFM*, is early flowering. Further analysis should be done to clarify the mechanism through which *G1L2* regulates flowering time. For this reason, we decided to focus our attention on the *g1l2* single mutant to better understand how this gene acts. Meristem size analysis of different meristem types highlighted that the reduction in branches formation is not related to a smaller meristem size such as in the *apo2* mutant [207] but might depend on regulation of *G1L2* target genes involved in branch initiation including also hormone pathways, such as Cytokinin and Auxin.

The results obtained in this study provide a more detailed insight into the role that *ALOG* genes play in inflorescence development in Arabidopsis and rice. However, further studies will be needed to statistically evaluate the inflorescence phenotypes and to unravel the molecular mechanisms by which they control inflorescence architecture. These experiments are at the moment on their way to our laboratory.

4. CONCLUSIONS AND FUTURE PERSPECTIVE

Inflorescence architecture is an agronomical trait finely regulated by different factors. Our results suggest that *ALOG* genes play a role in meristem maintenance and organogenesis in Arabidopsis and in rice, although the molecular mechanisms are still unclear.

LSH1 seems to be involved in the regulation of the development of AM by the secondary shoot whereas *LSH3* might have a role in stem elongation. However, the absence of an inflorescence phenotype in *lsh1, lsh3, lsh4* and in the *lsh3 lsh4* loss of function mutants might be related to redundant functions of these genes in this pathway. To test this hypothesis a cross between *lsh3 lsh4* and *lsh1* homozygous mutants has been done to obtain the *lsh1 lsh3 lsh4* triple mutant. F2 lines will be genotyped in order to select the triple mutant and phenotypical analysis will be done on this mutant but also on the *lsh1 lsh4* double mutant. Furthermore, to further investigate how *LSH1* regulates AM formation we are planning to investigate whether the expression of genes involved in AM development and those involved in the specification of the floral meristem are downregulated in this mutant background. Since auxin is involved in AM formation, we are planning to cross the *lsh1* mutant with auxin reporter lines that are already available in our laboratory. Analysis of these plants, using confocal microscopy, could provide insight if there is a defect in auxin signalling pathway. In parallel, histological analysis to study the stem elongation in the *lsh3* mutant might clarify the role of *LSH3* in stem elongation. Furthermore, the GA signalling pathway might also be studied since this phytohormone is an important regulator of stem elongation.

To further investigate the molecular mechanisms by which LSH factors work, a yeast 2-hybrid analysis could be performed to identify new interactors that could through the guilt-by-interaction principle give a better idea of their way of action in the control of inflorescence development.

For the rice ALOG family genes we confirmed that *G1L1* and *G1L2* play a role in inflorescence patterning, regulating the number of branches, spikelets and grains. In particular, among these genes, *G1L2* seems to be more promising than *G1L1* since it showed a role also in secondary branches formation and flowering time. However, to better understand how this gene regulates this process and which are its putative targets, in collaboration with Ross Sozzani's laboratory at NC State University, an RNA-seq experiment followed by bioinformatics analysis will be used to analyse the transcriptomes of WT and the *g1l2* single mutant, using N1/N2 meristems which correspond to the PB formation stage.

In parallel, at a different time points of inflorescence development the expression of genes involved in flowering time and the development of branches will be analysed in WT and the *g1l2* mutant

background. Unfortunately, all experiments were seriously delayed due to compromised growing conditions. We are now working to obtain the missing research data to get statistically sound data from which we can draw solid conclusions about the functions of the rice ALOG genes.

To further investigate the role of *G1L2* also in root growth development we will perform a 2D and a 3D root phenotyping analysis [191]on WT and *g1l2* plants in collaboration respectively with Ross Sozzani lab (NCSU University) and Philip Benfey lab (Duke University).

Furthermore, we are planning to perform a phenotypical analysis on the obtained *G1L1* and *G1L2* overexpression line in order to understand if these genes, like *TAW1,* will also produce panicles with more branches and more seeds. A phenotypical analysis will be also done comparing *g1l1 g1l2(+/-), g1l1 g1l2* double mutants with *g1l1, g1l2* single mutants to verify if the double mutants, and in particular *g1l1g1l2,* have a more severe phenotype than the single mutants and hence will elucidate if these genes work in the same pathway to regulate inflorescence architecture.

Last but not least to further investigate the putative relation between *g1l2* and hormone pathways, inflorescences of the marker lines that we generated in the WT and *g1l2* mutant background will be analysed. Furthermore, regarding the cytokinin marker line, a deeper analysis of plant tissues will be done to verify whether the new construct generated in our lab works well and whether it can be used for hormonally related analysis.

All planned experiments will contribute to a better understanding of the function that these genes have in inflorescence development. This knowledge could be useful for (molecular) breeding programs with the final aim to increase yield.

7. MATERIALS AND METHODS

7.1. PLANT MATERIAL AND GROWTH CONDITION

7.1.1 Arabidopsis thaliana

For the experiments, we use Columbia-0 (Col-0) ecotype of *Arabidopsis thaliana*. The plants were grown in soil first in Short Day (SD) conditions (10h day/14h night at 20-22°C) and moved, after 30 days, to LD conditions (14h day/10h night at 20-22°C) to induce flowering. For RNA expression analysis the seeds were sown in a plate containing MS medium (7g/L MS+ vitamins, 10g/L Sucrose, 1L ddH20, 7g/L Phyto agar, pH adjusted to 6.0 with KOH) and after 7 days, roots, hypocotyl and cotyledon were harvested.

7.1.2 Oryza sativa

For the experiments, we used *Oryza sativa*, *ssp. Japonica, cv Nibbonbare*. The plants were grown for 8-10 weeks in LD conditions (70% humidity, 16h day at 28°C/8h night at 26°C) and then moved in SD conditions (70% humidity, 12h day at 28°C/12h night at 26°C) to induce flowering. Plants germinated in MS-F medium (2,2 g/L MS + vitamins, 15 g/L Sucrose, 1L ddH2O, pH adjusted to 5.6 adding KOH, 2.5 g/L gelrite) and after 15 days were transplanted in soil.

7.2. RNA ISOLATION AND CDNA SYNTHESIS

In Arabidopsis, 100 mg per plant tissues (roots, hypocotyl, cotyledon, rosette and cauline leaves, inflorescence, siliques) were harvested and ground with N2 for total RNA extraction. Total RNA was extracted from three biological replicates of each sample using the LiCl extraction method as previously described *by Gregis et al., 2008* [208]. For rice a 50 mg for each tissue was harvested and ground and total RNA extraction, from three biological replicates for each sample, was done with NucleoSpin® RNA Plant kit (http://www.mn-net.com).

DNA contamination from RNA isolated in both species was removed using the TURBO DNA-free™ Kit according to the manufacturer's instructions (https://www.thermofisher.com). The RNA was Rverse transcribed using the ImProm-II™ Rverse Transcription System (https://ita.promega.com) and the cDNA was used as a template in RT-PCR reactions.

7.3. qRT-PCR ANALYSIS

The RT- PCR analysis was carried out in a final volume of 12 μL using a Biorad C1000™ thermal cycler and using 3 μL of a 1:10 dilution cDNA, 0,2 μM (stock 10mM) Forward and Reverse Primer, 6 μL eQ Sybr Green Super Mix 2X (Bio-Rad), 2,6 μl MQ H2O.

The expression levels of *LSH1(At5g28490), LSH3(AT2G31160)* and *LSH4(AT3G23290)* were evaluated using primers RT2545/RT2546, ATP6517/ATP6132 and ATP6519/ATP6135 respectively and was performed with the following conditions: 95°C 90'' 40 cycles (95°C 15'', 58°C 10'', 60°C 30'') and 60°C 10''.

The expression levels of *G1L1(LOC_Os02g07030), G1L2 (LOC_Os06g46030)* and *G1L5 (LOC_Os10g33780)* were evaluated using RT2541/RT2542, RT1387/ RT1389 and RT2543/ RT2544 respectively whereas the expression levels of *pACT1::G1L1*, *pUBI::G1L1* and *pUBI::G1L2* were evaluated using primers RT2728/OSP1841 (for *G1L1*) and OSP1387/OSP1389 (for *G1L2*). The RT-PCR was performed at 60° C instead of 58 °C.

Three biological replicates for each experiment were performed.

Arabidopsis reference gene ubiquitin *(At4g36800)* and Rice Elongation Factor 1 (EF1) (LOC_Os03g08010) were used as an internal reference during the experiments respectively. Primer sequences are listed in **Table 4.**

7.4. *In situ* HYBRIDIZATION

Rice Reproductive meristems from the main stem at different stages of early panicle development and Arabidopsis inflorescence were harvested and fixed in FAA [ethanol (Fluka) 50 %; acetic acid (Sigma-Aldrich) 5 %; formaldehyde (Sigma-Aldrich) 3·7 % (v/v)]. Subsequently, the samples were infiltrated under mild vacuum conditions for 15 min in ice and after 1h 45' were washed 3 times for 10' in EtOH 70% and conserved at 4°C; then the samples were dehydrated in a series of increasing graded ethanol series, transferred to bioclear (Bioptica) and then embedded in Paraplast X-TRA® (Sigma-Aldrich). To generate the sense and antisense probes, gene fragments were amplified from cDNA using gene specific primers **(Table 4),** cloned into pGEM®-T Easy Vector and confirmed by sequencing. Digoxigenin-labeled antisense and sense RNA probes were transcribed and labelled from pGEM®-T Easy with T7/SP6 RNA polymerase (Promega) according to the manufacturer's instructions, and using the DIG RNA labelling mix (Roche). Paraplast-embedded tissues were sliced on an RM2155 microtome (Leica) at 8 μm of thickness and hybridized as described by Coen et al. (1990)[209] with minor modification. Immunodetection was carried out with anti-digoxigenin-AP Fab fragment (Roche) and BCIP-NBT colour development substrate (Promega) as specified by the manufacturer.

7.5. CRISPR-CAS9 CONSTRUCT GENERATION

For the generation of *g1l1*, *g1l2* single knock-out mutants, 20-bp specific protospacers **(Table 4)** for each gene were selected using the CRISPR-P database (*http://cbi.hzau.edu.cn/crispr/*) and cloned into the BsaI site of pOs-sgRNA entry vectors under U3 promoter and then combined into the destination vector containing the Cas9 under maize Ubiquitin Promoter using the Gateway® LR Clonase II Enzyme mix following the procedure reported by Miao et al. (2013) [181]. For double (*g1l1*, *g1l2*) knockout lines, protospacers were designed containing BsaI sites according to Xie et al. (2015) [182], amplified with PCR using the pGTR plasmid as template and then ligated with Golden Gate (GG) and assembled with PCR. To make the Polycistronic tRNA-gRNA (PTGs) the PCR reaction was purified and digested with FokI and cloned into the destination vector pRGEB32 containing the Cas9 under the control of the UBI promoter.

For generation of *lsh1, lsh3* and *lsh4* single knock- out mutants, 20-bp specific protospacers **(Table 4)** for each gene were selected using CRISPR-P v2 database (http://crispr.hzau.edu.cn/CRISPR2/) and cloned into BbsI site of pEN-Chimera entry vector under Arabidopsis U6-26 promoter and then combined into destination vector pDe-Cas9, containing Cas9, by single site Gateway® LR reaction according to procedure reported by Fauser et al., 2014 [179].

In order to generate a different kind of combination of *lsh*s mutants a cross- fertilization of Arabidopsis plant has been performed according to instruction described by Ortrun Mittelsten Scheid (https://www.arabidopsis.org/download_files/Protocols/Crossing_of_Arabidopsis_Lab_Course.pdf)

7.6. OVEREXPRESSION LINE GENERATION

The CDS of *OsG1L1* and *OsG1L2* were amplified using primers OSP1893/OSP1894 and OSP1895/OSP1896 respectively using high-fidelity polymerase Q5 (NEB) following the protocol described on NEB website (https://www.neb.com) and using High GC enhancer buffer and also 0,03 ul GoTaq (Promega) (62 °C annealing). The CDSs were cloned respectively first into pDNR207(Invitrogen) entry clone and then into pH2GW7 destination vector containing rice actin promoter (pACT1) (provided by Fabio Fornara, Unimi) or into pCAMBIA5300 destination vector (provided by Hélène Adam and Stèphane Jouannic, IRD center, UMR DIADE) containing Ubiquitin promoter by the Gateway® LR reaction. Each Plasmid was checked by PCR and by sequencing.

7.7 MUTANT SCREENING IN TRANSGENIC PLANTS

Genomic DNA was extracted from T1 BASTA–resistant Arabidopsis plants and T0-hygromycin-resistant rice plants and genotyped by PCR using specific primers for Cas9 construct, ATP5575/ATP5578 (for Arabidopsis), ATP5706/5718 (for rice single CRISPR-Cas construct) and OSP1584/OSP1585 (for rice Multiplex CRISPR-Cas9 Construct **(Table 4)**. Subsequently, from the positive plants, DNA fragments across the target sites were amplified with PCR using the gene-specific primer pairs **(Table 4)**. The PCR amplicons were purified with NaAc 3M pH 5.2 and EtOH 100% and sequenced. The sequencing chromatograms were analysed with FinchTV carefully for mutations.

Then the mutant lines with fixed mutation in both species were genotyped by restriction enzymes. Specific primers were used to amplified DNA fragments of the *LSH1, LSH3, LSH4 G1L1* and *G1L2* genes **(Table 4)**. The PCR products were digested by BSS Sa1, MSE1, BLP1, AHD1, BBV1 respectively for each gene. To dilute the enzymes to the wanted concentration we used Biolabs 1x Diluent A (10 mM Tris-HCl, 1 mM DTT, 0.1 mM EDTA, 50% Glycerol, 200 µg/mL BSA, 50 mM KCl, at pH 7.4 at 25°C) and 1X Diluent B (300 mM NaCl, 10 mM Tris-HCl, 1 mM DTT, 0.1 mM EDTA, 500 µg/mL BSA, 50% Glycerol, at pH 7.4 at 25°C). Each digestion reaction was carry out in 25 uL: 5 µL Template (approximately 50ng/µL), 1 µL Biolabs Cutsmart buffer 10x, 0,4 µL Diluent 1X (A o B), 0,1 µL 1:5 restriction enzyme and 18,5 µL Millipore H20. The digestion run at 37°C for at least 1h **(Table 4).**

The T-DNA line insertion for *LSH3* and *LSH4* were genotyped using two couple of primers, first one amplified the mutant allele with FW primer on T-DNA and Rv primer on gene sequence (ATP1213/ATP5143 and ATP1213/ATP6134 respectively for *lsh3 T-DNA* and *lsh4 T-DNA*); the second one amplified the WT allele (ATP 5142/ ATP 5143 and ATP6134/ATP6520 respectively for *lsh3 T-DNA* and *lsh4 T-DNA).*

7.8. INTROGRESSION AND GENERATION OF AUXIN AND CYTOKININ MARKER LINES IN RICE

A new construct for fluorescent reporter line for CKs was generated. *TCSn* synthetic promoter with 35S minimal promoter and TMVΩ was amplified from Arabidopsis genome *TCSn:: GFP* marker line provided by Bruno Muller [188] [**Figure 60]**, using primers OSP1924/OSP1936 and Terra Taq polymerase (Clonotech). The 2-STEP PCR reaction was performed in 25ul according to the protocol described online (https://takara.co.kr/file/manual/pdf/PT5126-1_1206.pdf). The PCR-Product purified using NucleoSpin® Gel and PCR Clean-up (https://www.mn-net.com) was cloned first into

pDNR221 entry vector (Invitrogen) and then into pHGWFS7 destination vector (Invitrogen) containing eGFP by Gatway® LR reaction. The plasmids were checked by PCR and sequencing.

DR5::VENUS seeds and *DII::VENUS* construct was provided by Dabing Zhang Lab [187]. The Nipponbare *DR5::VENUS* seed were cross pollinated with *g1l2* mutants to obtain an auxin marker line also in the mutant background according to the protocol described by Susan R. McCouch (http://ricelab.plbr.cornell.edu/cross_pollinating_rice); whereas the *DII:VENUS* construct together with TCSn:eGFP construct were transformed in WT and *g1l2* embryonic calli by *Agrobacterium tumefaciens* infection.

7.9. BACTERIAL AND PLANT TRANSFORMATION

For bacterial transformation, we used *E.Coli* electrocompetent cell (DH10b strains) and Agrobacterium electrocompetent cell (EH105 strain).

All final constructs were introduced respectively in Arabidopsis plant by *Agrobacterium tumefaciens* infection with Floral Dip Method [10] and in embryogenic calli from *Oryza sativa* L. ssp. *Japonica* cv. Nipponbare seeds according to the methods described by Hiei et al. (1994) [22] and Toki (1997) [210].

7.10. PROTEIN- PROTEIN INTERACTION ANALYSIS

Yeast two-hybrid assays were performed in the yeast strains PJ69-4A and PJ69-4α [211]. The coding sequences of *LSH1, LSH3* and *LSH4* were amplified using primers ATP6397/ATP6398, ATP6399/ATP6400 and ATP6401/ ATP6402 respectively and cloned first in pDNR207 (Invitrogen) and then in the pDEST32 (bait vector, BD; Invitrogen) and in pDEST22 (prey vector, AD; Invitrogen) Gateway vector by Gatway® reaction. Each plasmid was verified by PCR and sequencing. The bait constructs were tested for autoactivation on selective yeast synthetic dropout medium lacking Leu, Trp and His supplemented with 1, 3, 5, 10 or 15 mM of 3-aminotriazole, in order to set the screening conditions. After mating, colonies were plated on the proper selective media and grown for 5 days at 28°C. The experiment was performed in collaboration with LangeBio (Irapuato University, in Stefan De Folter Laboratory).

The same coding sequences for *LSH1, LSH4* and CDS of *TCP15* (amplified using ATP4117/ATP4118 primers) were also cloned in the pYFPN43 and pYFPC43 vectors by Gatway® reaction, to perform the BiFC assay. The experiment was performed in collaboration with Niigata University, in Toshiaki Mitsui laboratory. Agrobacterium was used to infiltrate tobacco leaves. The abaxial surfaces of infiltrated leaves were imaged 3 d after inoculation. An LSH1-LSH4 heterodimer, which was not observed in the Y2H assays, was employed as a negative control for the infiltration,

whereas VDD-VAL heterodimer was used as a positive control for the infiltration [180]. Images were acquired at Leica SP8 confocal microscope.

7.11. PHENOTYPICAL ANALYSIS P-TRAP

To performed phenotypical analysis 15, 19 and 20 panicles from the main tiller were harvested respectively from each WT, *g1l1* and *g1l2* plant. Each panicle was attached on A3 white paper and on that all panicle branches were spread and blocked with transparent stick. Each paper with a panicle and scale bar was put on the Image capturing system consist of Portable Camera Stand and two RB 218N HF Lighting Units. The pictures were made by Canon Power Shot G12 Digital Camera and processed into P-TRAP software. The analysis was done as described in A L-Tam F et al., (2013) [184]. The results were statistically analysed by One Way ANOVA followed by Tukey test (http://vassarstats.net/anova1u.html) and represented with Graphpad Prism 8 (https://www.graphpad.com/scientific-software/prism/). Furthermore, panicles architecture was also graphically represented using R packages as described in (https://othomantegazza.github.io/ptrapr/index.html).

7.12. POLLEN AVAILABILITY TEST

To test pollen availability on WT and *g1l1g1l2* mutant, 3 WT and 3 *g1l1g1l2* spikelets before anthesis were harvested in Carnoy's fixative solution (6 alcohol: 3 chloroform:1 acetic acid) for a minimum of 2 hours and store at 4°C. The anthers were isolated from spikelets on slides and before samples were completely dried two/three drop of staining solution were added (10 mL 95% alcohol, 1 mL Malachite green (1% solution in 95% alcohol),50 mL Distilled water, 25 mL Glycerol, 5 mL Acid fuchsin (1% solution in water), 0.5 mL Orange G (1% solution in water), 4 mL Glacial acetic acid Add distilled water (4.5 mL) to a total of 100 mL). The test was then performed as described by Ross Peterson et al., 2010 [183]. The images are then taken on Leica® MZ 6 microscope.

7.13. HISTOLOGICAL ANALYSIS ON MERISTEM SIZE

WT and *g1l2* reproductive meristems at 12, 14 and 16 DAS (Day After Shift from LD to SD condition), stages at which the meristem progress respectively from N1 (Inflorescence Meristem), N2 (acquisition of first Primary Branch Meristems) and N3 (acquisition of first Secondary Branch Meristems), were sampled. They were fixed ad described above, *in situ* hybridization paragraph, and embedded in Paraplast Plus® Sigma-Aldrich. Embedded samples were sliced on the microtome at 8 μm of thickness, deparaffinised in Bioclear (Bioptica), rehydrated in a series of decreasing ethanol

concentrations, stained with Toluidine Blue, dehydrated in a series of increasing Ethanol concentration and store in Bioclear solution o/n according to the following protocol: Bio Clear 20',Bio Clear 20', 1:1 EtOH/Bio Clear 2', EtOH 100% 2', EtOH 95% 2', EtOH 75% 2', EtOH 50% 2', Toluidine Blue 5', EtOH 50% 2' , EtOH 75% 2', EtOH 95% 2', EtOH 100% 2', 1:1 EtOH/Bio Clear 2', Bio Clear 2', Bio Clear o/n) . The samples were mounted with Glycerol 40% and cover slides and then the pictures on meristems were taken using Zeiss Axiophot® microscope. Morphological traits were analysed on at least 6 meristems for each stage using ImageJ software and the analysis was performed as reported by Kawakatsu et al., (2006) [190] and Ta et al., (2017) [29].

Table 4. List of Primers

PRIMERS FOR qRT-PCR		
GENE	OLIGOS-ID	SEQUENCE
UBI A	RT147 (Fw)	CTGTTCACGGAACCCAATTC
	RT148 (Rv)	GGAAAAAGGTCTGACCGACA
LSH1	RT 2545(Fw)	GCTCTCTCTCCCCTCGTGTA
	RT 2546 (Rv)	AGAAGGCACAGTTCTGGTGG
LSH3	ATP6517(Fw)	CCAATTGATGGAAGGCTCTTCAG
	ATP6132(Rv)	TTGAGTTCGCCGATGGTGAG
LSH4	ATP6519(Fw)	GCTTTATGGGCACAACAAACAT
	ATP6135(Rv)	TTAGCTGGTTAGTCCCCGAG
EF1	RT1212 (Fw)	TGGTATGGTGGTGACCTTTG
	RT1213 (Rv)	GTACCCACGCTTCACATCCT
G1L1	RT2541 (Fw)	GCACACCACACCTACCATGA
	RT2542 (Rv)	GGCTGCAGAGATCGAAGTGT
G1L2	RT1387 (Fw)	TTGCAGTGGTCTTCTTCGCA
	RT1389 (Rv)	AGAGTTTGAGGTGCAGATGTGA
G1L5	RT2543 (Fw)	GAGCTGCTAGCCTCCTACG
	RT2544 Rv)	GCTAGTAGCAAGAGCAGCCTA
G1L1	RT2728 (Fw)	AGCTGGTGGAACAGGCGGT
	OSP1841(Rv)	GAAGTGCGCCGGGAACAAGAAGTG
PRIMERS FOR in-situ HYBRIDIZATION		
GENE	OLIGOS-ID	SEQUENCE
LSH1	ATP6128(Fw)	TCAACAGGCAGAAACCGCAAAC
	ATP6129(Rv)	CAACTAGTACAGAAACAAAAGCATC
LSH3	ATP6131(Fw)	CAGCTCCTCCATATCCATCAAG
	ATP6132(Rv)	TTGAGTTCGCCGATGGTGAG
LSH4	ATP6134(Fw)	CAAGCCTCCTCTCATCTTCACC
	ATP6135(Rv)	TTAGCTGGTTAGTCCCCGAG
G1L1	OSP1384 (Fw)	ACACCAAGCAGAAGCAGCAG
	OSP1385(Rv)	ATGCAAATCACCACGCATCC
G1L2	OSP1387 (Fw)	CACACTTCATGCACGGACAC
	OSP1388(Rv)	TGCTATATGCTGCTGATCTCTG
G1L5	OSP1390(Fw)	GCGTCAGCTACGAGAAGAAG
	OSP1391(Rv)	ATTAGATGCAGTAGCAGCAGC
PROTOSPACERS FOR SINGLE CRISPR/Cas9		
GENE	OLIGOS-ID	SEQUENCE
LSH1	ATP6677(+ve)	ATTGACGTGTGCGCCGCTACACGA
	ATP6678(-ve)	AAACTCGTGTAGCGGCGCACACGT
LSH3	ATP6679(+ve)	ATTGGAAGGCTCTTCAGCTTACGG

	ATP6680(-ve)	AAACCCGTAAGCTGAAGAGCCTTC
LSH4	ATP6374(+ve)	ATTGCGGGGACTAACCAGCTAAGC
	ATP6375 (-ve)	AAACGCTTAGCTGGTTAGTCCCCG
G1L1	OSP1012 (+ve)	GGCACATCCGCGACACGCAGTCCA
	OSP1013 (-ve)	AAACTGGACTGCGTGTCGCGGATG
G1L2	OSP1016 (+ve)	GGCACTGGAGCTGTCGCGGTGCAG
	OSP1017 (-ve)	AAACCTGCACCGCGACAGCTCCAG
PROTOSPACERS FOR MULTIPLEX CRISPR/Cas9		
GENE	OLIGOS-ID	SEQUENCE
G1L1	OSP1271 (+ve)	TAGGTCTCACGACACGCAGTCCAGTTTTAGAGCTAGAA
	OSP1272 (-ve)	CGGGTCTCAGTCGCGGATGTGCACCAGCCGGG
G1L2	OSP1273 (+ve)	TAGGTCTCAGTCGCGGTGCAGGTTTTAGAGCTAGAA
	OSP1274 (-ve)	CGGGTCTCACGACAGCTCCAGTGCACCAGCCGGG
PRIMERS FOR PRODUCING PTGs FOR pRGEB32 VECTOR		
GENE	OLIGOS-ID	SEQUENCE
L5AD5F	OSP1198	CGGGTCTCAGGCAGGATGGGCAGTCTGGGCAACAAAGCAC CAGTGG
L3AD5R	OSP1199	TAGGTCTCCAAACGGATGAGCGACAGCAAACAAAAAAAAAGC ACCGACTCG
S5AD5F	OSP1200	CGGGTCTCAGGCAGGATGGGCAGTCTGGGCA
S3AD5R	OSP1201	TAGGTCTCCAAACGGATGAGCGACAGCAAAC
PRIMERS FOR GENOTYPING TRANSGENIC PLANTS FOR Cas9		
	OLIGOS-ID	SEQUENCE
	Atp5706 (Fw)	GTGAAGCTCAATAGAGAGGACC
	Atp5718 (Rv)	CTTGATAATCTTGAGGAGGTCGTGG
	OsP1584 (Fw)	TGATCGAGACAAACGGCGAA
	OsP1585 (Rv)	ACCAGCACAGAATAGGCCAC
	Atp 5575	GGATTTCCAATTCTACAAGGTGAGGG
	Atp 5578	ACTCTTTCCCTTCTCAACCTTAGC
PRIMERS FOR GENOTYPING T-DNA line		
GENE	OLIGOS-ID	SEQUENCE
LSH3 T-DNA insertion	ATP1213 (Fw)	TGGTTCACGTAGTGGGCCATCG
	ATP 5143(Rv)	TCAAAGGCAGCTCGAAGACG
LSH3 WT allele	ATP 5142(Fw)	AAGGCTATTTAGTCCCTCCGAC
	ATP 5143(Rv)	TCAAAGGCAGCTCGAAGACG
LSH4 T-DNA insertion	ATP 1213 (Fw)	TGGTTCACGTAGTGGGCCATCG
	ATP 6520(Rv)	CTTAGTCTTGCCGAATTGGTCG
LSH4 WT allele	ATP 6134(Fw)	CAAGCCTCCTCTCATCTTCACC
	ATP 6520(Rv)	CTTAGTCTTGCCGAATTGGTCG
PRIMERS FOR AMPLIFYING TARGET SITE		
GENE	OLIGOS-ID	SEQUENCE
LSH1	ATP 6515 (Fw)	GGCTAGACATCTGCTTTGGCTTC
	ATP 5605 (Rv)	CGGTTTCTGCCTGTTGAC
LSH3	ATP 6131 (Fw)	CAGCTCCTCCATATCCATCAAG
	ATP 6518 (Rv)	GGACTTTTGTCTTACCGAACTGG
LSH4	ATP 6134 (Fw)	CAAGCCTCCTCTCATCTTCACC
	ATP 6520 (Rv)	CTTAGTCTTGCCGAATTGGTCG
G1L1	OSP 1840 (Fw)	GGAGATGGACATGATCGGCATGG
	OSP 1841 (Rv)	GAAGTGCGCCGGGAACAAGAAGTG
G1L2	OSP 1362 (Fw)	AGGTTTGCTGCTGCTTGTGC
	OSP 1363 (Rv)	TGAGACGAAGACGAGGAGGTG

PRIMERS FOR GENOTYPING BY RESTRICTRION ENZYME			
GENE	OLIGOS-ID	SEQUENCE	
LSH1	ATP 6515(Fw)	GGCTAGACATCTGCTTTGGCTTC	
	ATP 6516(Rv)	GAACTGGTCAAGGTAGCGGAGG	BSS SαI 37° C 8h
LSH3	ATP 7049(Fw)	CCAATTGATGGAAGGCTCTTCCGC	MSEI 1 37° C 1h
	ATP 6518(Rv)	GGACTTTTGTCTTACCGAACTGG	
LSH4	ATP 6134(Fw)	CAAGCCTCCTCTCATCTTCACC	
	ATP 6520(Rv)	CTTAGTCTTGCCGAATTGGTCG	BLPI 37° C 1,5 h
G1L1	OSP1841(Fw)	GCAGGTACGAGTCGCAGAAGC	AHD1 37° C 1h
	OSP1842(Rv)	GAAGTGCGCCGGGAACAAGAAGTG	
G1L2	OSP1842(Fw)	GAAGTGCGCCGGGAACAAGAAGTG	BBV1 37° C 2h
	OSP1363 (Rv)	TGAGACGAAGACGAGGAGGTG	
PRIMERS FOR AMPLIFYING CDSs			
GENE	OLIGOS-ID	SEQUENCE	
LSH1	ATP6397	GGGGACAAGTTTGTACAAAAAAGCAGGCTTCATGGATTTGATCTCTCACCAACCA	
	ATP6398(Rv)	GGGGACCACTTTGTACAAGAAAGCTGGGTTCATACTGTTGCACCCGAGTAATTAGC	
LSH3	ATP6399 Fw)	GGGGACAAGTTTGTACAAAAAAGCAGGCTGAATGGATATGATTCCCCAATTGATG	
	ATP6400(Rv)	GGGGACCACTTTGTACAAGAAAGCTGGGTCTTACTTCTCAAACTTTAATTGAGTAG	
LSH4	ATP6401 Fw)	GGGGACAAGTTTGTACAAAAAAGCAGGCTCTATGGATCATATCATCGGCTTTATGG	
	ATP6402(Rv)	GGGGACCACTTTGTACAAGAAAGCTGGGTGTTAATTAGGGCTACTTGAAATCGC	
TCP15	ATP4117 Fw)	GGGGACAAGTTTGTACAAAAAAGCAGGCTcGATGGATCCGGATCCGGATCAT	
	ATP4118(Rv)	GGGGACCACTTTGTACAAGAAAGCTGGGTgCTAGGAATGATGACTGGTGC	
G1L1	OSP 1891 Fw)	GGGGACAAGTTTGTACAAAAAAGCAGGCTAGATGGACATGATCGGCATGG	
	OSP 1892(Rv)	GGGGACCACTTTGTACAAGAAAGCTGGGTACTAGTTGAACACCGACAGTGG	
G1L2	OSP 1893 Fw)	GGGGACAAGTTTGTACAAAAAAGCAGGCTAGGACGTCATGCAGGGAGG	
	OSP 1894(Rv)	GGGGACCACTTTGTACAAGAAAGCTGGGTGCTAGTTAAACACGGACAGCG	
PRIMERS FOR AMPLIFYING TCSN			
	OLIGOS-ID	SEQUENCE	
	OSP1924	GGGGACAAGTTTGTACAAAAAAGCAGGCTAGTCAAAGATCTTTAAAAG	
	OSP1936(Rv)	GGGGACCACTTTGTACAAGAAAGCTGGGTCTGTAATTGTAATTGTAAATAG	

Figure 60. Sequence TCSn amplified, AttB site highlighted in yellow.

GGGGACAAGTTTGTACAAAAAAGCAGGCTAGTCAAAGATCTTTAAAAGATTTTGAAAG
ATCTCTCCAAAATCCTTTCAAAGATCTTTAAAAGATTTATAAAAATCTTTGCAAAATCC
AACCAAAGATTTTGTAAAGATTTTGCAAGATCCGATCAAAATCTTTAGCTAGTCAAAG
ATCTTTAAAAGATTTTGAAAGATCTCTCCAAAATCCTTTCAAAGATCTTTAAAAGATTT
ATAAAAATCTTTGCAAAATCCAACCAAAGATTTTGTAAAGATTTTGCAAGATCCGATC
AAAATCTTTAGCTAGCCAAGACCCTTCCTCTATATAAGGAAGTTCATTTCATTTGGAGA
GGATCTGTATTTTTACAACAATTACCAACAACAACAAACAACAAACAACATTACAATT
ACTATTTACAATTACAATTACAGACCCAGCTTTCTTGTACAAAGTGGTCCCC

REFERENCES

1.   Mantegazza, O. *et al.* Gene coexpression patterns during early development of the native Arabidopsis reproductive meristem: Novel candidate developmental regulators and patterns of functional redundancy. *Plant J.* **79**, 861–877 (2014).

2.   Harrop, T. W. R. *et al.* Gene expression profiling of reproductive meristem types in early rice inflorescences by laser microdissection. *Plant J.* **86**, 75–88 (2016).

3.   Cho, E. & Zambryski, P. C. ORGAN BOUNDARY1 defines a gene expressed at the junction between the shoot apical meristem and lateral organs. *Proc. Natl. Acad. Sci. U. S. A.* **108**, 2154–2159 (2011).

4.   Takeda, S. *et al.* CUP-SHAPED COTYLEDON1 transcription factor activates the expression of LSH4 and LSH3, two members of the ALOG gene family, in shoot organ boundary cells. *Plant J.* **66**, 1066–1077 (2011).

5.   Yoshida, A. *et al.* TAWAWA1, a regulator of rice inflorescence architecture, functions through the suppression of meristem phase transition. *Proc. Natl. Acad. Sci. U. S. A.* **110**, 767–72 (2013).

6.   Yoshida, A., Suzaki, T., Tanaka, W. & Hirano, H. Y. The homeotic gene long sterile lemma (G1) specifies sterile lemma identity in the rice spikelet. *Proc. Natl. Acad. Sci. U. S. A.* **106**, 20103–20108 (2009).

7.   Itoh, J. I. *et al.* Rice plant development: From zygote to spikelet. *Plant Cell Physiol.* **46**, 23–47 (2005).

8.   Laibach, F. Zur Frage nach der Individualität der Chromosomen im Pflanzenreich... (1907).

9.   Kaul, S. *et al.* Analysis of the genome sequence of the flowering plant Arabidopsis thaliana. *Nature* **408**, 796–815 (2000).

10. Clough, S. J. & Bent, A. F. Floral dip: A simplified method for Agrobacterium-mediated transformation of Arabidopsis thaliana. *Plant J.* **16**, 735–743 (1998).

11. Wang, M. *et al.* The genome sequence of African rice (Oryza glaberrima) and evidence for independent domestication. *Nat. Genet.* **46**, 982–988 (2014).

12. Sasaki, T. & Burr, B. International Rice Genome Sequencing Project: The effort to completely sequence the rice genome. *Curr. Opin. Plant Biol.* **3**, 138–141 (2000).

13. Ashikari, M. *et al.* Cytokinin oxidase regulates rice grain production. *Science* **309**, 741–5 (2005).

14. Arumuganathan, K. & Earle, E. D. Nuclear DNA content of some important plant species. *Plant Mol. Biol. Report.* **9**, 208–218 (1991).

15. Matsumoto, T. *et al.* The map-based sequence of the rice genome. *Nature* **436**, 793–800 (2005).

16. Jain, M., Tyagi, A. K. & Khurana, J. P. Genome-wide identification, classification, evolutionary expansion and expression analyses of homeobox genes in rice. *FEBS J.* **275**, 2845–2861 (2008).

17. Matsumoto, T. *et al.* The Nipponbare genome and the next-generation of rice genomics research in Japan. *Rice* **9**, 33 (2016).

18. Du, H. *et al.* Sequencing and de novo assembly of a near complete indica rice genome. *Nat. Commun.* **8**, (2017).

19. Yu, J. *et al.* A draft sequence of the rice genome (Oryza sativa L. ssp. indica). *Science (80-.).* **296**, 79–92 (2002).

20. Yu, J. *et al.* The genomes of Oryza sativa: A history of duplications. *PLoS Biol.* **3**, 0266–0281 (2005).

21. Schatz, M. C. *et al.* Whole genome de novo assemblies of three divergent strains of rice, Oryza sativa, document novel gene space of aus and indica. *Genome Biol.* **15**, 506 (2014).

22. Hiei, Y., Ohta, S., Komari, T. & Kumashiro, T. Efficient transformation of rice (Oryza sativa L.) mediated by Agrobacterium and sequence analysis of the boundaries of the T-DNA. *Plant J.* **6**, 271–282 (1994).

23. Clark, L. G., Zhang, W. & Wendel, J. F. A Phylogeny of the Grass Family (Poaceae) Based on ndhF Sequence

Data. *Syst. Bot.* **20**, 436 (1995).

24.   Gale, M. D. & Devos, K. M. Comparative genetics in the grasses. *Proc. Natl. Acad. Sci.* **95**, 1971–1974 (1998).

25.   Zhu, Z. *et al.* Genetic control of inflorescence architecture during rice domestication. *Nat. Commun.* **4**, 2200 (2013).

26.   Kellogg, E. A. *et al.* Early inflorescence development in the grasses (Poaceae). *Front. Plant Sci.* **4**, 1–16 (2013).

27.   Han, Y., Yang, H. & Jiao, Y. Regulation of inflorescence architecture by cytokinins. *Front. Plant Sci.* **5**, 669 (2014).

28.   Prusinkiewicz, P., Erasmus, Y., Lane, B., Harder, L. D. & Coen, E. Evolution and development of inflorescence architectures. *Science* **316**, 1452–6 (2007).

29.   Ta, K. N. *et al.* Differences in meristem size and expression of branching genes are associated with variation in panicle phenotype in wild and domesticated African rice. *Evodevo* **8**, 1–14 (2017).

30.   Ikeda-Kawakatsu, K. *et al.* Expression level of ABERRANT PANICLE ORGANIZATION1 determines rice inflorescence form through control of cell proliferation in the meristem. *Plant Physiol.* **150**, 736–47 (2009).

31.   Kurakawa, T. *et al.* Direct control of shoot meristem activity by a cytokinin-activating enzyme. *Nature* **445**, 652–5 (2007).

32.   Huijser, P. & Schmid, M. The control of developmental phase transitions in plants. *Development* **138**, 4117–4129 (2011).

33.   Schultz, E. A. & Haughn, G. W. LEAFY, a Homeotic Gene That Regulates Inflorescence Development in Arabidopsis. *Plant Cell* **3**, 771–781 (1991).

34.   Alvarez-buylla, A. E. R. *et al.* Flower Development. **2010**, 1–58 (2010).

35.   Irish, V. F. The flowering of Arabidopsis flower development. *Plant J.* **61**, 1014–1028 (2010).

36.   Hoshikawa, K. *The growing rice plant : an anatomical monograph*. (Nobunkyo, 1989).

37.   Ikeda, K., Sunohara, H. & Nagato, Y. Developmental Course of Inflorescence and Spikelet in Rice. *Breed. Sci.* **54**, 147–156 (2004).

38.   Yoshida, H. & Nagato, Y. Flower development in rice. *J. Exp. Bot.* **62**, 4719–4730 (2011).

39.   Lombardo, F. & Yoshida, H. Interpreting lemma and palea homologies: A point of view from rice floral mutants. *Front. Plant Sci.* **6**, 1–6 (2015).

40.   Boss, P. K., Bastow, R. M., Mylne, J. S. & Dean, C. Multiple pathways in the decision to flower: Enabling, promoting, and resetting. *Plant Cell* **16**, (2004).

41.   Sawa, M., Nusinow, D. A., Kay, S. A. & Imaizumi, T. FKF1 and GIGANTEA complex formation is required for day-length measurement in Arabidopsis. *Science* **318**, 261–5 (2007).

42.   Brambilla, V., Gomez-Ariza, J., Cerise, M. & Fornara, F. The importance of being on time: Regulatory networks controlling photoperiodic flowering in cereals. *Front. Plant Sci.* **8**, 1–8 (2017).

43.   Fornara, F. *et al.* response. *Dev. Cell* **17**, 75–86 (2009).

44.   Putterill, J., Robson, F., Lee, K., Simon, R. & Coupland, G. The CONSTANS gene of Arabidopsis promotes flowering and encodes a protein showing similarities to zinc finger transcription factors. *Cell* **80**, 847–57 (1995).

45.   Kardailsky, I. *et al.* Activation tagging of the floral inducer FT. *Science (80-.).* **286**, 1962–1965 (1999).

46.   Wigge, P. A. *et al.* Integration of spatial and temporal information during floral induction in Arabidopsis. *Science* **309**, 1056–9 (2005).

47.   Corbesier, L. *et al.* FT protein movement contributes to long-distance signaling in floral induction of

Arabidopsis. *Science* **316**, 1030–3 (2007).

48. Wils, C. R. & Kaufmann, K. Gene-regulatory networks controlling inflorescence and flower development in Arabidopsis thaliana. *Biochim. Biophys. Acta - Gene Regul. Mech.* **1860**, 95–105 (2017).

49. Abe, M. *et al.* FD, a bZIP protein mediating signals from the floral pathway integrator FT at the shoot apex. *Science (80-.).* **309**, 1052–1056 (2005).

50. Kaufmann, K. *et al.* Orchestration of floral initiation by APETALA1. *Science (80-.).* **328**, 85–89 (2010).

51. Weigel, D., Alvarez, J., Smyth, D. R., Yanofsky, M. F. & Meyerowitz, E. M. LEAFY controls floral meristem identity in Arabidopsis. *Cell* **69**, 843–59 (1992).

52. Yamaguchi, N. *et al.* A Molecular Framework for Auxin-Mediated Initiation of Flower Primordia. *Dev. Cell* **24**, 271–282 (2013).

53. Huala, E. & Sussex, I. M. LEAFY Interacts with Floral Homeotic Genes to Regulate Arabidopsis Floral Development. *Plant Cell* 901–913 (1992). doi:10.1105/tpc.4.8.901

54. Blázquez, M. A., Soowal, L. N., Lee, I. & Weigel, D. LEAFY expression and flower initiation in Arabidopsis. *Development* **124**, 3835–44 (1997).

55. Benková, E. *et al.* Local, Efflux-Dependent Auxin Gradients as a Common Module for Plant Organ Formation. *Cell* **115**, 591–602 (2003).

56. Bhatia, N. *et al.* Auxin Acts through MONOPTEROS to Regulate Plant Cell Polarity and Pattern Phyllotaxis. *Curr. Biol.* **26**, 3202–3208 (2016).

57. Saddic, L. A. *et al.* The LEAFY target LMI1 is a meristem identity regulator and acts together with LEAFY to regulate expression of CAULIFLOWER. *Development* **133**, 1673–82 (2006).

58. Wagner, D., Sablowski, R. W. M. & Meyerowitz, E. M. Transcriptional activation of APETALA1 by LEAFY. *Science (80-.).* **285**, 582–584 (1999).

59. Pastore, J. J. *et al.* LATE MERISTEM IDENTITY2 acts together with LEAFY to activate APETALA1. *Development* **138**, 3189–3198 (2011).

60. Winter, C. M. *et al.* LEAFY Target Genes Reveal Floral Regulatory Logic, cis Motifs, and a Link to Biotic Stimulus Response. *Dev. Cell* **20**, 430–443 (2011).

61. Wellmer, F., Alves-Ferreira, M., Dubois, A., Riechmann, J. L. & Meyerowitz, E. M. Genome-wide analysis of gene expression during early Arabidopsis flower development. *PLoS Genet.* **2**, 1012–1024 (2006).

62. Mandel, M. A., Gustafson-Brown, C., Savidge, B. & Yanofsky, M. F. Molecular characterization of the Arabidopsis floral homeotic gene APETALA1. *Nature* **360**, 273–7 (1992).

63. Ratcliffe, O. J., Bradley, D. J. & Coen, E. S. *Separation of shoot and floral identity*. (1999).

64. Grandi, V., Gregis, V. & Kater, M. M. Uncovering genetic and molecular interactions among floral meristem identity genes in Arabidopsis thaliana. *Plant J.* **69**, 881–893 (2012).

65. Irish, V. F. & Sussex, I. M. Function of the apetala-1 gene during Arabidopsis floral development. *Plant Cell* **2**, 741–753 (1990).

66. Bowman, J. L., Alvarez, J., Weigel, D., Meyerowitz, E. M. & Smyth, D. R. Control of flower development in Arabidopsis thaliana by APETALA1 and interacting genes. *Development* **119**, (1993).

67. Mandel, M. A. & Yanofsky, M. F. The Arabidopsis AGL8 MADS box gene is expressed in inflorescence meristems and is negatively regulated by APETALA1. *Plant Cell* **7**, 1763–1771 (1995).

68. Castillejo, C. & Pelaz, S. The balance between CONSTANS and TEMPRANILLO activities determines FT expression to trigger flowering. *Curr. Biol.* **18**, 1338–43 (2008).

69. Parcy, F., Bomblies, K. & Weigel, D. Interaction of LEAFY, AGAMOUS and TERMINAL FLOWER1 in maintaining floral meristem identity in Arabidopsis. *Development* **129**, (2002).

70. Litt, A. & Irish, V. F. Duplication and diversification in the APETALA1/FRUITFULL floral homeotic gene lineage: implications for the evolution of floral development. *Genetics* **165**, 821–33 (2003).

71. Gu, Q., Ferrándiz, C., Yanofsky, M. F. & Martienssen, R. The FRUITFULL MADS-box gene mediates cell differentiation during Arabidopsis fruit development. *Development* **125**, 1509–17 (1998).

72. Hempel, F. D. *et al.* Floral determination and expression of floral regulatory genes in Arabidopsis. *Development* **124**, (1997).

73. Ferrandiz, C., Gu, Q., Martienssen, R. & Yanofsky, M. F. Redundant regulation of meristem identity and plant architecture by FRUITFULL, APETALA1 and CAULIFLOWER. *Development* **127**, (2000).

74. Urbanus, S. L. *et al.* In planta localisation patterns of MADS domain proteins during floral development in Arabidopsis thaliana. *BMC Plant Biol.* **9**, 5 (2009).

75. McCarthy, E. W., Mohamed, A. & Litt, A. Functional divergence of APETALA1 and FRUITFULL is due to changes in both regulation and coding sequence. *Front. Plant Sci.* **6**, (2015).

76. Hartmann, U. *et al.* Molecular cloning of SVP: A negative regulator of the floral transition in Arabidopsis. *Plant J.* **21**, 351–360 (2000).

77. Yu, H., Xu, Y., Tan, E. L. & Kumar, P. P. AGAMOUS-LIKE 24, a dosage-dependent mediator of the flowering signals. *Proc. Natl. Acad. Sci. U. S. A.* **99**, 16336–16341 (2002).

78. Michaels, S. D. *et al.* AGL24 acts as a promoter of flowering in Arabidopsis and is positively regulated by vernalization. *Plant J.* **33**, 867–874 (2003).

79. Jeong, H. L. *et al.* Role of SVP in the control of flowering time by ambient temperature in Arabidopsis. *Genes Dev.* **21**, 397–402 (2007).

80. Li, D. *et al.* A Repressor Complex Governs the Integration of Flowering Signals in Arabidopsis. *Dev. Cell* **15**, 110–120 (2008).

81. Gregis, V., Sessa, A., Dorca-Fornell, C. & Kater, M. M. The Arabidopsis floral meristem identity genes AP1, AGL24 and SVP directly repress class B and C floral homeotic genes. *Plant J.* **60**, 626–37 (2009).

82. Liu, C. *et al.* Direct interaction of AGL24 and SOC1 integrates flowering signals in Arabidopsis. *Development* **135**, 1481–1491 (2008).

83. Yamaguchi, A. *et al.* The MicroRNA-Regulated SBP-Box Transcription Factor SPL3 Is a Direct Upstream Activator of LEAFY, FRUITFULL, and APETALA1. *Dev. Cell* **17**, 268–278 (2009).

84. Jung, J.-H., Ju, Y., Seo, P. J., Lee, J.-H. & Park, C.-M. The SOC1-SPL module integrates photoperiod and gibberellic acid signals to control flowering time in Arabidopsis. *Plant J.* **69**, 577–88 (2012).

85. Wang, J. W. Regulation of flowering time by the miR156-mediated age pathway. *Journal of Experimental Botany* **65**, 4723–4730 (2014).

86. Lal, S., Pacis, L. B. & Smith, H. M. S. Regulation of the SQUAMOSA PROMOTER-BINDING PROTEIN-LIKE genes/microRNA156 module by the homeodomain proteins PENNYWISE and POUND-FOOLISH in Arabidopsis. *Mol. Plant* **4**, 1123–32 (2011).

87. Khan, M. *et al.* Repression of lateral organ boundary genes by pennywise and pound-foolish is essential for meristem maintenance and flowering in Arabidopsis. *Plant Physiol.* **169**, 2166–2186 (2015).

88. Karlgren, A. *et al.* Evolution of the PEBP gene family in plants: Functional diversification in seed plant evolution. *Plant Physiol.* **156**, 1967–1977 (2011).

89.	Schultz, E. A. & Haughn, G. W. Genetic analysis of the floral initiation process (FLIP) in Arabidopsis. *Development* **119**, (1993).

90.	Shannon, S. & Meeks-Wagner, D. R. A Mutation in the Arabidopsis TFL1 Gene Affects Inflorescence Meristem Development. *Plant Cell* 877–892 (1991). doi:10.1105/tpc.3.9.877

91.	Telfer, A., Bollman, K. M. & Poethig, R. S. Phase change and the regulation of trichome distribution in Arabidopsis thaliana. *Development* **124**, 645–54 (1997).

92.	Kobayashi, Y., Kaya, H., Goto, K., Iwabuchi, M. & Araki, T. A pair of related genes with antagonistic roles in mediating flowering signals. *Science* **286**, 1960–2 (1999).

93.	Bradley, D., Ratcliffe, O., Vincent, C., Carpenter, R. & Coen, E. Inflorescence commitment and architecture in Arabidopsis. *Science* **275**, 80–3 (1997).

94.	Wang, Z. *et al.* The divergence of flowering time modulated by FT/TFL1 is independent to their interaction and binding activities. *Front. Plant Sci.* **8**, 1–16 (2017).

95.	Ho, W. W. H. & Weigel, D. Structural features determining flower-promoting activity of Arabidopsis FLOWERING LOCUS T. *Plant Cell* **26**, 552–564 (2014).

96.	Mutasa-Göttgens, E. & Hedden, P. Gibberellin as a factor in floral regulatory networks. *Journal of Experimental Botany* **60**, 1979–1989 (2009).

97.	Porri, A. *et al.* SHORT VEGETATIVE PHASE reduces gibberellin biosynthesis at the Arabidopsis shoot apex to regulate the floral transition Fernando Andrés1. *Proc. Natl. Acad. Sci. U. S. A.* **111**, (2014).

98.	Landrein, B. *et al.* Nitrate modulates stem cell dynamics in Arabidopsis shoot meristems through cytokinins. *Proc. Natl. Acad. Sci. U. S. A.* **115**, 1382–1387 (2018).

99.	Bartrina, I., Otto, E., Strnad, M., Werner, T. & Schmülling, T. Cytokinin regulates the activity of reproductive meristems, flower organ size, ovule formation, and thus seed yield in Arabidopsis thaliana. *Plant Cell* **23**, 69–80 (2011).

100.	Skylar, A. & Wu, X. Regulation of Meristem Size by Cytokinin Signaling. *Journal of Integrative Plant Biology* **53**, 446–454 (2011).

101.	Tokunaga, H. *et al.* Arabidopsis lonely guy (LOG) multiple mutants reveal a central role of the LOG-dependent pathway in cytokinin activation. *Plant J.* **69**, 355–65 (2012).

102.	Han, Y., Zhang, C., Yang, H. & Jiao, Y. Cytokinin pathway mediates APETALA1 function in the establishment of determinate floral meristems in Arabidopsis. *Proc. Natl. Acad. Sci. U. S. A.* **111**, 6840–6845 (2014).

103.	Han, Y. & Jiao, Y. APETALA1 establishes determinate floral meristem through regulating cytokinins homeostasis in Arabidopsis. *Plant Signal. Behav.* **10**, (2015).

104.	Werner, T. *et al.* Cytokinin-deficient transgenic Arabidopsis plants show multiple developmental alterations indicating opposite functions of cytokinins in the regulation of shoot and root meristem activity. *Plant Cell* **15**, 2532–50 (2003).

105.	Nishimura, C. *et al.* Histidine kinase homologs that act as cytokinin receptors possess overlapping functions in the regulation of shoot and root growth in Arabidopsis. *Plant Cell* **16**, 1365–77 (2004).

106.	Brambilla, V. & Fornara, F. Molecular Control of Flowering in Response to Day Length in Rice. *J. Integr. Plant Biol.* **55**, 410–418 (2013).

107.	Yano, M. *et al.* Hd1, a major photoperiod sensitivity quantitative trait locus in rice, is closely related to the Arabidopsis flowering time gene CONSTANS. *Plant Cell* **12**, 2473–2484 (2000).

108.	Hayama, R., Yokoi, S., Tamaki, S., Yano, M. & Shimamoto, K. Adaptation of photoperiodic control pathways

produces short-day flowering in rice. *Nature* **422**, 719–22 (2003).

109. Doi, K. *et al.* Ehd1, a B-type response regulator in rice, confers short-day promotion of flowering and controls FT-like gene expression independently of Hd1. *Genes Dev.* **18**, 926–936 (2004).

110. Itoh, H., Nonoue, Y., Yano, M. & Izawa, T. A pair of floral regulators sets critical day length for Hd3a florigen expression in rice. *Nat. Genet.* **42**, 635–8 (2010).

111. Zhao, J. *et al.* Genetic interactions between diverged alleles of Early heading date 1 (Ehd1) and Heading date 3a (Hd3a)/ RICE FLOWERING LOCUS T1 (RFT1) control differential heading and contribute to regional adaptation in rice (Oryza sativa). *New Phytol.* **208**, 936–48 (2015).

112. Zhu, S. *et al.* The OsHAPL1-DTH8-Hd1 complex functions as the transcription regulator to repress heading date in rice. *J. Exp. Bot.* **68**, 553–568 (2017).

113. Xue, W. *et al.* Natural variation in Ghd7 is an important regulator of heading date and yield potential in rice. *Nat. Genet.* **40**, 761–7 (2008).

114. Wei, X. *et al.* DTH8 suppresses flowering in rice, influencing plant height and yield potential simultaneously. *Plant Physiol.* **153**, 1747–58 (2010).

115. Lee, Y.-S. *et al.* OsCOL4 is a constitutive flowering repressor upstream of Ehd1 and downstream of OsphyB. *Plant J.* **63**, 18–30 (2010).

116. Tan, J. *et al.* OsCOL10, a CONSTANS-Like Gene, Functions as a Flowering Time Repressor Downstream of Ghd7 in Rice. *Plant Cell Physiol.* **57**, 798–812 (2016).

117. Matsubara, K. *et al.* Ehd2, a rice ortholog of the maize INDETERMINATE1 gene, promotes flowering by up-regulating Ehd1. *Plant Physiol.* **148**, 1425–35 (2008).

118. Wu, C. *et al.* RID1, encoding a Cys2/His2-type zinc finger transcription factor, acts as a master switch from vegetative to floral development in rice. *Proc. Natl. Acad. Sci. U. S. A.* **105**, 12915–20 (2008).

119. Matsubara, K. *et al.* Ehd3, encoding a plant homeodomain finger-containing protein, is a critical promoter of rice flowering. *Plant J.* **66**, 603–12 (2011).

120. Gao, H. *et al.* Ehd4 encodes a novel and Oryza-genus-specific regulator of photoperiodic flowering in rice. *PLoS Genet.* **9**, e1003281 (2013).

121. Song, L. K., Lee, S., Hyo, J. K., Hong, G. N. & An, G. OsMADS51 is a short-day flowering promoter that functions upstream of Ehd1, OsMADS14, and Hd3a1. *Plant Physiol.* **145**, 1484–1494 (2007).

122. Komiya, R., Yokoi, S. & Shimamoto, K. A gene network for long-day flowering activates RFT1 encoding a mobile flowering signal in rice. *Development* **136**, 3443–50 (2009).

123. Taoka, K. *et al.* 14-3-3 proteins act as intracellular receptors for rice Hd3a florigen. *Nature* **476**, 332–5 (2011).

124. Kobayashi, K. *et al.* Inflorescence meristem identity in rice is specified by overlapping functions of three AP1/FUL-Like MADS box genes and PAP2, a SEPALLATA MADS Box gene. *Plant Cell* **24**, 1848–1859 (2012).

125. Furutani, I., Sukegawa, S. & Kyozuka, J. Genome-wide analysis of spatial and temporal gene expression in rice panicle development. *Plant J.* **46**, 503–511 (2006).

126. Li, X. *et al.* Control of tillering in rice. *Nature* **422**, 618–621 (2003).

127. Liang, W. hong, Shang, F., Lin, Q. ting, Lou, C. & Zhang, J. Tillering and panicle branching genes in rice. *Gene* **537**, 1–5 (2014).

128. Tsuda, K., Ito, Y., Sato, Y. & Kurata, N. Positive autoregulation of a KNOX gene is essential for shoot apical meristem maintenance in rice. *Plant Cell* **23**, 4368–4381 (2011).

129. Takeda, T. *et al.* The OsTB1 gene negatively regulates lateral branching in rice. *Plant J.* **33**, 513–20 (2003).

130. Chen, L. *et al.* OsMADS57 together with OsTB1 coordinates transcription of its target OsWRKY94 and D14 to switch its organogenesis to defense for cold adaptation in rice. *New Phytol.* **218**, 219–231 (2018).

131. Komatsu, M., Maekawa, M., Shimamoto, K. & Kyozuka, J. The LAX1 and FRIZZY PANICLE 2 genes determine the inflorescence architecture of rice by controlling rachis-branch and spikelet development. *Dev. Biol.* **231**, 364–373 (2001).

132. Komatsu, K. *et al.* LAX and SPA: Major regulators of shoot branching in rice. *Proc. Natl. Acad. Sci. U. S. A.* **100**, 11765–11770 (2003).

133. Deshpande, G. M., Ramakrishna, K., Chongloi, G. L. & Vijayraghavan, U. Functions for rice RFL in vegetative axillary meristem specification and outgrowth. *J. Exp. Bot.* **66**, 2773–2784 (2015).

134. Ikeda-Kawakatsu, K., Maekawa, M., Izawa, T., Itoh, J. I. & Nagato, Y. ABERRANT PANICLE ORGANIZATION 2/RFL, the rice ortholog of Arabidopsis LEAFY, suppresses the transition from inflorescence meristem to floral meristem through interaction with APO1. *Plant J.* **69**, 168–180 (2012).

135. Ikeda, K., Nagasawa, N. & Nagato, Y. Aberrant panicle organization 1 temporally regulates meristem identity in rice. *Dev. Biol.* **282**, 349–360 (2005).

136. Rao, N. N., Prasad, K., Kumar, P. R. & Vijayraghavan, U. Distinct regulatory role for RFL, the rice LFY homolog, in determining flowering time and plant architecture. *Proc. Natl. Acad. Sci. U. S. A.* **105**, 3646–3651 (2008).

137. Ikeda, K., Ito, M., Nagasawa, N., Kyozuka, J. & Nagato, Y. Rice ABERRANT PANICLE ORGANIZATION 1, encoding an F-box protein, regulates meristem fate. *Plant J.* **51**, 1030–1040 (2007).

138. Nakagawa, M., Shimamoto, K. & Kyozuka, J. Overexpression of RCN1 and RCN2, rice TERMINAL FLOWER 1 CENTRORADIALIS homologs, confers delay of phase. **29**, (2002).

139. Kaneko-Suzuki, M. *et al.* TFL1-Like Proteins in Rice Antagonize Rice FT-Like Protein in Inflorescence Development by Competition for Complex Formation with 14-3-3 and FD. *Plant Cell Physiol.* **59**, 458–468 (2018).

140. Zhang, S. *et al.* TFL1/CEN-like genes control intercalary meristem activity and phase transition in rice. *Plant Sci.* **168**, 1393–1408 (2005).

141. Kobayashi, K., Maekawa, M., Miyao, A., Hirochika, H. & Kyozuka, J. PANICLE PHYTOMER2 (PAP2), encoding a SEPALLATA subfamily MADS-box protein, positively controls spikelet meristem identity in rice. *Plant Cell Physiol.* **51**, 47–57 (2010).

142. Liu, C. *et al.* A conserved genetic pathway determines inflorescence architecture in Arabidopsis and rice. *Dev. Cell* **24**, 612–22 (2013).

143. Gao, X. *et al.* The SEPALLATA-like gene OsMADS34 is required for rice inflorescence and spikelet development. *Plant Physiol.* **153**, 728–40 (2010).

144. Jiao, Y. *et al.* Regulation of OsSPL14 by OsmiR156 defines ideal plant architecture in rice. *Nat. Genet.* **42**, 541–544 (2010).

145. Miura, K. *et al.* OsSPL14 promotes panicle branching and higher grain productivity in rice. *Nat. Genet.* **42**, 545–9 (2010).

146. Huang, X. *et al.* Natural variation at the DEP1 locus enhances grain yield in rice. *Nat. Genet.* **41**, 494–7 (2009).

147. Xu, H., Zhao, M., Zhang, Q., Xu, Z. & Xu, Q. The DENSE AND ERECT PANICLE 1 (DEP1) gene offering the potential in the breeding of high-yielding rice. *Breeding Science* **66**, 659–667 (2016).

148. Lee, D. Y. & An, G. Two AP2 family genes, SUPERNUMERARY BRACT (SNB) and OsINDETERMINATE SPIKELET 1 (OsIDS1), synergistically control inflorescence architecture and floral meristem establishment in rice. *Plant J.* **69**, 445–461 (2012).

149. Zhu, Q.-H., Upadhyaya, N. M., Gubler, F. & Helliwell, C. A. Over-expression of miR172 causes loss of spikelet determinacy and floral organ abnormalities in rice (Oryza sativa). *BMC Plant Biol.* **9**, 149 (2009).

150. Ren, D. *et al.* MULTI-FLORET SPIKELET1, which encodes an AP2/ERF protein, determines spikelet meristem fate and sterile lemma identity in rice. *Plant Physiol.* **162**, 872–884 (2013).

151. McSteen, P. Hormonal regulation of branching in grasses. *Plant Physiol.* **149**, 46–55 (2009).

152. Yamamoto, Y., Kamiya, N., Morinaka, Y., Matsuoka, M. & Sazuka, T. Auxin biosynthesis by the YUCCA genes in rice. *Plant Physiol.* **143**, 1362–1371 (2007).

153. McSteen, P. *et al.* barren inflorescence2 encodes a co-ortholog of the Pinoid serine/threonine kinase and is required for organogenesis during inflorescence and vegetative development in maize. *Plant Physiol.* **144**, 1000–1011 (2007).

154. McSteen, P. Auxin and monocot development. *Cold Spring Harb. Perspect. Biol.* **2**, 1–18 (2010).

155. Morita, Y. & Kyozuka, J. Characterization of OsPID, the rice ortholog of PINOID, and its possible involvement in the control of polar auxin transport. *Plant Cell Physiol.* **48**, 540–549 (2007).

156. Zhang, D. & Yuan, Z. Molecular control of grass inflorescence development. *Annu. Rev. Plant Biol.* **65**, 553–78 (2014).

157. Yoshida, A., Ohmori, Y., Kitano, H., Taguchi-Shiobara, F. & Hirano, H.-Y. Aberrant spikelet and panicle1, encoding a TOPLESS-related transcriptional co-repressor, is involved in the regulation of meristem fate in rice. *Plant J.* **70**, 327–39 (2012).

158. Barazesh, S. & McSteen, P. Hormonal control of grass inflorescence development. *Trends in Plant Science* **13**, 656–662 (2008).

159. Gu, B. *et al.* An-2 Encodes a Cytokinin Synthesis Enzyme that Regulates Awn Length and Grain Production in Rice. *Mol. Plant* **8**, 1635–1650 (2015).

160. Sakakibara, H. CYTOKININS: Activity, Biosynthesis, and Translocation. *Annu. Rev. Plant Biol.* **57**, 431–449 (2006).

161. Hirose, N., Makita, N., Kojima, M., Kamada-Nobusada, T. & Sakakibara, H. Overexpression of a type-A response regulator alters rice morphology and cytokinin metabolism. *Plant Cell Physiol.* **48**, 523–539 (2007).

162. Li, Y., Li, X., Fu, D. & Wu, C. Panicle Morphology Mutant 1 (PMM1) determines the inflorescence architecture of rice by controlling brassinosteroid biosynthesis. *BMC Plant Biol.* **18**, 1–13 (2018).

163. Yamburenko, M. V., Kieber, J. J. & Schaller, G. E. Dynamic patterns of expression for genes regulating cytokinin metabolism and signaling during rice inflorescence development. *PLoS One* **12**, 1–18 (2017).

164. Zhao, L. *et al.* Overexpression of LSH1, a member of an uncharacterised gene family, causes enhanced light regulation of seedling development. *Plant J.* **37**, 694–706 (2004).

165. Iyer, L. M. & Aravind, L. ALOG domains: Provenance of plant homeotic and developmental regulators from the DNA-binding domain of a novel class of DIRS1-type retroposons. *Biol. Direct* **7**, 1–8 (2012).

166. Li, N., Wang, Y., Lu, J. & Liu, C. Genome-wide identification and characterization of the ALOG domain genes in rice. *Int. J. Genomics* **2019**, (2019).

167. Roeder, A. H. K., Ferrándiz, C. & Yanofsky, M. F. The role of the REPLUMLESS homeodomain protein in patterning the Arabidopsis fruit. *Curr. Biol.* **13**, 1630–5 (2003).

168. Bencivenga, S., Serrano-Mislata, A., Bush, M., Fox, S. & Sablowski, R. Control of Oriented Tissue Growth through Repression of Organ Boundary Genes Promotes Stem Morphogenesis. *Dev. Cell* **39**, 198–208 (2016).

169. Peng, P. *et al.* The rice TRIANGULAR HULL1 protein acts as a transcriptional repressor in regulating lateral development of spikelet. *Sci. Rep.* **7**, (2017).

170. Sato, D. S., Ohmori, Y., Nagashima, H., Toriba, T. & Hirano, H. Y. A role for TRIANGULAR HULL1 in fine-tuning spikelet morphogenesis in rice. *Genes Genet. Syst.* **89**, 61–69 (2014).

171. MacAlister, C. A. *et al.* Synchronization of the flowering transition by the tomato terminating flower gene. *Nat. Genet.* **44**, 1393–1398 (2012).

172. Levin, J. Z. & Meyerowitz, E. M. UFO: an Arabidopsis gene involved in both floral meristem and floral organ development. *Plant Cell* **7**, 529–48 (1995).

173. Hepworth, S. R., Zhang, Y., McKim, S., Li, X. & Haughn, G. W. BLADE-ON-PETIOLE-dependent signaling controls leaf and floral patterning in Arabidopsis. *Plant Cell* **17**, 1434–48 (2005).

174. Norberg, M., Holmlund, M. & Nilsson, O. The BLADE ON PETIOLE genes act redundantly to control the growth and development of lateral organs. *Development* **132**, 2203–13 (2005).

175. Xu, C., Park, S. J., Van Eck, J. & Lippman, Z. B. Control of inflorescence architecture in tomato by BTB/POZ transcriptional regulators. *Genes Dev.* **30**, 2048–2061 (2016).

176. Huang, X. *et al.* Control of flowering and inflorescence architecture in tomato by synergistic interactions between ALOG transcription factors. *J. Genet. Genomics* **45**, 557–560 (2018).

177. Takacs, E. M. *et al.* Ontogeny of the maize shoot apical meristem. *Plant Cell* **24**, 3219–3234 (2012).

178. Lei, Y., Su, S., He, L., Hu, X. & Luo, D. A member of the ALOG gene family has a novel role in regulating nodulation in Lotus japonicus. *J. Integr. Plant Biol.* **61**, 463–477 (2019).

179. Fauser, F., Schiml, S. & Puchta, H. Both CRISPR/Cas-based nucleases and nickases can be used efficiently for genome engineering in Arabidopsis thaliana. *Plant J.* **79**, 348–59 (2014).

180. Mendes, M. A. *et al.* Live and let die: a REM complex promotes fertilization through synergid cell death in Arabidopsis. *Development* **143**, 2780–90 (2016).

181. Miao, J. *et al.* Targeted mutagenesis in rice using CRISPR-Cas system. *Cell Res.* **23**, 1233–6 (2013).

182. Xie, K., Minkenberg, B. & Yang, Y. Boosting CRISPR/Cas9 multiplex editing capability with the endogenous tRNA-processing system. *Proc. Natl. Acad. Sci. U. S. A.* **112**, 3570–3575 (2015).

183. Peterson, R., Slovin, J. P. & Chen, C. A simplified method for differential staining of aborted and non-aborted pollen grains. *Int. J. Plant Biol.* **1**, 66–69 (2010).

184. A L-Tam, F. *et al.* P-TRAP: a Panicle TRAit Phenotyping tool. *BMC Plant Biol.* **13**, 122 (2013).

185. Wang, Y. & Jiao, Y. Auxin and above-ground meristems. *J. Exp. Bot.* **69**, 147–154 (2018).

186. Worthen, J. M. *et al.* Type-B response regulators of rice play key roles in growth, development and cytokinin signaling. *Development* **146**, dev174870 (2019).

187. Yang, J. *et al.* Dynamic regulation of auxin response during rice development revealed by newly established hormone biosensor markers. *Front. Plant Sci.* **8**, 1–17 (2017).

188. Zürcher, E. *et al.* A robust and sensitive synthetic sensor to monitor the transcriptional output of the cytokinin signaling network in planta. *Plant Physiol.* **161**, 1066–1075 (2013).

189. Tao, J. *et al.* A sensitive synthetic reporter for visualizing cytokinin signaling output in rice. *Plant Methods* **13**, 1–9 (2017).

190. Kawakatsu, T. *et al.* PLASTOCHRON2 regulates leaf initiation and maturation in rice. *Plant Cell* **18**, 612–25

(2006).

191.   Iyer-Pascuzzi, A. S. *et al.* Imaging and analysis platform for automatic phenotyping and trait ranking of plant root systems. *Plant Physiol.* **152**, 1148–1157 (2010).

192.   Binenbaum, J., Weinstain, R. & Shani, E. Gibberellin Localization and Transport in Plants. *Trends Plant Sci.* **23**, 410–421 (2018).

193.   Physiology of Woody Plants - Stephen G. Pallardy - Google Books. Available at: https://books.google.com/books?hl=en&lr=&id=lErfWWicYb4C&oi=fnd&pg=PP1&ots=VjQ8JN0hRH&sig= UdTkehczoLI30-tZ3GG0c5s6FFU#v=onepage&q&f=false. (Accessed: 26th September 2019)

194.   Zhou, X. *et al.* The ERF11 Transcription Factor Promotes Internode Elongation by Activating Gibberellin Biosynthesis and Signaling. *Plant Physiol.* **171**, 2760–70 (2016).

195.   Keller, T., Abbott, J., Moritz, T. & Doerner, P. Arabidopsis REGULATOR OF AXILLARY MERISTEMS1 controls a leaf axil stem cell niche and modulates vegetative development. *Plant Cell* **18**, 598–611 (2006).

196.   Uberti-Manassero, N. G., Lucero, L. E., Viola, I. L., Vegetti, A. C. & Gonzalez, D. H. The class i protein AtTCP15 modulates plant development through a pathway that overlaps with the one affected by CIN-like TCP proteins. *J. Exp. Bot.* **63**, 809–823 (2012).

197.   Kieffer, M., Master, V., Waites, R. & Davies, B. TCP14 and TCP15 affect internode length and leaf shape in Arabidopsis. *Plant J.* **68**, 147–58 (2011).

198.   Resentini, F. *et al.* TCP14 and TCP15 mediate the promotion of seed germination by gibberellins in Arabidopsis thaliana. *Mol. Plant* **8**, 482–5 (2015).

199.   Tabuchi, H. *et al.* LAX PANICLE2 of rice encodes a novel nuclear protein and regulates the formation of axillary meristems. *Plant Cell* **23**, 3276–3287 (2011).

200.   Li, Z., Li, P. & Zhang, J. Expression analysis of PIN-formed auxin efflux transporter genes in maize. *Plant Signal. Behav.* (2019). doi:10.1080/15592324.2019.1632689

201.   Nan, J. *et al.* Improving rice grain length through updating the GS3 locus of an elite variety Kongyu 131. *Rice (N. Y).* **11**, 21 (2018).

202.   Takano-Kai, N. *et al.* Evolutionary history of GS3, a gene conferring grain length in rice. *Genetics* **182**, 1323–34 (2009).

203.   Song, X.-J., Huang, W., Shi, M., Zhu, M.-Z. & Lin, H.-X. A QTL for rice grain width and weight encodes a previously unknown RING-type E3 ubiquitin ligase. *Nat. Genet.* **39**, 623–30 (2007).

204.   Ya-dong, Z. *et al.* Functional Marker Development and Effect Analysis of Grain Size Gene GW2 in Extreme Grain Size Germplasm in Rice. *Rice Sci.* **22**, 65–70 (2015).

205.   Horstman, A., Willemsen, V., Boutilier, K. & Heidstra, R. AINTEGUMENTA-LIKE proteins: Hubs in a plethora of networks. *Trends Plant Sci.* **19**, 146–157 (2014).

206.   Elliott, R. C. *et al.* AINTEGUMENTA, an APETALA2-like gene of Arabidopsis with pleiotropic roles in ovule development and floral organ growth. *Plant Cell* **8**, 155–68 (1996).

207.   Ikeda-Kawakatsu, K., Maekawa, M., Izawa, T., Itoh, J. I. & Nagato, Y. ABERRANT PANICLE ORGANIZATION 2/RFL, the rice ortholog of Arabidopsis LEAFY, suppresses the transition from inflorescence meristem to floral meristem through interaction with APO1. *Plant J.* **69**, 168–180 (2012).

208.   Gregis, V., Sessa, A., Colombo, L. & Kater, M. M. AGAMOUS-LIKE24 and SHORT VEGETATIVE PHASE determine floral meristem identity in Arabidopsis. *Plant J.* **56**, 891–902 (2008).

209.   Coen, E. S. *et al.* floricaula: a homeotic gene required for flower development in antirrhinum majus. *Cell* **63**,

1311–22 (1990).

210. Toki, S. Rapid and efficient Agrobacterium-mediated transformation in rice. *Plant Mol. Biol. Report.* **15**, 16–21 (1997).

211. de Folter, S. & Immink, R. G. H. Yeast protein-protein interaction assays and screens. *Methods Mol. Biol.* **754**, 145–65 (2011).